Preferred citation: F. Julien Saint Amand. Particle Separation Processes. In **The science of papermaking**, *Trans. of the XIIth Fund. Res. Symp. Oxford, 2001*, (C.F. Baker, ed.), pp 81–191, FRC, Manchester, 2018. DOI: 10.15376/frc.2001.1.81.

STOCK PREPARATION PART 2 – PARTICLE SEPARATION PROCESSES

François Julien Saint Amand

Centre Technique du Papier (CTP)
BP 251 – 38044 Grenoble Cedex – FRANCE
Francois.Julien-Saint-Amand@ctp.inpg.fr

ABSTRACT

The screening, cleaning, flotation and washing processes are treated in this second part "Particle Separation Processes" of the review paper about "Stock Preparation", which is focused on the process engineering aspects of the unit operations used in the production of virgin and recycled pulps. Chemical and physical-chemical aspects are out of the scope of this paper as well as the pulp dilution, transport and storage unit operations.

Particle separation processes refer to the unit operations aiming at separating different pulp components in order to remove or concentrate some of them in different fractions. The particle separation processes are essential in recycling to remove various contraries in a very large particle size range. Separation is mainly based on particle dimensions in screening and washing, on particle density in centrifugal cleaning and on particle surface properties in flotation. Fractionation is normally performed as an intermediate process between screening and washing, though the centrifugal process can also be used. Particle size and shape and hydrodynamic phenomena are decisive in the separation processes.

Fundamentals of centrifugal separation as well as flotation hydrodynamics have been extensively studied in the field of mineral processing, while fundamentals of pressure screening have not yet been investigated as much, since the technique is more recent and specific to the pulp and paper industry. The particle separation mechanisms are reviewed in this paper, with special emphasis placed on the description and analysis of physical mechanisms and on the theory developed about two main aspects:

– the large scale fibre suspension flows, which define particle transport and mixing;
– the particle separation micro-processes observed at the scale of the particles.

Finally, the effects of machine, operating and material parameters are briefly analysed with respect to the theoretical background.

INTRODUCTION

Stock preparation, in the broad sense of producing a fibre suspension in a suitable form for the paper machine from the various fibre resources, includes the manufacture of chemical pulps, high-yield pulps and non-wood pulps as well as the recycling of recovered papers in the fields of deinking and packaging. The mechanical processes used in one or several of these applications can be classified in two main groups:

– Pulp treatment processes: pulping, refining and hot dispersing: Part I;
– Particle separation processes: screening, cleaning, flotation and washing: Part II.

Chemical processes and physical-chemical aspects are out of the scope of this paper, as well as wood treatment processes, water treatment processes and pulp dilution, transport and storage. The particle separation processes reviewed in this second part are a concern in the various sectors of stock preparation.

In chemical pulp mills, the screening process is used to remove various contraries, from uncooked material in the coarse step to small shives, bark and impurities in the fine screening room. The washing process used in pulp mills differs from wash deinking, as it is not a particle separation process. Displacement washing is not reviewed in this paper. Cleaning is used in pulp mills to remove bark, sand and low-density plastics.

In the manufacturing of high-yield pulps, the screening systems associated to the second refining stage are essential to reach the pulp quality requirements in terms of shives removal and fibre developments. Cleaners are used to complete the removal of shives.

Non-wood fibres are produced by chemical or high-yield pulping processes and more recently by the promising bivis extrusion process, which has been adapted to the pulp and paper industry and investigated at CTP [1]. The bivis extrusion process is basically a mechanical pulping process, with a defibering action between grinding and refining [2]. The bivis extruder is used as high temperature short time reactor and it is also a pulp washer since chemicals can be added and dissolved material removed as the pulp moves along the two extrusion screws [3,4]. The bivis process is used in the manufacture of printing and packaging papers from wood [1–4] and annual plants [5,6].

The recycling of recovered papers is essentially a combination of mechanical and physical-chemical pulp treatment and particle separation processes. Recycling chemistry is more important in the deinking process, which normally includes pulp bleaching steps, than in the recycling of brown grades for packaging papers. The increasing amount in the recovered papers of various kinds of contraries introduced by the paper printing and converting processes and during waste paper collection, has led to the development of more and more complex recycling lines. A detailed analysis of the different systems used for the recycling of the various raw materials and the production of various paper grades or market deinked pulp is out of the scope of this paper.

The optimisation of the pulping step is a prerequisite in any recycling line to ensure a sufficient defibering of the recovered papers, separate the contraries from the fibres if necessary, and keep them as large as possible to make their removal easier in the subsequent screening, cleaning and flotation steps.

In the field of packaging, screening is clearly the most important separation process. Some deflaking is achieved in the first screening steps after the pulper to minimise the fibre losses. High consistency cleaning has then to be implemented to remove coarse heavy particles such as sand, grids and metals in order to protect downstream equipment. Fine high-density cleaning should be implemented before slot screening to remove fine sand and reduce the wear of the screen cylinders in the fine screening steps. Low-density cleaning contributes to the removal of various lightweight particles such as plastic films and hot melt glues. Current trends are to replace hot dispersing by fine screening, since hot dispersing does not remove contaminants but only disperse them, and consequently does not solve the problems of deposits on the paper machine. Refining is generally implemented on a long fibre fraction in a fractionation and contaminant-screening step. Flotation and washing, which could remove problematic colloid matter and improve the paper strength properties, have not yet been used in the recycling of packaging papers because of their negative impact in terms of yield and treatment costs.

In the field of deinking, the optimisation of the ink detachment and subsequent removal by flotation or washing has led to the development of two or three loops deinking lines, with intermediate hot dispersing steps to detach the inks which have not been detached from the fibres in the pulping step. The optimisation of the pulping step is even more important than in the recycling of brown grades, because of the pulping chemistry added for the detachment of the inks, and also because the removal of stickies from pressure sensitive adhesives (PSA) is more crucial, since the adhesive material is weak and might be more or less dissolved or fragmented in small particles down to the microscopic size. The pulping chemistry (alkaline to neutral conditions) should also be adapted to the type of ink in the recovered papers, especially in the case of water based inks [7].

The coarse cleaning and screening steps are similar in deinking lines and in packaging recycling lines, except that coarse screening is normally performed under more gentle screening conditions to minimise the fragmentation of the stickies. Fine slot screening, high-density cleaning and low-density cleaning are then used in various system designs to remove most of the contaminants in the first deinking loop. Most of the free ink is then removed by flotation or washing (normally used in tissue mills). At the end of the first deinking loop, pulp is thickened to the consistency required for the hot dispersing step and process water is returned to the pulper. The main role of hot dispersing is to detach the residual attached ink and remove it in the post-deinking step. Additionally, the high consistency, high temperature treatment modifies the size and shape of the residual stickies. PSA particles become more spherical, namely in the case of kneading, and their subsequent removal is enhanced especially by flotation and cleaning [8]. Bleaching is normally combined to hot dispersing to make use of high temperature and efficient mixing. The optimisation of process water treatments and water circuit design is essential to improve the deinking yield and the removal of inks and colloid material. Refining also becomes important in deinking to develop the paper strength and surface properties. It might be combined to screening to improve the removal of shives and coarse fibres, especially as deinked pulp is incorporated in high quality graphic papers.

The pulp separation processes reviewed and analysed in this paper refer to the unit operations aiming at separating the different pulp components in order to remove various contraries or to concentrate some of the pulp components in different fractions. Particle separation is based on particle size for barrier separation techniques, i.e. screening, fractionation, washing and

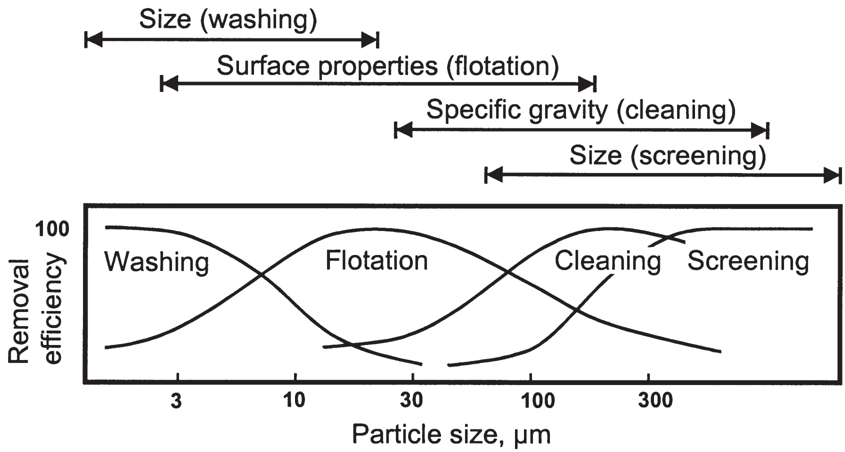

Figure 1 Optimum efficiency range of unit operation efficiency versus particle size.

thickening, on particle density for centrifugal cleaning and on particle surface properties and deinking chemistry for flotation.

Particle size is a key factor in all the separation processes as shown in Figure 1. These curves were proposed to describe the contribution of the separation processes to the removal of inks in deinking lines [8]. However, it is clear that particle shape and other properties are decisive factors as well. Stiff round shaped particles are easier to remove by screening with fine slots than thin particles, neutral buoyancy particles are not removed by cleaning and hydrophilic particles are normally not removed by flotation.

Pulp fractionation can be defined as the separation of the pulp components in two fractions, which are used separately (for different paper grades, machines or layers) and/or submitted to different treatments (typically selective refining of the coarse fibre fraction). Fractionation is normally performed with screens to separate the long and coarse fibres from the short fibres and fine components. The use of washing to remove fine components (fines, fillers, inks) might also be considered as a fractionation process, as far as the fine components are reused instead of usually rejected (wash deinking). Besides barrier separation technology, centrifugal cleaning can also be used for the fractionation of pulps according to other fibre properties.

SCREENING

Contaminant screening can be defined as the retention of the contaminants by the barrier and the passage of practically all the pulp through the openings in the barrier. Depending on the application in the stock preparation line, contaminant screening is performed in one single stage or in a multistage system. The barrier is normally a screen plate with holes or slots.

Fractionation screening requires basically the use of screen plates with small openings combined with specific screening conditions. Long and coarse fibres concentrate with the shives and contaminants in the reject stream (long fraction) while short fibres are accepted. Fine contaminant screening is always associated with fractionation within the screening systems.

SCREENING TECHNOLOGY

Considerable progress has been achieved in screening technology over the last 50 years with the development of pressure screens, which replaced the old side-hill and vibrating screens to increase capacity, consistency and screening efficiency. Open screens are however still used at the coarse screening steps. A complete overview of the various equipment used in recycled fibre systems has been given in several papers [1,2]. The analysis and results reported in this section focus on fine screening, though effective coarse screening is a pre-requisite to improve the overall contaminant removal efficiency.

Coarse screening is performed with holes. Pulper screens (secondary pulpers) equipped with flat smooth screen plates are normally implemented after the pulper [3,4]. Pulpers include the first screening step in the case of low consistency and drum pulpers. Various types of tail screens, with different designs (open or pressurised, flat screen plate, cylinder or half cylinder, continuous or discontinuous) have been developed to treat coarse screening rejects [1,2]. In pulper screens, the feed side volume is large to accept the accumulation of large contraries. The rotor is designed to provide some optimised deflaking but the screening conditions on the screen plate are not homogeneous because of the radial feed pressure gradient produced by the rotation of the pulp.

Fine screening is performed with slots in pressure screens. Screen cylinders are used to increase the open area and to optimise the hydrodynamic screening conditions. Basket screens are also used for coarse screening with smaller holes than in pulper screens. Several screen designs have been developed by the equipment suppliers, as shown in Figure 2. The most common screen

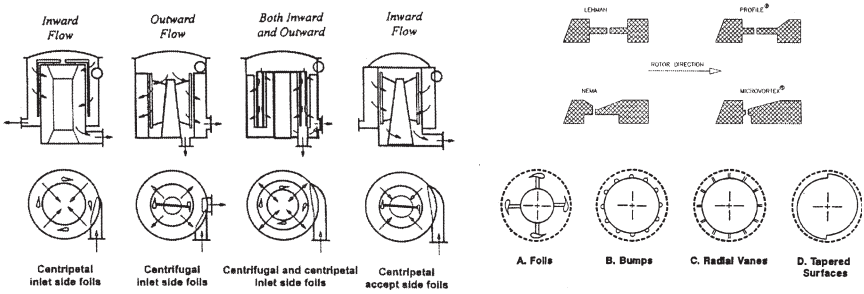

Figure 2 Examples of pressure screen configurations [5], milled screen plate designs [6] and rotor designs [7].

design configuration is the centrifugal design with outward flow and the rotor located at the inlet of the screen basket, mainly for mechanical reasons. The centripetal design with inward flow and the rotor located around the screen basket was developed to improve the removal of heavy contraries and to reduce the pressure pulses at the screen accepts for headbox screen applications [5].

The rotor is normally implemented at the feed side of the screen basket to control the flow conditions and avoid pulp flocculation. The implementation of the pressure pulse generating elements, i.e. the rotor or static means in the case of a rotating basket, at the accept side avoids the fragmentation of fragile contraries. The rotating basket in centripetal configuration improves the removal of heavy contraries such as sand [8,9] but should reduce the removal of lightweight contraries.

The first role of the rotor is to avoid the formation of a fibre mat by the reverse flow created by the pressure pulse elements such as foils. Typically the rotor velocities are in the range of 10 to 25 m/s and the duration between two pulses about 20 ms depending on the type of rotor (Figure 2). Open rotors are equipped with foils of various shapes or with long blades [10]. Closed or cylindrical rotors are characterised by the fact that pulp is forced to pass between the screen plate and the pulse generating elements. These include bumps [11], radial vanes with internal dilution [12], tapered or lobed rotor shape [13,14] and various other elements such as foils or short steps placed on the cylinder.

One of the most important developments in screen cylinders occurred in the early 1980's with the development of grooved (contoured or profiled) screen plates [15,16], such as shown in Figure 2. Profiled screen plates are currently used in all the fine screening applications because of their advantages over smooth screen plates. As initially observed with flow interrupter bars welded on the screen plate [5] the profiles improve the screening capacity since pulp flocculation is reduced because of the higher turbulence and the effectiveness of the rotor is increased. Efficiency can then be improved by using smaller slots in a given screening system.

Smooth screen plates with holes are still used for coarse screening (typically 4 mm diameter holes in a secondary pulper) and pulp fractionation (basket screens with holes down to 1 mm). Profiled screen plates are currently used in all the other applications of basket screens, with holes down to 1.2 mm as well as with slots down to 0.10 mm in the field of deinking and mechanical pulps or 0.15 mm in the field of packaging.

Various designs of the profile and slot section have been developed as well as different manufacturing techniques, including milled profiles and slots, laser and water jet cut slots and the wedge wire construction [17–18]. Progress has been achieved recently in both manufacturing techniques to improve the weak points, i.e. to increase the slot width precision with wedge wire cylinders and to reduce slot width, increase open area and improve slot and profile shape with milled cylinders.

SCREENING THEORY: BASIC RELATIONS

The theory of screening and the fundamental relations to describe screen performance were investigated by different authors [20–24] before fundamental research work started about the hydrodynamic separation mechanisms in pressure screens [25–30].

The theory of screening and the fundamental relations to describe screen performance were first established in the 1950's on the basis of probabilistic separation [20,21]. Kubat and Steenberg developed the statistical ideas of screening by treating the case of charging a screen with particles of only one type, having a size so chosen that they can pass the apertures of the screen. There was assumed to be sufficient agitation of the liquid in the upstream (feed/rejects) and downstream (accepts) compartments to ensure uniform concentration in each part, and the particle concentrations were assumed to be sufficiently low for the particles to behave as statistical independent units. The pulsation effect in pressure screens was taken into account, i.e. there exists flows through the screening element in both directions, the net flow being equivalent to the throughflow (accept flow). By using the following symbols and indices:

q	flow rate (water)
P	average particle passage probability
C	particle concentration
i, a, r	inlet, accepts, rejects
u, d	upstream, downstream compartments
1, 2	throughflow, reverse flow directions

the net flow of particles is given by the relation:

$$P_1 q_1 C\mathrm{u} - P_2 q_2 C\mathrm{d} = P q\mathrm{a}\, C\mathrm{u}$$

where P_1 and P_2 vary from 0 for the particles completely retained by the screen to 1 for the particles which follow the suspending fluid. With $q\mathrm{a} = q_1 - q_2$ and $\alpha = q_2/q\mathrm{a}$ the relation becomes:

$$P = P_1\ (1 + \alpha)/(1 + \alpha P_2)$$

Kubat and Steenberg established this definition of the screen permeability index P and used α as a suitable measure of the pulsation effect. They noticed that P might have values above unit because of the pulsation and that, even if the probabilities P_1 and P_2 are independent of the flow conditions, increasing the pulsation will always increase P.

Screen performance Equations based on fundamental mass and flow balances of single closed screening units, on particle passage probabilities and on the derivation of these Equations along the screen basket have been reviewed and developed by Wahren [22], Nelson [23] and Gooding and Kerekes [24]. The influence of re-circulation of rejects to feed has been treated by Norman et al. cited in [22]. It is convenient to use the time-averaged particle passing probabilities on a single aperture, i.e. the permeability P of an elementary screen area or cylinder section, to derive the screen performance Equations. Gooding and Kerekes defined the passage ratio of a particle by the ratio $C\mathrm{s}/C\mathrm{u}$, which is equal to the screen permeability P, as the consistency $C\mathrm{s}$ of particles in the flow through the slots is equal to the consistency $C\mathrm{a} = C\mathrm{d}$ of the particles in the accept flow under the hypothesis of uniform concentration in the downstream compartment.

Some of the basic relations established for all screens or for particular internal flow models in the upstream compartment are reported below. The symbols are indicated in Figure 3, where Q are the flow rates, C the pulp consistencies, M the mass flow rates, $R\mathrm{v}$ the ratio of reject to feed flow, $R\mathrm{w}$ the reject rate by weight and S the contaminant contents (symbol for shives content).

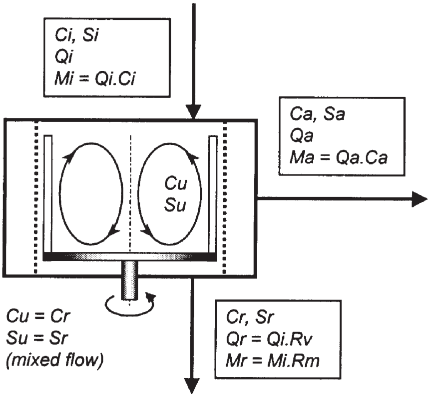

Figure 3 General screening symbols and Equations of mixed-flow model.

The mixed-flow model corresponds to the perfect mixing case, i.e. to uniform particle concentrations in the upstream compartment. This model might be used to describe the flow in pressure screens with open rotor and high radial turbulence and/or high axial internal re-circulation as illustrated in Figure 3. Feed pulp is perfectly mixed to the rejects; the upstream and downstream consistencies are respectively equal to the reject and accept consistencies. The passage ratio is then given by $P = Ca/Cr$.

The plug-flow model described in Figure 4 assumes there is no axial mixing

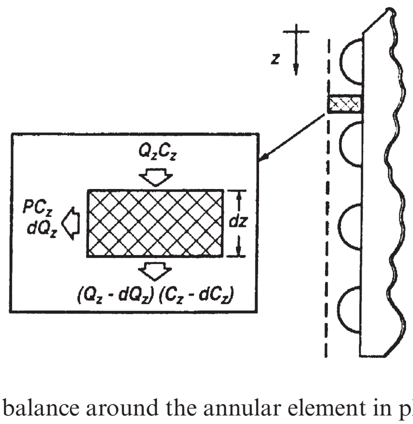

Figure 4 Material balance around the annular element in plug-flow model [24].

in the annular screening zone (upstream axial plug flow from the feed to the reject section) and perfect radial mixing at each location z [24]. This model might be used to describe the flow in pressure screens with cylindrical rotor, small annular thickness and high basket length with respect to the basket diameter. The plug-flow model corresponds to single mixed-flow elementary screens in cascade (rejects of one stage feed the next stage) with common accepts, as described in [21] to analyse the side-hill screen.

The performances of screens can be predicted according to these flow models assuming no interactions between the suspended particles and constant particle passage ratios P_x over the screen plate, the subscript x identifying the particle type [24]. The Equations giving the reject thickening factor ($T = C\mathrm{r}/C\mathrm{i}$) are only valid for homogeneous particles:

$T = 1/(P - R\mathrm{v}P + R\mathrm{v})$ for the mixed-flow model
$T = R\mathrm{v}^{(P-1)}$ for the plug-flow model

In the hypothesis of homogeneous fibres with a passage ratio P_F and contaminants with a passage ratio P_K, the ratio $\beta = P_K/P_F$ was shown to be simply related to the standard efficiency definitions and to the screening quotient Q [23], which found widespread use in pulp screening [24]:

$E_R = R\mathrm{w}S\mathrm{r}/S\mathrm{i}$ Reject (removal) efficiency
$E_C = 1 - S\mathrm{a}/S\mathrm{i}$ Cleanliness efficiency
$\mathrm{Q} = E_C/(E_C + \mathrm{Rw} - E_C\mathrm{Rw}) = E_C/E_R = 1 - S\mathrm{a}/S\mathrm{r}$
$E_R = \mathrm{Rw}/(\mathrm{Rw} + \beta - \beta\mathrm{Rw})$ or $\mathrm{Q} = 1 - \beta$ for the mixed-flow model
$E_R = \mathrm{Rw}^{\beta}$ for the plug-flow model

The above Equations, which apply to probability screening, can be modified to include barrier screening. If b is the ratio of the amount of "barrier" contaminants ($P_K = 0$) to the total amount of "barrier + probability" contaminants in the feed pulp, they become [24]:

$E_R = \mathrm{b} + (1 - \mathrm{b})\mathrm{Rw}/(\mathrm{Rw} + \beta - \beta\mathrm{Rw})$ for the mixed-flow model
$E_R = \mathrm{b} + (1 - \mathrm{b})\mathrm{Rw}^{\beta}$ for the plug-flow model

In real situation, the passage ratio distributions of the contaminants and pulp components have to be included in the calculation to establish the models of screening systems. If the pulp is composed of homogenous fibres with a passage ratio P_F and fine particles with a passage ratio of 1 (such as fillers, fines or ink particles following the fluid), the pulp passage ratio is given by $P_P = a + (1 - a)\, P_F$ where a is the fine particles fraction [31].

SCREENING HYDRODYNAMICS

The probability screening process is governed, besides barrier separation, by complex hydrodynamic separation phenomena inside the pressure screen, which can be divided into "macro-flow" and "micro-flow" phenomena [29]. The rotor ensures the transport of the particles in the upstream compartment, by the "macro-flow" generated inside the screen basket in the tangential and axial directions. The rotor also generates the pressure pulses (Figure 5) which control the radial slot velocity variations during the positive pulse (screening phase) and the negative pulse (reverse flow to clean the screen).

The unsteady "micro-flow" conditions at the surface of the screen plate and through the slots depend strongly on the characteristics of the rotor and on the design of the screen plate (Figure 6). These flow conditions govern the

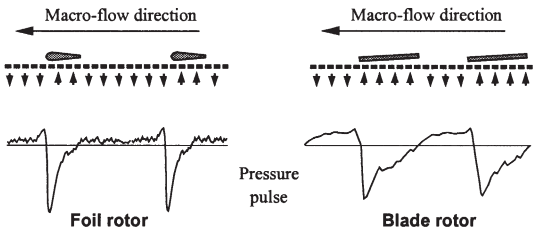

Figure 5 Typical pressure pulse produced by a rotor with conventional short foils and by a rotor with long blades [32].

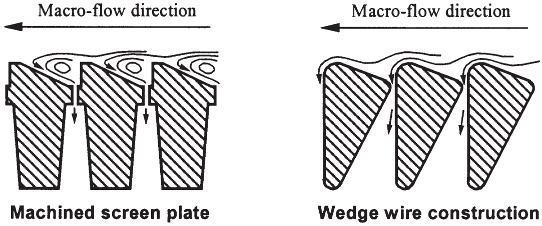

Figure 6 Example of the micro-flow streamlines at the feed side of machined and wedge wire screen plates [33].

probabilities for the particles to be captured from the main stream by the "exit layer" and then to pass through the slots.

Pulp Transport and Mixing

In low consistency screens, the suspension in the macro-flow area is highly turbulent and behaves like water, which allows the fluid dynamics theory and CFD simulation tools to be used for the evaluation of the flow characteristics and the optimisation of pressure screen design [34–40]. The velocity at the surface of the screen plate depends on the rotor velocity and design (gap clearance, foil/blade angle), on the feed conditions and on the screen plate design. The reverse pulse is created by the pressure decrease produced by the acceleration of the fluid in the gap between the rotor and the screen cylinder. The pressure pulse is roughly proportional to the square of the rotor velocity. It is increased as the velocity difference between the rotor and the pulp is increased.

The pressure pulses shown in Figure 4 were measured with an experimental industrial sized pressure screen [32] at the same rotor velocity (23 m/s), pulse frequency (4 foils or 4 blades) and gap clearance (4 mm). The negative pressure pulses were about 200 kPa for the foil rotor and 150 kPa for the blade rotor. With such relatively high negative pressure pulses a minimum accept pressure is required to avoid cavitation.

Computational Fluid Dynamics (CFD) has been used to predict pressure pulses and optimise rotor design. The choice of the turbulence model, standard k-ε, k-ε RNG (renormalization group) or others might however lead to discrepancies as illustrated in Figure 7 showing results obtained with the code Fluent [39]. The roughness of the screen cylinder has also to be taken into account for the CFD simulation. Grégoire et al. used a "two-layer zonal model" to compute the flow at the surface of the screen plate [40]. The results showed to be consistent with the classical logarithmic law if the origin was taken at the crests of the profiles (Figure 8). Another model was used and adapted to rough surfaces in order to treat the problem with suction flow through the surface.

In high consistency screens, more energy has to be dissipated in the macro-flow at the feed side of the screen plate to avoid pulp flocculation, which basically reduces the separation between the different pulp components and might lead to blinding of the screen as the pulp passage is reduced [41]. It is beyond the scope of this section to review the literature about turbulence flocculation interactions and the non-Newtonian behaviour of fibre suspensions at low shear rate and increasing consistency. Basic results and theory can be found in several papers including [42–47]. The shear stress required for

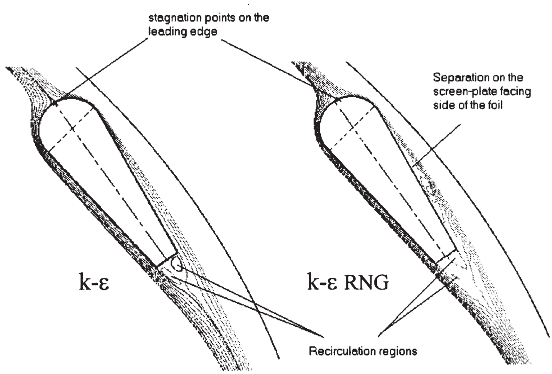

Figure 7 Numerical simulation of the flow around a foil showing discrepancies between the standard k-ε turbulence model and the k-ε RNG turbulence model [39].

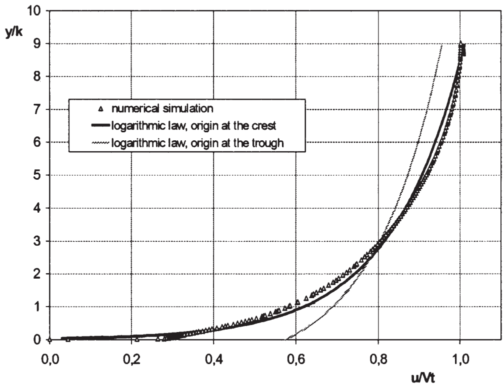

Figure 8 Numerical simulation of the velocity profile over the rough surface of a screen plate (without suction) and comparison with the logarithmic law [40].

the disruption of the fibre network and the onset of complete pulp deflocculation, i.e. pulp fluidisation, is generally assessed by the yield stress function:

$$\tau = aC_{\mathrm{w}}{}^{b}$$

where the consistency C_w is given as weight % and a and c depend on the type of pulp. The shear forces generated between the rotor and the screen cylinder in high consistency screens were evaluated recently using an apparent pulp viscosity [48]. The authors used the apparent pulp viscosity evaluated on the basis on the above yield stress function [46]. The Bingham model has been used recently to define the rheology of the pulp for the numerical simulation of the flow and pressure pulses in high consistency screens [38].

Shear is however not the only way to de-flocculate the pulp by the induced turbulence. Elongational stress in convergent flow [45] and turbulent elongational stress [49] can effectively contribute to the destruction of the fibre flocs. In addition, it is believed that yield stress function should not be used to evaluate the shear stresses at lower scales than the floc sizes, i.e. in the slots of high consistency screens.

Practically, since the disruptive shear stress required for pulp de-flocculation increases drastically and the re-flocculation time decreases strongly as the pulp consistency is increased, screens in the high consistency range (3 to 5%) are operated at higher rotor velocity than low consistency screens. A higher reverse pulp frequency is also necessary to avoid blinding of the screen cylinder as the accumulation of fibres or flocs is higher.

Pulp flocculation may also influence the screening process in a positive way as it occurs in the accept side of the screen plate during the reverse pulse. The re-flocculation, after turbulence decay, of the pulp passing the slots during the screening phase might reduce the thickening of the pulp on the feed side, by the dilution effect produced during the reverse flow phase if flocs are formed and retained on the accept side of the screen plate. This phenomenon characterised by an increase of the pulp passage ratio (up to above 1 with consequently a lower reject than feed consistency in certain cases) should only concern high consistency screens equipped with extended reverse pulse rotors to give enough time to the fibres to flocculate (see re-flocculation time in decaying turbulence reported in [45]). It was observed with the tapered surface rotor shown in Figure 2 [13] and with the long blade rotor shown in Figure 4 [50].

Particle Separation

Fundamental research work about the fibre separation mechanisms in screens has started in the 1980's, in connection with the development of profiled screen plates [51–56]. Both the flow conditions and the motion of fibres were investigated since the fibre trajectories, orientations and external forces, which determine the passage probability of the fibre through the slots, are governed by the velocity field near the screen plate.

The flow characteristics were studied by numerical simulation [25,27,30,52,54] or experimentally by visualisation with water or smoke [35,53,55,] in transparent channels with a single slot or several slots after a sufficient channel length to fully develop the velocity profile at the surface of the model screen. The experimental "channel screens" were also used to study the motion of fibres near the slots at extremely low consistency [25,26,53,56]. A "channel screen" has been equipped with a pressure pulse generating device on the accept side to determine the fibre passage ratios at higher consistency and simulate real screening conditions [27,54].

All the CFD simulations and the flow and fibre motion visualisations were performed in the plane of the slots and tangential velocities (*Vs* and *Vt*). The hypothesis of a 2D simulation of the flow at the feed surface of the screen basket is on average relevant regarding industrial screening conditions, since the tangential velocity induced by the rotation of the rotor is high with respect to the axial velocity. The hypothesis of a 2D flow is however not rigorous with cylindrical rotors, especially in the feed section where the axial velocity is higher, as well as with rotors producing axial velocity pulses such as the bump rotor (Figure 2).

The flow patterns given as examples in Figure 5 correspond respectively, in the machined screen plate drawing to usual flow conditions ($Vt > Vs$) with fine slots as reported in [36] and shown in the Figures 12–15, and in the wedge wire screen plate drawing to a higher slot width and Vs/Vt ratio. A round shaped profile top as shown in the drawing of the wedge wire screen plate (Figure 2) contributes to avoid the boundary layer release, i.e. the fluid tends to sticks to the wall as a result of the boundary forces (Coanda effect). A similar flow pattern visualised on a wedge wire screen plate has been reported in [35]. The intensity of the vortex created at the slot inlet increases with increasing slot width and Vs/Vt ratio [36]. It has to be pointed out that the vortex rotates in the same direction during the screening and the reverse flow phases. This contributes to further reduce the time lag between the maximum negative pressure pulse and the maximum reverse flow velocity. CFD simulations performed recently [39] without taking the rotation of the vortex into account showed that the inertia of the fluid in the slot could be neglected since the calculated time lag was shown to be about two orders of magnitude lower than the pressure pulse period.

Fibres were introduced in the numeral simulation later [57,59], since the problem is much more complicated, even at low consistency assuming no fibre interactions. Lawryshyn and Kuhn [57] used the Equations previously established for large and small deflection analysis of flexible cylindrical fibres [60]. The formulae used to evaluate the drag coefficient with respect to a cross flow are reported in the section devoted to centrifugal cleaning. Chains of prolate spheroids with flexible links were recently used to simulate flexible fibres [58,59].

Gooding [25,51] showed that fibre separation in a “channel screen” with a single non-profiled slot took place by two mechanisms: a “wall effect” that lowered the concentration of stiff fibres in the flow layer entering the slot and a “turning effect” that caused these stiff fibres to rotate rather than bend as they turned into the slot. These rotating fibres tended to be swept away from the slot by the mainstream flow whereas more flexible fibres tended to bend and enter. Five “fibre motion types” were reported:

1. The fibre moves past the slot without either entering the slot or touching the slot wall.
2. One end of the fibre enters the slot and touches one of the walls, but is then swept out of the slot and back into the main stream.
3. One end of the fibre enters the slot and the fibre is immobilised – balanced on the downstream edge of the slot (commonly called “stapling”).
4. The fibre passes through the slot after contacting one (or both) of the sidewalls.
5. The fibre passes through the slot without contacting either slot wall.

The fibre motions experimentally observed by Gooding [25] were later observed by the fibre motion simulation of Lawryshyn and Kuhn [57] except type 3. In the simulations it was observed that fibres which approach the channel and slot junction can be grouped into five general categories according to their initial wall contact, as follows:

A. The fibre first contacts the upstream slot corner: observed in cases where the initial fibre position is close to the wall as shown in Figure 9. Rigid

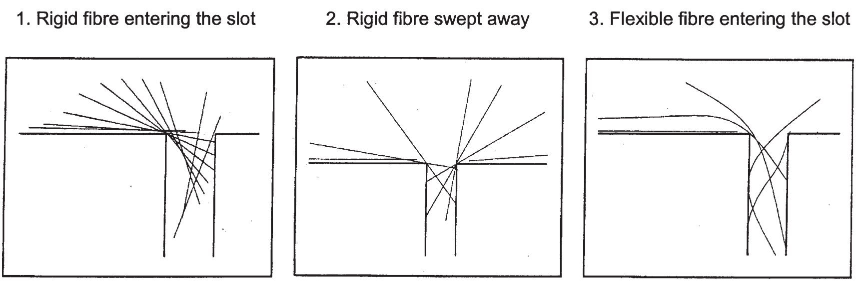

Figure 9 Numerical simulation of category A motion for rigid and flexible fibres [57].

fibres either enter the slot at high Vs/Vt ratio (Figure 9-1) or rotate and are swept out of the slot at low Vs/Vt ratio (Figure 9-2). Flexible fibres tend to bend with the streamlines and are less prone to be swept away by the main stream (Figure 9-3).

B. The fibre enters the slot without any contact: observed for short fibres.
C. The fibre first contacts the downstream slot wall: observed for most fibres that enter the slot, with similar cases than in category A.
D. The fibre first contacts the downstream channel wall: observed for fibres which generally do not enter the slot. Long fibres usually staple the slot. Short fibres rotate and either enter the slot at high Vs/Vt or are swept out of the slot at lower Vs/Vt.
E. The fibre does not contact any walls and simply flows downstream in the channel.

Kumar [26,61] further investigated the behaviour of fibres at extremely low concentrations in the “channel screen” used by Gooding and showed that the fibre passage ratio was a function of the ratio Vs/Vu (see Figure 10), which was termed “normalised slot velocity”. This ratio determines the thickness of the layer of fluid that turns into the slot (the “wall effect”), but not necessarily the magnitude of the hydrodynamic drag forces through and past the slot (the “turning effect”). Kumar showed that, under ideal conditions, the passage ratio of given fibres (length l) through the slots (width W) was well characterised by a dimensional penetration number, Pe, given by:

$$Pe = \frac{W Vs}{l Vu}$$

Olson [27,62] further investigated the influence of fibre length. A theoretical expression for fibre passage ratio was derived based on a fibre concentration gradient at the screen plate surface [63]. It was shown that the fibre concentration gradient created near a smooth wall by the rotation and the impacts of the fibres on the wall was proportional to the fibre length [27]. This mechanism characterised in the model by the concentration gradient height (δ in Figure 10) was assumed to occur at the screen plate surface. The model also assumes that fibres only pass the slots as they originate beyond the exit layer and that the velocity Vt is constant at the screen plate surface, i.e. the exit layer height is given by $W\ Vs/Vt = l\ Pe$ (physically, $Pe = H/l$ can be interpreted as the exit layer height relative to fibre length). The model, where m and k are two experimentally determined constants, gives the fibre passage ratio P as a function of the penetration number Pe_t calculated with respect to the rotor velocity Vt instead of the upstream velocity Vu.

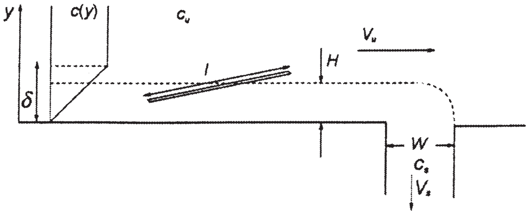

Figure 10 Flow hypothesis and symbols used in the fibre fractionation model [63].

$$P = \frac{Pe_t}{2mk} \quad \text{if } P < 1/2 \qquad\qquad P = 1 - \frac{mk}{2Pe_t} \quad \text{if } P \geq 1/2$$

The predictions of the model were shown to agree reasonably well with the fibre ratio distributions ($P(l) = C_s(l)/C_u(l)$ in Figure 10) experimentally determined with a cross sectional pressure screen and a softwood TMP at 1% consistency. Fibre length is thus the primary characteristic, which determines a fibre's tendency to pass through a slot while flexibility plays a second role according to the fibre motion simulations [57].

Lawryshyn and Kuhn [57] solved both the inertial and inertialess Equations of motion of fibres (using a typical fibre coarseness of 30 mg/100 m) and obtained similar motions, with however a more "lethargic" fibre motion as the inertia was taken into account. The influence of particle inertia is much more pronounced with particles with larger diameter and fluid/particle density difference than the fibres, typically sand particles and bubbles.

High-density particles tend to escape from the vortex at the slot inlet (Figure 11), while low-density particles migrate towards the vortex core, because of the high acceleration in the exit layer around the vortex [64]. CFD simulation showed that the acceleration was in the range of 10^3 to 10^4 m/s^2 depending on the slot and tangential velocities [36]. Such a high acceleration should induce a significant slip of high-density particles, which might lead to

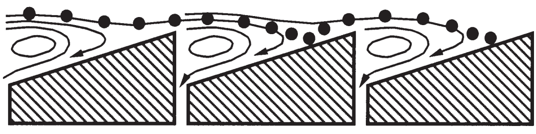

Figure 11 Motion of high-density particles due to acceleration induced particle slip [64].

increased wear of the profiles by sand particles at the impact point. Pictures of worn screen plates reported in [65] seem to confirm this analysis.

Referring to the Equation of particle slip in a vortex (Stokes' law) and to the symbols used in the section about centrifugal cleaning, the slip distance Δr of a small particle of diameter d over a half turn around the vortex at a tangential velocity V is given by:

$$\Delta r = \frac{\pi}{18\mu} d^2 \left(1 - \frac{\rho_s}{\rho_L}\right) V$$

The application of the formula to a mineral particle of 10 μm and a velocity of 3 m/s shows that the slip distance is about 0.1 mm. It is much higher for a fine sand particle of about 100 μm (the particle *Re* becomes too large to apply the Stokes' law).

Julien Saint Amand further investigated the probabilistic approach to characterise the behaviour of the particles and their accumulation at the screen surface [31,66] and suggested that the orientation of long and flat shaped particles should also be examined in the axial direction of the screen basket (screening theory was essentially studied in a 2D cross sectional plane), to address the separation mechanisms in screens [67].

The passage ratio of a given particle type was analysed as the result of the particle passage probabilities in both directions (as in [21]), i.e. during the screening phase and the reverse flow phase, and the mean passage probability during the screening phase was regarded as the result (taking fibre accumulation and slot velocity variation into account) of the instantaneous passing probabilities defined as:

$$Pi = Pc\,Ps$$

where Pc is the instantaneous probability for a particle to be captured in the fluid layer feeding the slot (the exit layer) and Ps is the subsequent instantaneous probability for the particle to pass the slot [66]. It was suggested that the probability Pc should essentially be determined by the flow lines at the surface of the screen plate, namely by the ratio of the radial flow through the slots to the tangential flow above the screen plate profiles

The probability Ps was then assumed to depend mainly on the characteristics of the slot and on the slot velocity and related positive pressure pulse. Hard spherical contaminants may for instance have a high capture probability ($Pc = 1$), especially in the case of neutral buoyancy particles, but no possibility to pass the slots ($Ps = 0$) if larger than the slot width. On the other hand the slot passing probabilities of soft and flat or long shaped contaminants should be high, especially with high positive pressure pulses.

The analysis of the dependence of the passage probability on the slot velocity shows the interest to consider instantaneous passage probabilities since the instantaneous slots velocities (Vs) might vary in a very large range up to about ±15 m/s in the case of rotor producing large positive and negative pressure pulses [31,66], even if the resultant passing velocity (Vp calculated from the accept flow rate and screen open area) is much lower (typically 1 to 2 m/s). This means large variations of the instantaneous normalised slot velocity (Vs/Vt) during the screening phase ($Vt = 15$ m/s is typical for the tangential velocity at the feed surface of the screen cylinder).

The model proposed for the accumulation of fibres on the screen surface during the screening phase was illustrated by an application under simplified hypothesis in order to allow formal calculation:

– The fibre passing probability p and the slot velocity V are assumed to be constant during the screening phase (constant positive pressure pulse), which is a quite realistic assumption for a foil rotor and a relatively high passing velocity.
– The upstream consistency C increases with time t but is assumed to be locally constant over a given height h, which corresponds to the assumption of a local and sufficiently high turbulence to ensure a complete mixing of the fibres in this pulp layer.
– The consistency C_0 at the beginning of the screening phase ($t = 0$) is equal to the local feed consistency Ci, keeping in mind that the initial consistency (C_0) depends in fact on the final consistency reached at the end of the previous positive pressure pulse and on the dilution effect achieved during the negative pressure pulse.

The fibre accumulation dm over a screen plate area A having a total slot area S is established by a material balance in the volume Ah:

$$dm = (SVCi - SVpC)dt = AhdC$$

The integration of the Equation with respect to the variable ($Ci/p - C$) gives for $p \neq 0$:

$$C = \frac{Ci}{p} - \left(\frac{Ci}{p} - C_0\right)\exp - \frac{pSV}{Ah}t$$

If the fibre does not pass the screen plate ($p = 0$), the consistency is:

$$C = C_0 + \frac{SVCi}{Ah}t$$

The amount of fibres accumulated on the screen plate can also be calculated in terms of equivalent grammage $G = h\,(C\text{-}C_0)$ to asses the risk of mat formation at the end of the screening phase. This calculation might be used to evaluate the fibre accumulation on the accept side of the screen plate during the reverse flow phase since the hypothesis of high local turbulent diffusion is not relevant on the accept side. The introduction of the two probabilities *Pc* and *Ps* at the feed side is interesting to distinguish the fibre accumulation phenomena above and between the profiles as reported in [68].

Particle capture probability

The analysis of the particle motions described below was established on the basis of the characteristics of the flow (water without fibres) determined by CDF simulation at the feed side of the screen plate [36]. The motion of fibres has not yet been simulated. The drawings shown in the Figures 12–15 were only proposed to point out the 3D particle orientation mechanisms which might occur as fibres or flat shaped particles approach the screen surface and penetrate the exit layer [33,67].

The numerical simulation showed that the thickness (e) of the exit layer is roughly proportional to the ratio of the slot flow rate to the tangential velocity Vt beyond the boundary layer, i.e. proportional to the ratio $W\,Vs/Vt$. This ratio is included in the penetration number ($W\,Vs/Vt = Pe/l$) if Pe is calculated with Vt.

The fibre fractionation model established for a smooth screen plate [63] might thus be applicable to profiled screen plates, even if some of the hypothesis of the model are questionable in the case of profiled screen plates with suction flow. The concentration gradient in the exit layer should be significantly affected by: the turbulence increase produced by the profiles as noticed in [63]; the flow through the screen which reduces the time to fully develop the concentration gradient; the fact that the profiles strongly modify the fibre wall contacts, which contribute to create the concentration gradient, since fibres can penetrate the exit layer in the profile grooves without any wall contact.

With the simplified hypothesis that the particle capture probability is proportional to portion of the particle area included in the exit layer, i.e. proportional to the thickness (e) of this fluid layer, the capture probability of fibres (length l, mean angle α with the screen surface), would then be given "on average" by the relation of proportionality:

$$Pc \approx \frac{e}{l \sin \alpha} \approx \frac{WVs}{lVt \sin \alpha} \approx Pe$$

This very simplified relation (not based on any rigorous calculation) is consistent with the fractionation model and includes the 3D orientation of the fibres with respect to the plane of the screen plate. The analysis of the fibre orientation in the 2D normal plan only considers the projected fibre length which might be much lower than the real fibre length, as illustrated in the Figures 12 and 13.

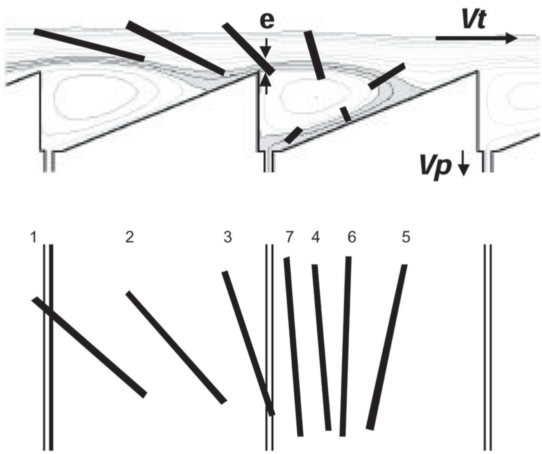

Figure 12 Side view and top view of one possible screening mechanism of rods [67].

The behaviour of individual fibres at the screen plate depends on their initial 3D orientation as illustrated in the Figures 12 and 13, showing the side and top views of possible motions of rigid fibres (rods) in diluted suspension. If the leading end of the fibre penetrates first the exit layer, the flow lines around the vortex tend to turn the fibre and align it with the slot inlet (Figure 12). If the trailing end of the fibre is inside the exit layer while the leading edge is outside, typically a fibre not captured in the previous situation, the flow lines tend to orient the fibre in the plane of the screen plate and parallel to the slot (Figure 13). In both situations the flow lines contribute to improve the capture and slot passing probabilities of the fibres, as they tend

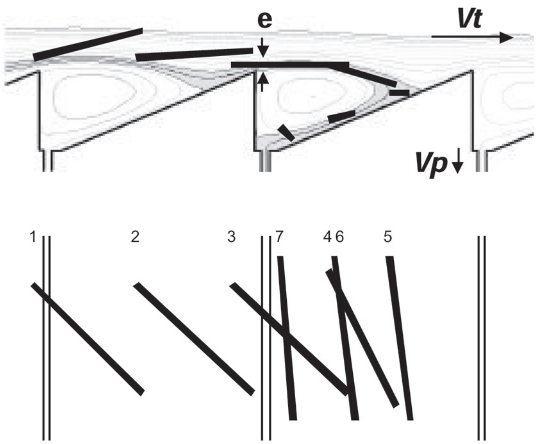

Figure 13 Side view and top view of another possible screening mechanism of rods [67].

to align themselves with the slot. The fibres drawn in the Figures 12 and 13 correspond to long and very stiff fibres of about 2.5 mm length.

The Figures 14 and 15 illustrate possible motions of small and stiff flat shaped particles, i.e. 0.5 mm^2 discs with a diameter (0.8 mm) about 3 times

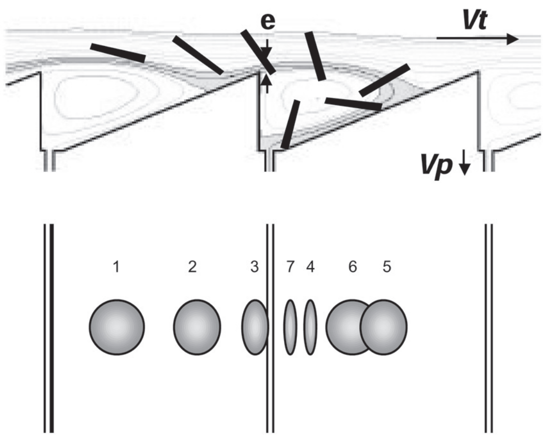

Figure 14 Side view and top view of one possible screening mechanism of discs [67].

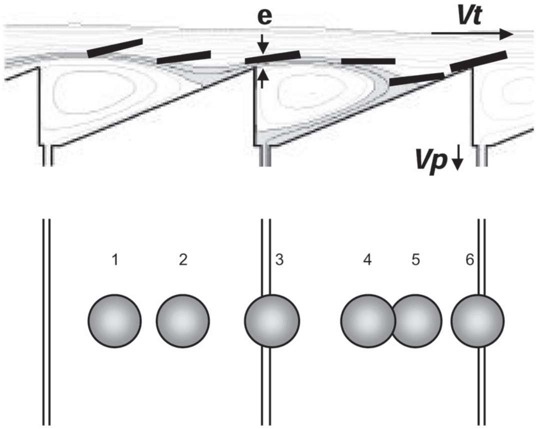

Figure 15 Side view and top view of another possible screening mechanism of discs [67].

lower than the length of the rods shown in the Figures 12 and 13. The size of these discs was chosen to illustrate typical probabilistic contaminants which are difficult to remove in recycled pulps and corresponds to the model contaminants used for the screening tests reported in [31–33]. The flow lines at the feed side of the screen plate should affect the capture probability of discs in a different way compared to rods.

In the case of discs with the leading edge initially located at the surface of the screen plate (Figure 14), the discs tend to turn in such a way to get finally oriented in the plane of the slot. Following the trajectory shown in Figure 14 the disc would then pass the slot with the accept pulp. If the disc in position 6 gets in contact with the inclined wall of the profile, the velocity drop of the trailing end tends to inverse the rotation of the disc and to orient it in the fluid layer along the inclined wall of the profile. The leading end of the disc would then hit the vertical wall of the profile and might be rejected in the upstream vortex flow, instead of passing the slot.

In the case of discs with the trailing edge initially located close to the surface of the screen plate (Figure 15), the discs tend to get oriented parallel to the screen plate surface, as with fibres, but might be rejected from the exit layer, since there is no possibility for a disc to align with the slot in the area of the first stagnation point of this fluid layer.

The particle trajectories described in the Figures 12–15 are extremely simplified. The real situation is much more complicated. Several other aspects should be analysed, such as other initial particle orientations, particle stiffness and particle slip with respect to particle size, density and associated fluid mass. In addition, the micro-flow conditions are unsteady over a relatively short time period with respect to the duration of the mechanisms described, and fibre flocculation at high consistency might completely change these mechanisms. However, the proposed analysis of the 3D particle orientation and capture mechanisms gives new insight in low consistency screening mechanisms.

The mechanisms of fibre alignment with the slot are believed to be decisive regarding the possibility to remove flexible films of much smaller diameter than the fibre length. In addition, the initial orientation of discs with respect to the slot direction (shown parallel in the Figures 14 and 15) should also influence their final orientation in the vortex flow at the slot inlet. If the discs are initially oriented in a plane perpendicular to the slot, their passing probability will be drastically reduced. The orientation of prolate spheroids (to simulate rods) and oblate spheroids (to simulate discs) in shear flows is a very complex issue, as reviewed in [69].

Particle slot passing probability

The mechanisms of fibre passage through the slots, which define *Ps*, depend on the vortex flow at the slot inlet and on the slot width and design. The trajectories of fibres at the slot inlet have been studied rigorously by visualisation and recently by numerical flow simulation. The drawings below were proposed to explain the experimental results about the influence of screen plate design, which were obtained with particular milled screen plates and typical wedge wire screen plates [33].

The drawings in the Figures 12–14 show that the probability to pass the slot should be lower with discs than with fibres, for a given stiffness, since the fibres tend to get aligned with the slot direction, while the discs only tend to get oriented in the plane of the slots. A large portion of the discs in the area of the slot inlet might be located in the upward vortex flow, since the whole diameter is concerned with discs while only the project length is concerned with rods, as shown by the side view pictures.

The drawings in the Figures 16 and 17 illustrate rigid fibres and flat shaped contaminants (Figure 16) and “soft contaminants” such as stickies, fibres bundles or flocs (Figure 17) as they enter the slot, in the case of the tested milled and wedge wire screen plates [33]. The design of the slots should influence the slot passing probabilities of fibres and probabilistic contaminants since both the particle passing mechanisms (wall contacts) and the flow

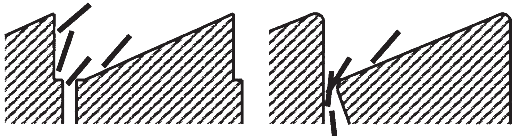

Figure 16 Possible slot passing mechanisms with milled (left) and wedge wire slots (right) in the case of rigid films or fibres [70].

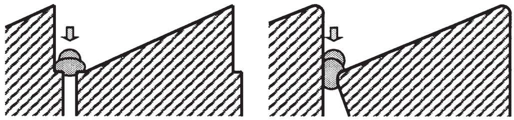

Figure 17 Possible slot passing mechanisms with milled (left) and wedge wire slots (right) in the case of soft particles [70].

conditions are changed. The location of the slots in the grooves might also influence the slot passing probabilities.

Thin particles are assumed to enter more easily the slots in the case of a convergent inlet section and as the slot is aligned with the "vertical" profile wall, since the wall contacts should be reduced. Soft particles of larger diameter than the slots (spherical particles or cylindrical particles along the slot inlet) should also enter more easily the slots under the same conditions, as they are pushed through the slots by the pressure distribution at the slot inlet. The normal stress exerted on the particle at the slot inlet depends on the flow velocity around the particle, i.e. on the slot velocity induced by the positive pressure during the screening phase, in the case of round shaped particles. It is higher and roughly given by the positive pressure in the case of long shaped particles along the slot inlet.

The experimental results showing that the wedge wire design improved the passage of fibres and flat shaped contaminants through the screen plate [33] were explained by:

– the higher particle capture probability as a result of the higher effective passing velocity due to the lower pressure drop coefficient given by the convergent inlet and divergent outlet;
– and subsequently by the higher particle passing probability through the slot as a result of the rounded edge at the slot inlet and of the higher effective passing velocity, compared to milled or laser cut slots.

Increasing the viscosity of the suspending liquid should promote the particle passing probability as a result of the higher fluid drag and improved slippage between the particle and the solid wall, as demonstrated in a recent paper reporting a large increase of the fibre passage ratios as the viscosity was increased by adding CMC [71]. However, under usual mill conditions the viscosity of the suspending liquid does not change strongly with temperature or dissolved matter content and should consequently not affect significantly the screening process as far as the particle properties are not modified.

Behaviour of "stickies"

The specific behaviour of PSA stickies in recycling lines has been extensively discussed in several papers reporting mill experience [72] or dealing with the optimisation of screens [48,73,74] or with the development of new recycling friendly adhesives for the paper industry. Deformation and disintegration phenomena of stickies observed in pressure screens have been reported with PSA under so called "aggressive" screening conditions compared to "gentle" screening conditions [48,73,74].

The behaviour of stickies is basically not different from the behaviour of other types of contaminants, as far as particle size, shape, density and flexibility are concerned, keeping in mind that particle flexibility is a function of particle size and shape and of the elastic modulus of the material. The specific behaviour of PSA is due to the fact that we are dealing with visco-elastic polymers.

The deformation and fracture of visco-elastic PSA in screens are generally associated to "aggressive" screening conditions [73] typically used in the high consistency range and to the high shear rates required for pulp "fluidisation" [48,74]. High consistency screens, which are operated at high rotor velocity to produce the required shear rates, generally produce higher pressure pulses than low consistency screens. On the other hand, pilot screening tests performed in large consistency and rotor velocity ranges showed no significant fragmentation or deformation of the tested adhesive particles, a mixture of relatively small (less than about 5 mm length) acrylic and rubber based PSA particles, even after several passes in the screen [70].

At low consistency, some of the hydrodynamics forces exerted on stickies in pressure screens can be evaluated more easily [67]. The shear flow produced by the rotor at the surface of the screen plate causes the particles to rotate (Figure 18) at a mean velocity which depends on the particle size and shape and on the shear rate [69]. The rotation of a particle on its own axis produces accelerations on the outer parts of the particle. Typically with a long shaped

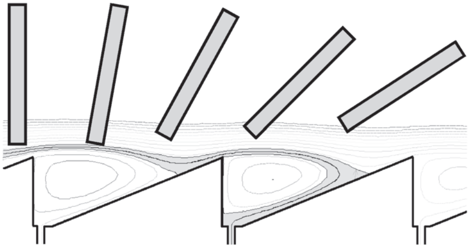

Figure 18 Shear induced rotation of long shaped particles close to the screen plate [67].

particle, the opposite accelerations at the ends produce tensile stresses concentrated in the middle of the particle.

The analysis of the flow conditions in pressure screens shows that the shear induced acceleration should be relatively low (in the order of magnitude of 10^2 m.s^{-2} for rods of about 5 mm length and a mean shear rate in the order of magnitude of 10^3 s^{-1} in the logarithmic law area of the turbulent boundary layer in Figure 8) if the particles are not in contact with the screen plate or with the rotor [67]. As the particle comes closer to the screen plate (Figure 19) and one end touches the profiles as it is captured in the fluid layer which feeds the slot, the velocity drop imparted to the other end induces a deceleration up to one order of magnitude higher, in the range of 10^3 m.s^{-2}.

This level of shear and contact induced acceleration in pressure screens produces stresses in the order of magnitude (10^{-2} N/mm^2) of the tensile strengths of very soft particles such as acrylic adhesives after soaking [48,74], but only with long shaped and relatively large particles of several mm length. Shear and contact induced acceleration in screens might thus only lead to the fragmentation of very soft and relatively large stickies such as some "soaked" stickies at high process temperature. This analysis is limited to low consistency screens. Additional stresses due to complex interactions between the stickies and the fibres and fibre flocs at higher screening consistency might be responsible for the reported stickies fragmentation phenomena. A long shaped adhesive particle might for instance be submitted to high tensile stresses, as it is included in a fibre floc disrupted under the high shear stresses in high consistency screens.

The other important issue to investigate in pressure screening is the extrusion of stickies through the slots. Other types of stresses are involved as the particles reach the slot inlet. As already discussed a long shaped adhesive

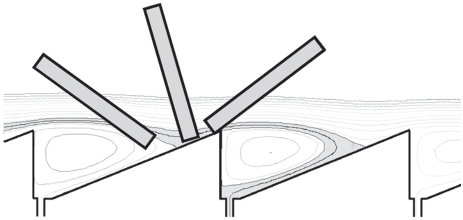

Figure 19 Shear and wall contact induced particle rotation closer to the screen plate [67].

particle of higher thickness than the slot width tends to blind the slot inlet as it is oriented by the vortex flow in the slot direction. The maximum normal stress exerted on the particle is then given by the positive pressure pulse, which is in the same range of the stresses discussed before (> 10^{-2} N/mm^2).

An important aspect to deal with in the case of adhesive materials is visco-elasticity, which means that the deformation of an adhesive particle is strongly time dependent. The characteristic time of the elongation process of the adhesive particle, which is given by the elastic modulus to viscosity ratio (E/μ), might fall in the order of magnitude of the duration of the screening phase, especially at high screening temperature. The extrusion of such stickies would then be limited by the fact that the time required for the particle deformation is higher than the duration of the positive pressure pulse.

ANALYSIS OF THE EFFECT OF BASIC SCREENING PARAMETERS

The performance of a single screen as a function of screening parameters is generally represented in terms of removal of coarse components (contraries or coarse fibres) from the accept pulp versus reject rate. Typically, the practical results reported in several papers deal with the removal of various types of heterogeneous particles, shives in high yield pulps or contraries and stickies in recycled pulps [4–19,35,41,48,64,65,75–78]. The analysis of the reported results is difficult as the efficiencies depend strongly on the characteristics of the contraries. Particles size distributions can be assessed, but none of the various methods available for the measurement of contaminants in mills provides any valuable information about particle shape, a key parameters in the screening process. Methods exist to evaluate stickies in recycled pulps, but should be improved to enable counting more particles [79]. The laboratory screening method is questionable for the evaluation of screening efficiencies in mills, and it cannot be used to evaluate the ability of contraries to be removed by screening under industrial conditions [80]. Practically, it is fairly difficult to establish statistically sound contaminant measurements in mills, even when counting several hundred particles, since the contaminants are heterogeneous and one should consider the particle counts in several classes of homogeneous contaminants.

The analysis of screening performance in terms of particle passage ratios gives a better insight in the screening process. Therefore, tests were performed with homogeneous contaminants of relevant size and shape and with an experimental equipment simulating a slice of industrial sized screens to assess the effect of screening parameters [31–33,50]. The experimental data reported were the fibre or pulp passage ratios, which controlled reject thickening and screening capacity, and the accept pulp cleanliness as a function of the pulp passage ratio, which illustrated the screening selectivity and further the final system efficiency with respect to fibre losses. The main results obtained in this study with 0.10 to 0.25 mm slots and different virgin and recycled pulps containing shives or flat shaped model contaminants (0.5 mm^2 films) are summarised below with reference to other studies, field experience and theoretical background.

Machine and Operating Parameters

With the probabilistic contaminants used in the study, i.e. flat or long shaped particles with lower thickness than the slot width, the efficiency results were particularly sensitive to the hydrodynamic screening conditions. Increasing slot width or passing velocity improved the pulp passage ratio, reduced the cleanliness efficiency at constant reject flow rate and did not significantly affect the screening selectivity. In other words, the parameters which improved the passage of the fibres unfortunately increased the passage of probabilistic contaminants through the slots.

The influence of the passing velocity showed to depend on the rotor velocity and design. Compared to the foil rotor with short reverse pulse, the blade rotor with long reverse pulse (see Figure 5) increased the pulp passage ratio, reduced the accept pulp cleanliness and did not significantly improve the screening selectivity. These results and the lower influence of the passing velocity always observed with the blade rotor were attributed to the high effective passing velocity produced with this rotor during the screening phase. The influence of the passing velocity showed also to be lower as the velocity of the rotor was increased, for the same reason since the higher pressure pulse produced at higher rotor velocity increases the effective passing velocity

[50,70]. The influence of passing velocity has been much debated. Contradictory results reported previously about the effect of the passing velocity with stickies and others contaminants [75–77] might have been due to the fact that different rotor velocities and designs were used, as well as different mixtures of barrier and probabilistic contaminants.

The velocity of the rotor strongly affected the screening capacity as expected, but showed on average no large influence on the fibre and contaminant passage ratios [50]. This was attributed to the fact that the normalised slot velocity does not depend on the rotor velocity under the following hypothesis: The mean tangential velocity is roughly proportional to the rotor velocity, the mean positive pressure pulse is proportional to the square of the rotor velocity, the effective passing velocity is roughly proportional to the square root of the pressure drop across the screen plate during the screening phase, and the mean pressure drop is roughly equal to mean positive pressure pulse. Pilot screening tests with high yield pulps showed by contrast a more or less pronounced increase of the pulp passage ratio [81–83] and a decrease of the fractionation selectivity (removal of the R14 fraction) as the velocity of the rotor was increased [81,82].

Concerning the influence of screen plate design, milled and wedge wire screen plates of the type shown in the Figures 16 and 17 and with a profile height of 1.2 mm were tested. Compared to the milled screen plates at given slot width, the wedge wire screen plates improved strongly the pulp passage ratio and reduced the cleanliness in the accept pulp. Again, the selectivity was not significantly improved since the passage ratios of both the fibres and the probabilistic contaminants used in the tests were increased, for the reasons previously discussed. The 0.12 mm wedge wire slots gave about the same results than the 0.15 mm milled slots at the same passing velocity, and at the same screen basket size since both cylinders had the same open area (80% open length with the milled slots compared to 100% with the wedge wire slots). Pilot screening tests reported recently showed however a higher screening selectivity regarding the removal of TMP shives, with a milled cylinder compared to a wedge wire cylinder [84].

Profile height is known to have a great impact on the pulp passage ratio (contoured screen plates have replaced smooth surface screen plates because of their higher production). The optimum profile height seems to be about half the fibre length as far as fibre passage is concerned. A reduction of the profile height down to 0.6 mm [33,68] or 0.3 mm [82] reduced the fibre passage ratio, but showed to improve the shives removal and fractionation selectivity with high yield pulps [33,82]. The better selectivity reported at reduced profile height might be explained by an increase of the wall contacts leading to a decrease of the particle capture probability, which should be higher with stiff particles (shives or films) compared to flexible fibres. Slot location is known to influence the fibre passage ratio [54]. Profile design was recently shown to influence the screening capacity at equal slot width and passage ratio. The lower capacity observed with the profiles having the lower volume between the profiles was believed to be due to the lower accumulation capacity (higher local consistency increase during the screening phase) in this volume of the fibres caught in the exit layer and retained by the slots [68].

The general pressure screen design (Figure 2) and the screening system design define the pulp transport and mixing conditions along the feed side of the screen plates used in the system. The macro-flow conditions along the screen cylinder and the de-flocculation state of the pulp suspension [10,13,41–48,55,83,85] might strongly influence the screening performance, especially if the screen is not properly designed. The differences observed between the slice screen and full size screens regarding the effect of rotor velocity are interesting to analyse in this respect. The low effect of rotor velocity observed with the slice screen corresponds to stabilised macro-flow conditions and pulp de-flocculation since the slotted section (100 mm width or less and 500 mm diameter) is placed between two profiled cylinder sections of the same width [50]. If the rotor velocity is increased in full size screens, the macro-flow conditions might for instance change from plug-flow type to mixed-flow type, as shown in Figure 3, and thus increase reject thickening and the passage ratio evaluated with a given model. Increasing rotor velocity is also assumed to create a more homogeneous slot velocity distribution in the screen because of the higher pulp rotation speed, which might improve efficiency.

The control of the pulp de-flocculation state is important in high consistency screening. Pulp might for instance be initially flocculated in the feed section of the screen cylinder, then de-flocculated by the rotor and finally re-flocculate as the consistency increases in the reject section. In addition, the heterogeneity along the screen cylinder of the particle separation conditions in terms of pulp flocculation might be increased by the fact that the pressure pulse depends on the rotor and pulp velocities. Typically, the pressure pulse is higher in the inlet section and lower in the outlet section as the pulp has been entrained by the rotor. Under these conditions, it is clear that the effect of rotor velocity on screening performance is very complex. The screening capacity is clearly increased at high rotor velocities but other means have been developed by the equipment suppliers, including special rotor designs to optimise pulp transport, pulp fluidisation and feed conditions onto the screen cylinder, optimised cylinder height and static de-flocculation devices and/or internal dilution means.

Screening installations typically include 3 stages of pressure screens in cascade or feed forward systems with screens in series in secondary stages in some cases. Multistage feed forward assemblies of up to 3 screening stages in one single machine have been developed recently to simplify the screening systems [85,86]. The optimisation of multistage screening systems has been extensively discussed in [87] on the basis of a simulation program. The feed forward systems showed to be more economical and more efficient if the degree of debris reduction in the screens is high, while cascade systems achieved higher efficiency with low contaminant size reduction. Simulation on the basis of fibre and contaminant passage ratio distributions is believed to be a powerful tool for the optimisation screening systems [88].

Material Parameters

Fibre length distribution and fibre consistency are the main parameters which define the type of screening technology and the fine screening limits, in mill applications. The influence of the consistency on the screening process (pulp passage ratio and efficiency) showed to be low, up to 2 or 3% depending on the fibre length, with the slice screen as long as the pulp was assumed to be well de-flocculated [31–33]. The influence of the consistency might be higher in industrial screens for the reasons already discussed.

Long fibres are known to concentrate in the rejects and thus to cause pulp fractionation. The effect of fibre length on the passage ratio was shown to be much higher than fibre stiffness in several studies including [25–28,32,57]. The relation between the passage ratio P and the fibre length l was approximated by a negative exponential function:

$$P = \exp - (l/\lambda)^{\beta}$$

where λ was experimentally shown to increase approximately linearly with the aperture diameter with $\beta = 1$ in the case of pilot plant fractionation with holes, while the best fit value was given by $\beta = 0.5$ in the case of fractionation with slots [89]. The theoretical flow models can then be used to help the optimisation of fractionation systems [90].

Fibre coarseness is linked to fibre flexibility and was shown to have a higher influence than flexibility on the fibre passage ratio, with high-yield pulps, since thick fibres, fibres bundles or fibres with split ends can be retained by barrier with fine slots [32,35].

The size and shape distribution of the contaminants is practically the most important parameter, which defines the removal ability of given contraries as well as the global efficiency of screening systems, for a given contaminant control method. In the case of thin particles the relevant parameter is the stiffness of the particle as far as its thickness is significantly lower than the slot width. With particles larger in a least one dimension than the slot width, the viscoelastic properties of the particles have also to be considered, as discussed in the section about stickies. The lack of methods to measure correctly the size and shape distribution of any kind of contaminants is a major difficulty as screening efficiency has to be evaluated under mill conditions with real contaminants. Depending on the type of adhesive and pulping conditions, PSA particles might be rather flat, long or round shaped, and become more spherical after kneading [91].

Particle density should also influence the separation process because of particle slip (Figure 11) in the case of particle such sand. The results reported about comparative pilot tests of centrifugal and centripetal screens performed with sand particles [78] indicate that particle slip due to the high acceleration in the micro-flow at the slot inlet had more influence on the removal of sand than particle slip induced by the rotation of the pulp. The situation should be different in the case of a rotating screen basket [9] since the pulp velocity is higher at the screen cylinder surface. The slip conditions, which promote the removal of high-density particles normally, reduce the removal low-density particles, but practically the effect should be limited since most of the low-density contaminants are close to neutral buoyancy.

Screening temperature should affect the removal of adhesives, which become softer at increased temperature, while the viscosity variations should have a limited effect.

To summarise about the effects of hydrodynamic parameters it seems that the published models agree quite well with the experience. The ratio of the effective slot flow rate during the screening phase to the surface flow velocity at the feed side of the screen plate appears to be a key parameter in the probabilistic screening process.

This ratio governs the capture probabilities of particles in the fluid layer to the slot inlet. The possibilities to increase this ratio and consequently the probability for fibres, and unfortunately thin probabilistic contaminants, to be captured in the exit layer, include:

– increasing slot width, which is detrimental to the “barrier” screening efficiency;
– increasing the effective passing velocity, which is observed at high positive pressure pulses produced at high rotor velocity and with extended reverse pulse rotors;
– decreasing the surface flow velocity, by static means or by special feed conditions;

– decreasing the friction factor through the slots, which increases the effective passing velocity, typically with wedge wire screen plate designs compared to milled slots.

The subsequent probability for the particles to pass the slots should then be increase by:

– the increase of the slot width and the increase of the effective passing velocity by various means such as by the reduction of the slot friction factor, as for the increase of the capture probability;
– the use of convergent slot inlet designs, and the proper location of the slot, which is typically obtained with the rounded edges of wedge wire screen plates.

The challenge with respect to the primary objective of screening, i.e. high contaminant removal efficiencies with low fibre losses, is then to increase the screening selectivity, which means to avoid the increase of the passing probabilities of the contaminants as the screening conditions are changed to increase the fibre passing probabilities.

The solution is obviously to reduce the slot width in the case of hard round shaped contaminants, but the problem is much more difficult to solve with thin probabilistic contaminants, and with particularly soft particles, since most of the criteria improving the passage of the fibres should also improve the passage of the contaminants. Further progress is however expected in screening technology such as screen plate design to improve the selectivity of the screening process.

In high consistency screening, the strong interactions between the fibres and with the contaminants suggest that models describing the motion of single fibres should not be valid, though low consistency and high consistency screens show similar influence of the screening parameters.

CLEANING

Centrifugal cleaning refers to the separation of fibres and contaminants in a centrifugal or vortex flow field. Such a separation is produced in hydrocyclones, known as cleaners in the pulp and paper industry, and in various rotating equipment including centrifuges. Cleaners are used in multistage systems to remove high-density and/or low-density contaminants and to fractionate pulp in some applications including high yield pulps.

The hydrocyclone was invented in 1891 and was first used in the paper industry in 1906. However, it was not commonly used until the 1950's.

Hydrocyclones have been the subject of countless papers published in the field of paper and mining industries. The applications of hydrocyclones in the mining industry were the first to be developed on a large scale. Most of the fundamental research on hydrocyclones has been devoted to ore grinding and other applications such as hydrocyclones for oil and water separation, and gas cyclones for the separation of solids, liquids and gas mixture.

CLEANING TECHNOLOGY

The conventional cleaner operates on the following principle: A swirling motion is created by the tangential inlet flow. As the stock accelerates along a helical path down the conical section of the cleaner, a substantial portion of the feed flow reverses its axial direction and swirls into a tighter inner spiral back up toward the vortex finder at the top of the cleaner. The vortex motion creates centrifugal forces which cause the particles having higher density than the stock to migrate to the outside of the cleaner, while particles having a lower density than the stock migrate toward the vortex core.

Detailed reviews of cleaning technology can be found in several papers including [1].

High-Density Cleaning

High-density or "forward cleaners" are used to remove high-density contaminants. Coarse cleaning is performed at high consistency to remove heavy particles such as sand and metals and protect downstream equipment. Large cleaners (head diameter > 200 mm) are generally used in one stage. The current trends in recycling are to add a secondary stage and/or to reduce the consistency, in order to improve the removal of fine sand to reduce the wear of the screen cylinders in the fine screening step.

Fine cleaning is generally performed at low consistency (about 1%) with small and medium size cleaners (60 to 200 mm head diameter) in multistage cascade systems. It is used to remove fine sand, shives, bark and various high-density polymeric contaminants in recycled pulps such as large ink particles, PVC and some adhesives. High-density cleaners are typically operated at 100 to 200 kPa pressure drop. The tangential feed velocity is normally between 5 and 10 m/s and the acceleration in the range of 10^3 m/s^2 (100 times the gravity acceleration g) and more in the vortex core.

The particular designs developed to improve cleaner performance include helical inlet, divergent accept outlet to recover the kinetic energy of the vortex core [2,3] and various reject outlets to improve the extraction of the contaminant [4–7]. The advantages of stepped or spiral cones (reduction of reject thickening) over smooth cones (unaltered vortex flow) are still debated. Very small cleaners can be equipped with a common reject outlet to increase the outlet size and avoid plugging [6,7].

Low-Density Cleaning

Low-density or "reverse cleaning" is performed in the low consistency range to remove low-density contaminants such as polyethylene, hot-melt glues and some other stickies, as well as air bubbles and associated matter. Various types of low-density cleaners have been developed (Figure 20) since the first commercial application (1969) of a three-stage reverse cleaning system in a deinking unit [8]. Reverse cleaners are normally operated at lower consistency than forward cleaners to improve the efficiency.

The combination cleaner or "core bleed cleaner" is a conventional high density cleaner equipped with an additional low-density contaminant outlet in the vortex core. This version is normally operated at a higher feed pressure and provides additional removal of air and low-density contaminants, with low additional equipment costs. However, the efficiency is limited because low-density contaminants have to cross the accept streamlines to be removed in the air core. Under these conditions, the time available for low-density contaminant cleaning in the upward accept flow is extremely short. The low density contaminant removal efficiency of combination cleaners can be increased by extending the length of the accept outlet to increase the residence time in the vortex core, or by adding a second low density outlet in the reject tip at the opposite side [9].

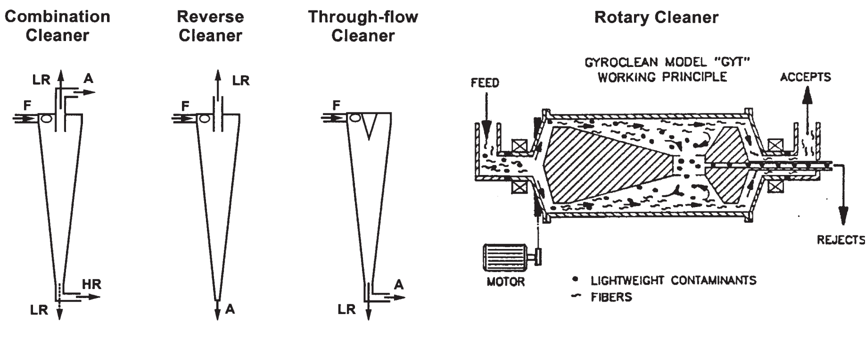

Figure 20 Working principle of the different types of low density cleaners F: feed, A: accepts, HR/LR: high/low density rejects.

The reverse cleaner is basically a conventional forward cleaner with reversed functions. The heavy fraction flow rate is increased (increased outlet diameter) to become accepts and the light fraction is reduced (smaller outlet diameter) to become rejects. Small size and some medium size reverse cleaners are available on the market [8,10,11]. The high reject flow rates of reverse cleaners (30 to 50%) requires 3 to 4 cleaning stages.

Through-flow cleaners are modified reverse cleaners, i.e. cleaners with reversed function characterised by a much lower reject flow rate (about 10%) obtained by the reversed "through-flow" pattern created inside the cleaner instead of reverse flow pattern [12]. Various small size and some medium size through-flow type cleaners are available on the market [10–13] as well as a cylindrical version [14] and a large diameter conical version equipped with a rotating inlet head [1].

Conventional and through-flow reverse cleaners can be associated in reverse cleaning systems to optimise the efficiency, energy and reject rates [11]. Combined high density and low density cleaning systems have been reported [14].

The rotary cleaner was basically developed at EFPG on the laboratory scale [15,16], constructed and tested at CTP on the pilot scale [17] and developed on the industrial scale with E&M Lamort in the early 1980's [17–19]. The current version, with a rotating drum diameter of 750 mm and a rotation velocity of 1250 rpm has much higher capacity than the first version with a rotating drum diameter of 500 mm.

The working principle involves a rotating cylinder where stock is introduced and accelerated by the rotating inlet head acting as a pump. The maximum pulp tangential velocity is somewhat higher than the velocity of the cylinder (typically + 5 m/s) in order to optimise the turbulence level, a function of the pulp velocity with respect to the wall. The accepts are collected at the opposite end by a second rotating head which also recovers the main part of the kinetic energy imparted by the inlet head. Low-density contaminants are extracted in the vortex core. The Gyroclean utilises high centripetal acceleration (about 700 g due to the high velocity > 50 m/s) and increased retention time (a few seconds) to achieve high efficiencies, which can be obtained at consistencies as high as 2% and reject rates as low as 0.1% by weight in one single stage.

CENTRIFUGAL CLEANING MECHANISMS AND THEORY

The flow in hydrocyclones has been the subject of intensive research for many years. The work of Kelsall [20], Bradley [21], Rietema [22] and others has established a good general understanding of the basic flow phenomena and particle trajectories in a hydrocyclone. Numerous models have been proposed to simulate the flow configuration and the separation process in hydrocyclones. All these models, generally based on the Stokes' law, were combinations of empirical and theoretical analysis [21] and thus required some experiments for accurate cleaner characterisation.

Progress achieved during the last decade in flow modelling techniques and theory of turbulence has opened new possibilities for the modelling of centrifugal separation. Improved models were developed to calculate the flow patterns using a modified k-ε turbulence model (where k is the turbulent kinetic energy and ε its dissipation rate). Particle motion was then described by iterative computation of slip velocities using drag coefficients as a function of particle slip Reynolds number and assuming no large influence of particle motion on the liquid phase velocities [23,24]. The k-ε model, which is valid for isotropic turbulence, has been recently compared to the Reynolds stress model to describe the flow structure in a cleaner [25]. Contrary to the k-ε model, the Reynolds stress model showed good correlation with the tangential velocity profiles predicted by the theory (Figure 2), since turbulence is not isotropic in a vortex flow. The simulated particle tracks showed also quite good agreement with measured efficiency.

Vortex Flow Field

The first step in the analysis of centrifugal separation is, as for the screening process, to define correctly the macro-flow conditions in the vortex, which ensure the transport of the suspended particles. The flow field in the hydrocyclone has been described in numerous publications based on experimental data and/or on numerical flow simulation. The flow patterns and the velocity component profiles in the three coordinates shown in the Figure 21 were postulated on the basis of order of magnitude analysis [26] and experimental measurements [21].

Basically, the convergent structure of the mean flow pattern in a hydrocyclone allows the high tangential velocities, and thus the high acceleration, to be maintained as the wall and internal friction losses are compensated by the tendency to increase these velocities, i.e. to keep constant the kinetic momentum of the rotating fluid. The theoretical free vortex law is given by $V_T = k/r$ for non-viscous irrotational flow.

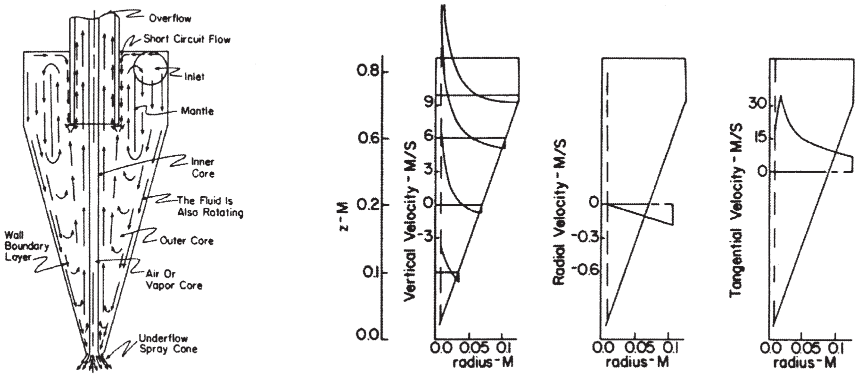

Figure 21 Descriptive flow patterns in a hydrocyclone and postulated velocity profiles [26].

The Equation below, which is obtained by integration of the axial component of the Reynolds Equations (the Navier-Stokes Equations in cylindrical coordinates) can be used to approximate the tangential velocity variations of the flow along the axis of cylindrical or slightly conical static or rotating cleaner walls [16]:

$$\frac{\partial}{\partial x}\left[\int_{0}^{R_0(x)} 2\pi \rho_L r^2 V_X V_T dr\right] dx = 2\pi R_0^{\,2} \tau_{T0}\, dx$$

where V_X and V_T are the axial and tangential velocity components, R_0 and τ_{T0} the radius and the tangential stress at the wall and ρ_L the liquid density.

In the downstream flow of the hydrocyclone, the velocity increases as the stock follows a helical path towards the small diameter end of the cone. The tangential velocity profile which is characteristic of the free vortex flow given by:

$$V_T = k/r^n \qquad \text{where } 0.5 < n < 0.9$$

has been determined experimentally. Consequently the centripetal acceleration:

$$\gamma = V_T^{\,2}/\, r = \omega^2 r \approx dP/\rho_L\, dr$$

becomes very high when the radius decreases as shown in Figure 21. Typically, the centripetal acceleration in a small cleaner increases from about 100 g in the upper part of the downstream flow to about 1000 g and more in the upstream flow of the vortex core.

Toward the tip of the cleaner, the pulp flows upward in a quick forced vortex motion. Due to the very high rotation, an air core can be observed. The maximum centripetal acceleration γ and radial pressure drop dP/dr are reached in the upward accept flow. There is an intermediate tangential velocity profile in the area between the downward "free vortex" flow and the upward "solid body rotation" flow ($V_T = k\ r$).

The short circuit flow observed on the top wall of the cleaner (Figure 21) is due to the Ekman boundary layer effect. Some heavy particles may be entrained and carried to the accept outlet. Equipment suppliers have provided several cleaner head designs to reduce short circuit flow that could otherwise reduce efficiency. They include rectangular inlet, helical roof, two tangential openings and vortex finder designs. Increasing the length of the vortex finder reduces the short circuit, but also reduces the time available for the particle separation in the upward vortex flow. An optimum length therefore exists, dependent upon cleaner design and type of particles to be separated [21].

The axial velocity profile in the upward vortex core is strongly influenced by the design of the cleaner outlets and by other characteristics such as the cone angle. The axial velocity profile defines the separation area between the accept and the reject streams and consequently influences the cleaning efficiency and reject rate. CDF flow simulation has become a powerful tool for the optimisation of cleaner design in this respect.

Particle Separation

The mechanisms, or micro-processes, involved in the separation of particles suspended in a vortex flow field are basically the same as those involved in natural particle settling and flotation, except that the separation forces are amplified by the factor $G = \gamma/g$. Particles with higher density than the fluid are migrating in the centrifugal direction while particles of lower density are migrating toward the vortex core.

The main forces acting on these particles are the centrifugal force, the buoyancy force, the drag force and the lift force, the latter being neglected in the Stokes' Equation, which gives the radial particle slip velocity with respect to the fluid. In the Equations below the drag force is given for small spherical particles (diameter d, density ρ_S) assuming creeping flow around the sphere.

Centrifugal force	$F_C = (\pi\ d^3/6)\ \rho_S \gamma$
Buoyancy force	$F_B = (\pi\ d^3/6)\ \rho_L \gamma$
Drag force	$F_D = 3\pi\ \mu\ d\ U$

The balance of the forces on the particle ($F_D = |F_C - F_B|$) gives the particle slip velocity, which corresponds to the Stokes' law in a centrifugal flow field:

$$U = \frac{d^2}{18\mu}(\rho_S - \rho_L)\gamma$$

The centrifugal force on a particle results from the rotary motion of the particle, which is assumed to rotate at the same mean velocity as the surrounding fluid in the Equations. This assumption is not rigorous for relatively large particles as they move in the radial direction and their tangential velocity is no more equal to the tangential fluid velocity.

A buoyancy force results when a solid body is submerged in a stationary fluid with a linear pressure distribution. There also is an imbalance of the surface forces on a particle that is carried in the fluid flow in a hydrocyclone, which has a non-linear pressure gradient in the radial direction. The buoyancy force for a spherical particle may be approximated by assuming that the pressure gradient on the flow field, in this instance, the buoyancy force in the radial direction, is dependent on the radial position and the swirl velocity components.

The drag force has mainly to be considered in the radial direction, since the gravity force is insignificant with respect to the centrifugal force, and it can be assumed, in a first approximation, that the particles follow the fluid in the tangential direction. The drag force is a function of the radial slip velocity U and of the drag coefficient C_D, which depends on the particle size, shape and orientation with respect to the direction of the slip velocity.

The drag coefficient of a particle of cross section A is experimentally determined [27] as a function of the particle Reynolds number ($\mathrm{Re}_p = \rho_L\ U\ d/\mu$) defined for the flow around the particle. The general expression of the particle slip velocity becomes:

$$U^2 = \frac{4}{3}\frac{d}{C_D}\frac{(\rho_S - \rho_L)}{\rho_L}\gamma \qquad \text{with} \quad C_D = \frac{F_D}{1/2\rho_L A U^2}$$

The Stokes' law (which corresponds to $C_D = 24/\mathrm{Re}_p$) is valid for particle Reynolds numbers up to about 1. The slip velocity is then overestimated for intermediate particle flow regimes. The turbulent flow ($0.47 < C_D < 0.43$ for

$10^3 < Re_p < 10^5$ with spheres) is not relevant with respect to particle sizes and slip velocities in cleaners.

The slip velocities of fibres in a centrifugal field can be assessed in the case of transversal flow (fibre perpendicular to the radial direction) by using drag coefficient formulae of cylinders such as the Lamb formula indicated below [28] or the different formulae of White [29] cited in [30] and [31].

$$C_D = \frac{8\pi}{\mathrm{Re}_p(2 - \log \mathrm{Re}_p)}$$

Theoretically, the slip velocity of a fibres assimilated to a cylinder depends on the fibre density (mean wet density including the water in the lumen) and specific surface, which are linked to the fibre coarseness [30] and not on the fibre length and stiffness, contrary to the lift force which depends on the fibre length and stiffness.

The lift force is a transverse force generated by the modifications of the pressure distribution created around a particle by the shear flow and by the particle rotation, which is generally induced by the shear. The Cameron force due to the shear flow is directed away from the wall, while the direction of the Magnus force, due to the rotation of a particle moving in a steady fluid, depends on the rotation velocity of the particle with respect to the direction of the slip velocity and to the related particle Reynolds number [27]. Just as the Magnus force on a spinning ball moving through a fluid will result in a curved trajectory, the transverse lift force on a particle that is carried in the flow field of the hydrocyclone has an effect on its trajectory.

Predicting the lift force is very complex. It is greater for larger particles, such as shives. Therefore, the effect of the lift force can be an important factor in hydrocyclone design when shive removal is a key objective. The lift force is generally directed inward when the particle lags behind the fluid motion, which is the case for solid particles that move from regions of lower velocity to regions of higher velocity. A model of the lift force, based on a combination of empirical and theoretical analysis, has been reported [3].

The particle separation mechanisms are much more difficult to predict with flat of long shaped particles than with round shaped particles with known drag coefficient. Basically, the Stokes' law indicates the slip direction, the strong separation efficiency decrease as particle size is decreased in the microscopic size range, the fact that neutral buoyancy particles should normally not be removed by pure centrifugal separation and the impact of the acceleration and of the cleaning temperature.

Turbulence plays a major role in the centrifugal separation process [32]. Small particles with low migration velocity are continuously re-mixed by the

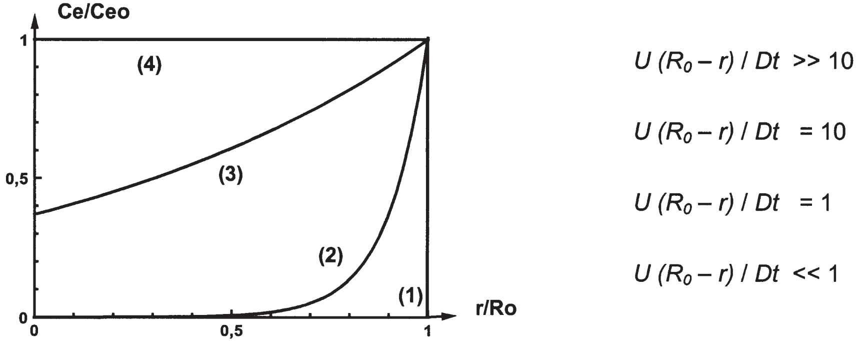

Figure 22 Effect of turbulent diffusion on radial consistency distribution at equilibrium [16].

turbulent diffusion while heavy particles which have reached the wall are not carried back by the turbulence. Figure 22 shows the theoretical consistency distributions of high density particles at equilibrium, i.e. by neglecting the effect of the initial conditions and under a constant centripetal acceleration, which were calculated by the Equation [16,32]:

$$\frac{Ce}{Ce_0} = \exp - \frac{U(R_0 - r)}{Dt}$$

where Ce and Ce_0 are the equilibrium consistencies at the radius r and R_0 (cleaner wall) U is the particle slip velocity and Dt particle turbulent diffusion coefficient, which can be assimilated to the turbulent diffusion coefficient of the fluid for small particles.

The purpose of cleaners is to separate high density or low-density particles. Turbulence, on the other hand, re-mixes the separated particles. As a consequence, turbulence is detrimental in most cases. However some turbulence is necessary to avoid pulp flocculation and reduce reject thickening. In addition, it has to be recalled that the Stokes' law has been established for a particle having established slip velocity (relatively low slip velocity in a steady swirling flow) which means that the phenomena due to the particle history are not taken into account. If a heavy particle moves from a low to a higher velocity zone, its tangential velocity is somewhat lower than the fluid velocity which may send the particles back to the vortex core. Such mechanisms associated with the lift force might explain the removal of neutral buoyancy particles observed with asymmetrical cleaner cone [7].

Consistency is known to be a decisive factor in the centrifugal cleaning process because of its considerable impact on the particle contacts in fibre suspensions. Collision probability calculations established to assess the free path of spherical particles moving through random oriented rigid fibres have shown that the mean distance between fibres is about 0.5 mm at 0.2% consistency, and about 0.1 mm at 5% consistency, for fibres with a diameter of 20 μm and a density of 1.2 g/cm^3 [15,16]. As these distances are much lower than the fibre length and in the size range of the contaminants to remove, fibre consistency will have a large effect on centrifugal cleaning efficiency. By contrast, fillers will have much lower effect. Coarse fillers, which concentrate in the reject area, might however reduce the separation efficiency in high-density cleaning systems.

The various models proposed to predict the efficiency of the hydrocyclone in mineral processing applications are generally based on the calculation of the diameter, d_{50}, of a particle having a predicted efficiency of 50% in the conditions considered for the calculation. The efficiency for a particle of equivalent diameter d (d is the diameter of a sphere having the same slip velocity than the particle according to Stokes' law), is then calculated according to probabilistic separation efficiency curves.

Among these efficiency models, the Bradley-Svarovsky model [33] combining empirical and theoretical analysis based on the Stokes' law, has been tested and adapted to fibre suspensions by Bermond [34]. The adapted model is described by the Equation below:

$$d_{50} = K\left(\frac{D^3}{Q}\right)^{1/2}\left(\frac{\mu}{\rho_S - \rho_L}\right)^{1/2}(1 - R_v)^{1/2}\exp(kC^n)$$

where K is the Bradley constant, D the cleaner head diameter, Q the feed flow rate, R_v the reject flow rate, k the Svarowsky constant and n the exponent introduced to adapt the model regarding the specific influence of the consistency C with pulp.

A modified form of the Rosin-Rammler-Bennett Equation of probability which was shown to fit with experimental particle separation curves in mineral processing [22] was used in the model to predict the removal efficiency E:

$$E = 1 - \exp-\left(\frac{d}{d_{50}} - 0.115\right)^3$$

This model showed to be adapted to the prediction of the filler and fibre reject rates provided that some experiments are performed to identify the constants of the cleaner and of the fibres at each cleaning stage. The effects of cleaning parameters such as pressure drop and consistency on speck removal efficiency were well predicted by the model, after pulp and cleaner identification, but differences were observed regarding the cleaner tested and the effects of other parameters such as the temperature were not in accordance with the predictions of the model [35].

A simplified cleaning index I has been proposed by Julien Saint Amand [36] in order to give a rough prediction of the efficiency level of a conventional cleaner. The cleaning index includes the most important cleaner operating and design parameters and is in accordance with the Bradley model [37]:

$$I = \frac{GT}{D}$$

G Centripetal acceleration (in g), $G = (G_i\ G_p)^{1/2}$ with:
- $G_i = V_i^2/r_i$ — with V_i injection velocity; r_i injection radius
- $G_p = dp/\rho_l dr$ — with dp pressure drop between inlet and accepts, ρ_l fluid density and $dr = (D - r_a)/2$ with r_a accept radius

T Residence time (in s), $T = (T_r\ T_s)^{1/2}$ with:
- T_r real residence time, based on cleaner flow rate and real internal volume.
- T_s standard residence time calculated for a "standard" cleaner with same flow rate and head diameter, a "standard" total length of 10 times the head diameter and a "standard" cylindrical part length of 3 times the head diameter.

D Cleaner head diameter (in mm).

The definition of the cleaning index is based on the assumptions that the removal probability of a given particle in a given pulp (consistency, temperature) is proportional to the ratio of its radial slip distance $\Delta r = U\ T$ to the cleaner head diameter D, the slip velocity being proportional to the mean centripetal acceleration G. The cleaning index (dimension: s^{-1}) becomes dimensionless by introducing the Stokes' law in this ratio:

$$\frac{UT}{D} = \frac{d^2}{18\mu}(\rho_S - \rho_L)\,\frac{GT}{D}$$

The cleaning index written in the form $Iir = Gi\ Tr/D$ is directly related to the Bradley model by a constant K_{irB} which depends on the cleaner dimensions, feed flow rate and constants which have to be determined experimentally in the Bradley model:

$$d_{50}^{2}\frac{\rho_S - \rho_L}{\mu} = K_{irB}(1 - R_V)I_{ir}$$

The cleaning index was introduced in a non-dimensionless form since the aim was only to evaluate the efficiency level of different cleaners and not to predict the influence of material parameters. It includes the influence of the feed flow rate and pressure drop on the basis of empirical relations and was not defined with standard units for practical reasons, but does not need any experiment for the identification of cleaner constants.

The influence of the cleaner head design is evaluated by using a mean value G of the acceleration in the upper part of the cleaner, which is calculated from the acceleration G_i produced by the injection velocity in the feed area and from the mean acceleration G_p which is calculated by the mean radial pressure gradient and takes the influence of the acceleration increase in the area of the accept outlet flow into account.

The influence of the cleaner body design is taken into account by using a standard residence time T_s in order to correct the residence time T used in the cleaning index. Indeed, if a cleaner is too long, the friction of the fluid against the long cone down to the reject tip will lead to lower velocities and thus, lower centripetal accelerations in this part of the cleaner, compared to a standard cleaner. So the centripetal acceleration G used in the cleaning index will be "overestimated" since it is calculated in the cleaner head and is assumed to represent a mean centripetal acceleration in the whole cleaner. Using a residence time T that is lower than the real residence time compensates this. By contrast, if the cleaner is very short, there will be a very high centripetal acceleration in the whole cleaner, and this is compensated for in the calculation of the cleaning index by using a residence time T which is higher than the real residence time.

The influence of the flow conditions in the reject area are not taken into account, though the influence of the reject flow rate might be assessed by dividing I by $(1 - R_v)$ on the basis of the Bradley model. However, reject thickening and reject outlet design might have a strong influence on the cleaning efficiency, which is evaluated in this approach. As discussed in [38] the vortex flow field has to be optimised and adapted to the type of pulp and contaminants, both in the separation zone where contaminants migrate to the area of the boundary layer and in the isolation zone where the flow is split between the rejects and the accepts of the cleaner.

The cleaning index is roughly proportional to the square root of the pressure drop and allows different cleaners to be compared using the same pulp. Cleaning trials performed on small and medium size cleaners showed good correlation between efficiency and cleaning index. The comparative study of 10 cleaners of various sizes between 24 mm and 152 mm diameter and different designs has been carried out on deinked pulp over a wide range of cleaning conditions [35]. The correlation between the cleaning index and the efficiencies obtained on the different cleaners tested at about 1% consistency and between 120 and 200 kPa pressure drop is shown in Figure 23. A similar correlation was obtained at about 1.5% consistency.

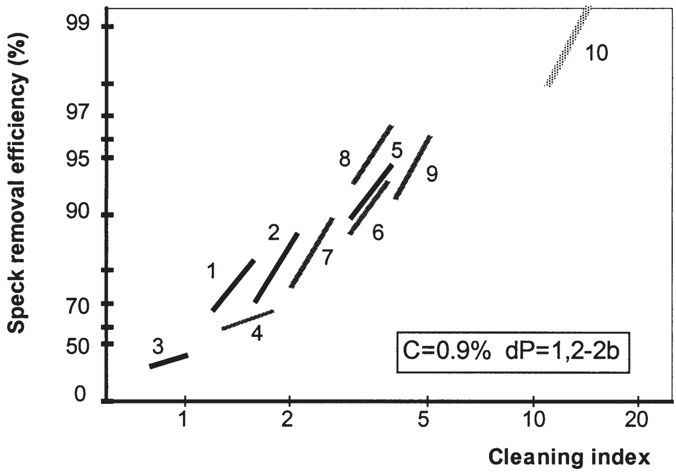

Figure 23 Correlation between cleaning index and speck removal efficiencies obtained with medium cleaners (1,2,3,5) small cleaners (4,6,7,8,9) and a 24 mm cleaner [35,37].

On average, the small cleaners (60–100 mm) gave better results than the medium cleaners (130–152 mm) did. The smallest cleaner n°10 (24 mm) had the highest efficiency, but some differences in cleaner design showed a significant effect. The medium size cleaner n°5 (150 mm) with low capacity had for instance a higher efficiency and cleaning index than the small cleaner n°4 (75 mm) having a slightly higher capacity. The reduced efficiency of the small cleaner n°4 is due to low injection velocity and residence time. This is also true for the medium size cleaner n°3 (130 mm). It has to be pointed out that the results were obtained with flat-shaped specks (UV varnish particles with about 0.2 to 1 mm diameter, 5 μm thickness, and a density of 1.35 g/cm^3). However, it is believed that the conclusions drawn from the analysis if the results in Figure 23 can be extended to more spherical contaminants but not to very long and stiff particles such as shives because of hydrodynamic effects due to the lift force.

The cleaning index gives a valuable prediction of the efficiency range of conventional cleaners as far as proper swirling motion is maintained in the whole cleaner. It was found that the effect of increased retention time within the cone was overshadowed by the loss of a cohesive vortex within the increased cone length [39]. On the other hand, the development of a high efficiency small diameter cleaner with increased centrifugal acceleration and residence time has been reported [38].

Centrifugal separation in high-density cleaners and centripetal separation in low-density cleaners are based on the same principles. Consequently the same conditions have to be respected to achieve high efficiency, i.e. high centrifugal acceleration, high residence time and low radial slip distance for the contaminants to escape from the accept flow.

Reverse cleaners with high cleaning index, i.e. small cleaners with low capacity and high pressure drop are assumed to be the most efficient, provided that they are operated at a sufficient reject flow rate, depending on the cleaner design. This approach has been used recently for the development of a new reverse cleaner [11]. The author defined the Necessary Average Radial Velocity (NARV = radial distance at the inlet/retention time in the cleaner) which is the average velocity a particle must travel to reach the air core, and the Cleaning Value Factor (CVF = (Vt^2/r)/NARV) which is a measurement of the centripetal acceleration on the particle versus the average velocity to reach the air core. Increasing the Cleaning Value Factor, which is equal to two times the Cleaning Index when using the same units, served as design tool for the new cleaner. The experimental results showed that the efficiency increased with these factors.

Reverse cleaners of the through-flow type have lower reject flow rate than conventional reverse cleaners, and the reject outlet has a very small diameter down to 10 mm. These reject conditions lead to high shear flow which can help to remove some long-shaped contaminants (long shives, synthetic fibres, etc.) by the lift force. However the small diameter of the separation area between light rejects and accept pulp makes it difficult to avoid some turbulent mixing between the reject and accept streamlines.

In combination cleaners low-density contaminants have to be separated from the upward accept flow in the very small volume of the inner vortex zone, which can be regarded as a small "fictive" low density cleaner having high centripetal acceleration, very small diameter and extremely short residence time. The latter characteristic and turbulent mixing are thought to be responsible for the limited efficiency. If the vortex finder of the combination cleaner is extended, it can be considered as a through flow cleaner in series. If the combination cleaner is provided with a second lightweight contaminant outlet, it can be considered partly as a through flow cleaner in the lower part and mainly as a combination cleaner in the upper part.

As already described, the rotary cleaner is characterised by a high acceleration, a long residence time and a relatively small pulp flow thickness in the outer separation zone. If the calculation is based on flow thickness and dwell time in this cleaning zone, the cleaning index of the rotation cleaner is comprised between 20 and 40 in the typical operating range of the large model. This high cleaning index is in agreement with the high efficiency of the rotary cleaner [15–19,40,41].

Comparative pilot tests were performed with different low-density cleaners including combination cleaners, small diameter reverse cleaners available at the time of the tests (conventional and through-flow type) and the rotary cleaner. The results in Figure 24-left were obtained with plastic beads and bleached chemical softwood or hardwood pulps at low consistency [17]. The highest efficiencies were observed with the rotary cleaner and the lowest efficiencies with the combination cleaners, which is in accordance with the cleaning index. The results were obtained with granular polyethylene or polypropylene particles mechanically fragmented and classified on laboratory

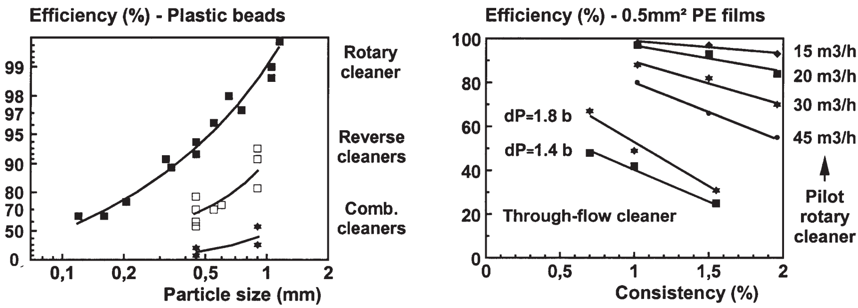

Figure 24 Comparative tests of different low-density cleaners. Results obtained with plastic beads – left [17] – and with polyethylene films – right [41].

wire screens. The particle sizes in Figure 24-left correspond to the mesh sizes used in the classification, which means that most of the particles retained on a given mesh size should easily pass slots of the corresponding width if treated in a pressure screen.

The results in Figure 24-right, which were obtained with bleached hardwood pulp and a pilot sized rotary cleaner, confirmed the high efficiency and the possibility to increase the consistency with the rotary cleaner in the case of small flat shaped particles (0.5 mm^2 polyethylene films), which were shown to be difficult to remove by screening [41].

ANALYSIS OF THE EFFECT OF BASIC CLEANING PARAMETERS

The effects of the most important parameters on the performance of cleaning systems have been described in several papers reporting pilot tests and mill experience. Some results are briefly discussed below to illustrate relations between theory and practice.

Machine and Operating Parameters

The influence of cleaner design parameters as well as the effects of the cleaner operating parameters, i.e. the feed flow rate and the associated pressure drop, the consistency and the reject flow rate, are included in the cleaner models and/or in the cleaning index.

A consistency increase always reduces strongly the efficiency of forward and reverse cleaning systems, mainly because of the drastic increase of the particle interactions. Pulp flocculation should not be observed in low consistency cleaners, because of the high shear forces at the cleaner wall and to a lesser extent in the vortex flow. The influence of consistency should be higher with large long or flat-shaped contaminants than with small round shaped contaminants. Typically small high-density particles such as fine sand can be removed efficiently at higher consistencies [7] than other particles having the same settling velocity in water. The comparative study of several cleaners at 9 and 14 g/l consistency showed a larger positive influence of a pressure drop increase at the higher consistency, which was attributed to the fact that increasing the feed flow rate helps to maintain a complete de-flocculation of the pulp in the whole cleaner [35].

Increasing the feed flow rate and pressure drop (roughly proportional to the square of the feed flow rate) was shown to increase continuously the efficiency in the tested range, i.e. no optimum pressure drop was observed regarding the cleaning efficiency [35]. Similar trends were observed with reverse cleaners tested up to 400 kPa pressure drop [11,42]. This behaviour is consistent with the predictions of the cleaning index and means that turbulent diffusion (particle re-mixing) does not increase sufficiently to overshadow the positive effect of a feed flow rate increase through the acceleration increase.

The rotary cleaner showed to be particular, as increasing the feed flow rate reduced the efficiency since the residence time is reduced while the acceleration, mainly produced by the rotating cylinder, is only slightly increased. On average, the efficiency depends only on the production (for a given type of pulp and contaminants) since the negative effect of a consistency increase can be compensated by an increase of the residence time obtained at constant production and correspondingly lower feed flow rate. This specific behaviour was observed with plastic beads as well as with films [18–20,41].

Cleaners are designed to be operated in a defined reject rate range. Forward and reverse versions sometimes exist for a given cleaner design. Continuity of the efficiency curves has been observed in such cases with respect to the reject rate [35]. Reducing the reject flow rate is known to increase the consistency of heavy rejects and to reduce the consistency of low-density rejects.

High-density and low-density cleaners (with the exception of the rotary cleaners) are operated in multistage systems (2 to 4 stages and more) so that increasing the reject flow rate means more cleaning stages. Various cleaning system designs have been compared in several papers [14,18,43]. The performance of the single cleaner has much more impact than system design on the overall cleaning efficiency for given fibre losses.

Material Parameters

Pulp composition influences centrifugal separation efficiency. It depends mainly on the fibre fraction consistency and on the fibre length l, while fillers and fines consistency has low impact. Long fibre pulps require a higher dilution than short fibre pulps in both high-density or low-density cleaning systems (or a higher cleaning capacity with the rotary cleaner) to maintain the efficiency, because individual long fibres generate more hindrance than short fibres to the radial slip of the contaminants [16]. In addition, fibre networks, which appear at lower consistency with long fibres compared to short fibres since the number of inter-fibre contacts is proportional to l^2 [44], further increase the hindrance to the radial motion of the contaminants with respect to the pulp.

Concerning the influence of the cleaning temperature, it is interesting to note that, if the impact on reject thickening is as predicted by the theory, i.e. higher reject thickening at increased temperature due to the higher slip velocity induced by the viscosity decrease, the influence of the temperature depends on the cleaning conditions. The speck removal efficiency of high-density cleaners was shown to decrease slightly as the temperature was increased [35], which was attributed to the increase of the fibre-particle interactions induced by the higher consistency in the reject area. By contrast, a temperature increase improves the efficiency and reduces the reject rate in low-density cleaning since the viscosity decrease increases the slip velocities of pulp components and contaminants in opposite directions and consequently improves the separation.

Reject thickening depends on the type of pulp since the fibre slip velocities and trends to flocculate depend on their characteristics. The possibility to use cleaners to fractionate pulps according to the fibre properties such as cell wall thickness and to remove fines has been reported in several papers [16,30,45–50]. In principle, fibres can be separated in all cleaners according fibre coarseness (fibre density in water) and specific surface (drag coefficient), while the lift force depends on the fibre length and stiffness. Recent research has been devoted to the optimisation of the pulp fractionation conditions and cleaner design for applications to virgin pulps.

The most decisive cleaning parameters are clearly the density and the size and shape of the contaminants as predicted by the theory, confirmed by field experience and reported in several papers already cited and in others [51–54]. The weak point of centrifugal cleaning is the separation of close to neutral buoyancy contaminants such as pressure sensitive adhesive (PSA) particles. Increasing the fluid to particle density difference, such as by chemical treatment with laser inks [52], increasing the temperature with hot melt glues [16] or mismatching the temperature [54], can improve the situation.

Particle fragmentation phenomena observed with PSA particles in cleaners have been reported and were attributed to the acceleration in the cleaner [55]. In fact one should not consider the bulk acceleration produced in the vortex flow field, but the shear induced acceleration exerted on the particles. The bulk acceleration affects the whole particles and does not produce any tensile stress, since the radial acceleration gradient is low.

The acceleration produced by the rotation of the particle in the shear flow can be evaluated as previously discussed in the section about screening. Shear is observed in the whole vortex flow, except in the solid rotation area of the vortex core. The shear rate due to the fluid rotation velocity increase towards the vortex axis (given by the maximum value of $2Vt/r$ for the free vortex law) is normally much lower than the shear rate at the cleaner wall. Compared to the shear rates in low consistency screens [56], the shear rate at the cleaner wall should be in the same order of magnitude than the shear rate at the screen plate (10^2 m.s^{-2}) or lower since the tangential injection velocities are generally lower than the rotor velocities, i.e. less than 10 m/s. This is also the case with the rotary cleaner where the velocity difference between the rotating body and the pulp injected at the inlet head is normally lower.

In the case of high density PSA particles, one should however consider a higher shear and contact induced acceleration, in the order of magnitude of 10^3 m.s^{-2}, since the contact probability of such adhesive particles with the cleaner wall is increased by the centrifugal particle slip. At this shear and wall contact induced acceleration level, some soft and long shaped stickies might be fragmented in cleaners.

The results reported about the influence of the cleaner's construction material [55] might be due to the surface properties of the cleaner wall. As the particle slip velocity during the contact should be higher with a smooth cleaner wall surface compared to a rough surface, the deceleration exerted on the adhesive particle end in contact with the wall should be reduced. Increasing the cleaning temperature should slightly increase the stress on the particle at wall contact since the fluid viscosity is reduced. A temperature increase improves normally the cleaning efficiency as the particle slip velocities are increased, but might increase the fragmentation of some PSA as the wall contact probability and stress are increased and the strength (elastic modulus and viscosity) of the adhesive material is decreased.

Concerning the characteristic time to consider with respect to the deformation of visco-elastic particles submitted to shear and wall contact induced acceleration, it has to be pointed out that the residence time in a cleaner is in the range of a second, which is two order of magnitude higher than the duration of the micro-processes in pressure screens. As already mentioned the fragmentation probability of stickies increases with particle size, i.e. with particle length in the case of long shaped adhesives. Indeed, large stickies should normally be removed at the fine screening step before cleaning. The fragmentation of small residual stickies in cleaners should then be less significant in modern deinking processes with efficient fine screening systems.

As a final comment about cleaning, it is believed that, despite considerable progress achieved recently in fine screening, which made cleaning significantly less competitive, there is still a need for centrifugal cleaning to remove some problematic contaminants that cannot be removed by screening and also to fractionate pulps according to different fibre properties than with screens.

FLOTATION

Froth flotation technology has been developed and used for many decades in the mineral processing industry before the technology was transferred to the pulp and paper industry for the deinking of waste papers in the late 1950's. The growth of installed flotation units has then been relentless in the field of deinking. Today, flotation deinking is the most significant stage in the waste paper recycling process for the production of graphic grades. Improved flotation conditions in terms of ink and speck removal efficiency and controlled rejects are requested to fulfil the brightness and cleanliness requirements of high quality paper products.

Flotation involves basically the subsequent steps of collision and attachment between ink particles and air bubbles, and the selective removal of the particle-bubble aggregates. Among these individual micro-processes, the mechanisms of attachment of ink particles onto the air bubbles are mainly driven by physical-chemical interactions, while the collision and removal of the inked bubbles processes are driven by hydrodynamics.

Extensive theoretical and experimental studies on the various aspects of froth flotation, including fluid dynamics, surface chemistry and broadly speaking colloid science, were carried out for the mining industry [1,2]. However, many of the fundamentals are believed to be applicable to deinking flotation because of major similarities.

The most significant differences between deinking flotation and mineral flotation are to be found in the development of specific equipment and especially in the particular characteristics of waste paper pulp suspensions including:

– the wide distribution of size, shape and surface properties of the particles to be removed: mainly ink particles from about 1 μm to 1 mm, generally hydrophobic (except for water-based inks) and flat shaped for the large particles, as well as stickies;
– the low density of these particles: polymeric particles with specific gravity close to that of the water (fillers should not be completely removed in most cases to avoid excessive losses except if deashing is required);
– the trend of cellulose fibres to flocculate at consistencies above about 1%, as soon as the turbulence level is decreased as observed in the separation zone of deinking cells;
– the chemicals added in the pulper to release the ink particles from the fibres and to enhance the flotation process (calcium soap and caustic soda or other deinking chemicals to be used under alkaline or neutral conditions),

as well as the various chemicals in the recovered papers (especially surfactants used in the coating colour).

The basic investigations in flotation deinking were first focused on physical chemistry, because of the very complex properties of recycled fibre suspensions in terms of dissolved, suspended and colloidal components as well as added deinking chemicals and surfactants from the recovered papers [3–13]. Several theories have been proposed to explain the mechanisms of ink collection onto air bubbles.

Investigations about flotation deinking hydrodynamics were carried out more recently. They included theoretical studies based on the scientific knowledge gained from mineral flotation, as well as experimental studies carried out on laboratory equipment [14–34].

Several papers reviewing flotation deinking technology have been published [29,35–39]. The characteristics of the different types of deinking cells in the aeration, mixing and separation steps were compared and analysed in [38] in order to define the most relevant hydrodynamic flotation conditions to be investigated experimentally.

FLOTATION TECHNOLOGY

The flotation systems currently used in deinking mills show a large diversity of designs (Figure 25), but also similarities regarding some basic principles. Detailed characteristics have been reported in several papers published by the equipment suppliers [40–59]. Flotation cells or cyclones may be very different in size and shape, but the key elements ensuring aeration, ink collection and bubble separation are always present. In fact, ink collection under turbulent mixing conditions is always more or less included in the aeration and separation processes. This mixing process involves collision, attachment and unwanted detachment of ink particles and bubbles. Depending on the design of the flotation unit, this decisive step of the flotation process is mainly achieved within the aeration elements or within the flotation unit in connection with bubble separation.

Aeration and Collection

Aeration refers to the introduction of air into the fibre suspension in a correct form and amount. Since the number and size of air bubbles crucially affect the probability of collision between bubbles and inks, the aeration conditions have to be characterised by relevant parameters such as bubble size

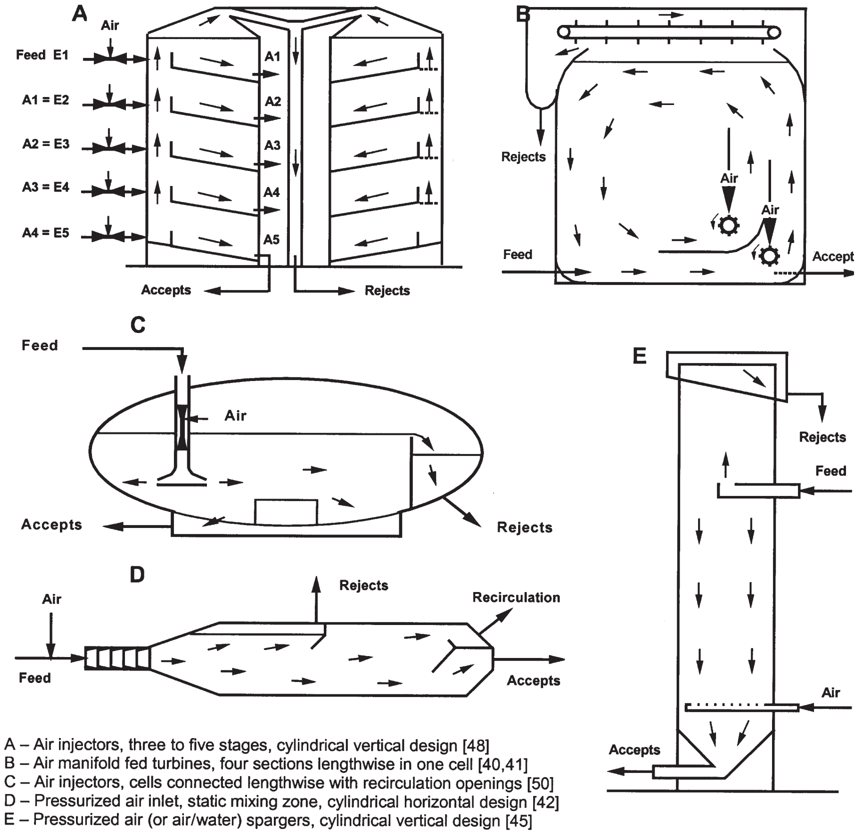

Figure 25 Different deinking flotation cells [38] – Figures redrawn from the literature cited.

distribution and volumetric air to pulp ratio [15]. The air ratio, or air flow rate, can be defined at each aeration step if pulp and air are supplied through the same inlet, or globally for a flotation unit or a complete installation, on the basis of the cumulated air flow (evaluated at the mean pressure in the flotation units). In fact the relevant parameter should be the effective air ratio, based on the air removed in the foam with the collected inks. However, the difference between removed and consumed air flow rate should be very small as generally only small bubbles, which do not contribute significantly to the air ratio, might not be removed in the foam.

Increasing the amount of air effectively used in the flotation process, and more particularly the specific phase interface [21,22] involved in the collection of ink particles, may be regarded as a preferred means to improve ink removal, at each aeration step. However there are limits, depending on bubble size distribution and pulp consistency, to the amount of air which can be introduced into a fibre suspension in order to keep a sufficiently free motion of bubbles and fibres. As a general rule, larger amounts of air can be mixed in the pulp as the bubble size is increased and a lower specific energy is required to create the interface. On the other hand large bubbles are less effective than small bubbles, but are easier to remove from the pulp suspension.

Different aeration systems have been developed by the equipment suppliers. They include various air introduction systems, under pressure or by self suction, and hydrodynamic or mechanical mixing in the pulp, at the inlet or within the flotation cell.

The mechanical method is based on a pumping rotor and generally stator elements, designed to achieve pulp circulation, air suction and mixing. This concept, developed and still widely used for mineral flotation, was the first to be adapted to deinking flotation but has now been dropped by the equipment suppliers who introduced it to the market. Other suppliers have then developed the mechanical aeration method further. Air is injected under pressure through a manifold on a turbine [40,41] or through holes to the axis of a rotor [59] in order to generate and disperse the air bubbles and to provide multiple pulp re-circulation within long retention time cells.

Several other methods of pressurised air introduction are currently used without mechanical dispersion: air is injected in the pulp flow through openings or porous media and subsequently dispersed under turbulent flow conditions [42–45]. Separate zones may be provided for the aeration step and for the subsequent mixing step [42]. The turbulence increase in the mixing zone is then assumed to reduce the size of the bubbles, which were produced in the aeration zone under lower turbulence and shear. Concerning the effect of pressurisation, it must be pointed out that the pressure level within the flotation unit compared to the pressure variations in the aeration and mixing zone, should have little influence on bubble size distribution and on nucleation and growth of micro-bubbles as far as this mechanism is concerned.

In cyclone flotation, initially developed for the mineral industry and adapted to deinking, air is sparged through the porous wall of a cleaner-type flotation unit, dispersed in the downward vortex flow and removed in the upward vortex core [43]. The latest design of cyclone flotation has been modified in such a way as to increase the amount of air sparged in the flotation cleaner and entrained in the downward outlet flow in order to be further removed in a conventional flotation cell [44]. Under these conditions the cyclone unit is essentially used to provide aeration and collection, separation being limited to the removal of excess air. The removal of excess air should correspond to large bubbles since the centrifugal separation effect has been reduced in the new cyclone design.

A new centrifugal flotation process, using a rotating cell where air is introduced through a rotating perforated wall, has been developed on a laboratory scale [56]. High air flow rates, up to 50 times the pulp flow rate which is far beyond the air ratios of industrial flotation cells (see Table 1) can be achieved with this technology, since the centrifugal flow field improves the separation of the air bubbles and can be maintained over a longer time than in cleaner type units used for conventional cyclone flotation.

In column flotation, a technology also adapted from mineral flotation where it showed to be very cost effective, the sparger system is arranged at the bottom of the column [45]. Spargers made up of holes in which a mixture of air and water is injected and released in the cell, or porous spargers are used.

A comparison of the various aeration systems using pressurised air supply, is not easy in terms of bubble size distribution. However it can be considered that smaller bubbles are produced as the air injection velocity (or air flow rate) and the size of the pores or openings are decreased, and as the pulp-flow velocity in the air-injection area is increased. A decrease of the pulp surface tension also reduces bubble size. If turbulence is increased after air injection, bubble size may be further decreased in the turbulent mixing zone. Under these conditions it is very difficult to evaluate, without measurements, bubble size distributions for such different air injection methods as, for example air sparged through very small pores in the low turbulence flow of column flotation, and air blown through a much larger opening onto a high-speed turbine.

The hydrodynamic method, based on the self suction and mixing of air according to the Venturi principle, has become the most common aeration technique since the first injector cells were specifically developed for deinking flotation [46–48]. Injectors of various sizes and designs have been investigated and constantly improved by the equipment suppliers and adapted to different designs of flotation units [48–58].

Referring to the pulp injection diameter, the size of the injector is regarded as a key design parameter to control the pulp jet velocity, the suction effect, the surface of phase interface and the turbulence level within the injector, in relation to pressure drop and injector capacity. It is suggested that the hydraulic diameter (4 × area/perimeter) of pulp injection be used to define the injector size in the case of injector designs using numerous or non-circular injection openings. Large injectors have been dropped and currently the injector flotation cells are equipped with various arrangements of small and medium size injectors, between 12 and 30 mm diameter [46,51,53], or less in terms of hydraulic diameter [48].

The amount of air introduced depends on the injector size and design. The various possibilities applied to increase the air ratio include, a high jet velocity, a small hydraulic diameter, a large area around an unstable jet to promote air suction by jet droplets, a low outlet pressure and pressurised air supply. High air flow rates up to 200%, and increased flotation efficiency on a pilot scale, have been reported under self-suction conditions for a small injector [22]. However, the injectors used on industrial equipment are generally operated at a lower air ratio, in the range of 30 to 70%, since it was found by experiment that beyond certain limits of the ratio no further increase in the flotation effect was possible [48, 49].

The size distribution of the bubbles produced by the injector depends on the turbulence available to mix the air in the pulp, as well as on the air ratio and on the surfactants in the pulp. A high turbulence is required to produce small bubbles. Such high turbulence is achieved by small injectors operated at high jet velocity. Injectors with turbulence generating devices in the mixing and distribution section have been developed in order to increase turbulence intensity and scale in such a way to produce air bubbles in a large size range [50,51]. Depending on the design of the pulp injection nozzle the feed pressure is partly or almost completely transformed in kinetic energy to achieve the required injection velocity (theoretically 10 to 20 m/s for 50 to 200 kPa pressure drop without friction loss). Injection velocities of 9 m/s for about 100 kPa feed pressure [50] and about twice as much for a small injector fed at 200 kPa [46] have been reported. Much higher jet velocities of about 50 m/s have been reported recently for a particular high pressure injector using a thin, clear liquid jet to mix the air in the suspension [55].

The effects of air ratio and liquid surface properties on bubble size distribution were investigated (in the frame of previous, unpublished studies) in the case of a commercial 12 mm injector. Bubble sizes were measured on video frames taken from a transparent channel connected at the outlet of the injector. Clear water with and without surfactant as well as deinking process water were tested at different air flow rates set by a valve at the air inlet. Much smaller bubbles were obtained by adding surfactants or with process water. Bubble size was clearly decreased as the air flow was reduced and very small bubbles where observed at low air ratio. This result was assumed to be due to the large suction effect achieved as the air valve was progressively closed: as a vacuum is created around the suspension jet and the turbulence is assumed to be unaffected by the pressure level, less air is contained in a given bubble volume so that bubble size will decrease as the jet kinetic energy is recovered and the pressure increased.

Investigations on different small injectors tested with water also showed the increase of bubble sizes with the air ratio [22]. Bubble size distributions were measured by using a new optical method based on bubble volume measurement in a capillary. By contrast no significant variations of the bubble size distribution curves were observed with deinked pulp. The specific phase interface was thus proportional to the air ratio. However it must be pointed out that these results were obtained at high air ratios (50 to 200%) while our results on a single 12 mm injector were obtained in a lower range of less than 50% air.

Concerning the micro-bubbles which may be generated from dissolved air during pressure release, it has been suggested that they may be formed on ink particles and thus improve flotation efficiency [32], while other authors reported, from experimental and theoretical considerations, that it is unlikely that new bubbles can be nucleated and grown on the surface of fibres or ink particles [60].

As already mentioned, aeration and collection are closely linked, because the collection process (collision and attachment between ink particles and air bubbles) begins as soon as air is mixed in the pulp, while the aeration process (air introduction and bubble production) really ends as no more bubbles are produced in the pulp suspension. The technological approach to achieve the aeration and related collection steps is thus of critical importance for the flotation efficiency.

Current technology is compared in Table 1. The comparative data are based on typical deinking flotation installations recommended by equipment suppliers to achieve high removal efficiencies on detached ink particles under usual flotation conditions. The number of aeration steps or flotation units in series may vary according to waste paper grade, deinked pulp quality requirements and flotation consistency [52].

Secondary flotation (treatment of flotation rejects), as well as post-flotation (additional flotation step implemented after a hot dispersion step to further detach ink particles from the fibres) which normally requires less

Table 1 Aeration conditions of current flotation installations [38].

Aeration method	Pressurised air			Air injector		
Literature	[44]	[42]	[40] [41]	[48]	[51]	[49] [50]
Air ratio per aeration (%)	70–100	300	600–1000	50	60	50
Number of aeration steps	1	1	Int. rec.	5	1	1
Number of flotation units	3	3	1	1	4	4 – 6
Total air ratio (%)	210–300	900	600–1000	250	240	200–300

aeration steps or flotation units in series, are not considered in Table 1. Under these conditions the total air ratio varies between 200 and 300% for injector cells [47–52]. About 3 times more air is recommended for pressure aerated cells [40–42], which is assumed to correspond to larger air bubbles.

Collection and Separation

High turbulent mixing in connection with pulp aeration at the inlet or within the cell is generally used to promote ink collection by increasing the probability of particle bubble collision. However these favourable conditions are only achieved over a very short time to keep the energy consumption within limits. Turbulence is then quickly decreased, as the pulp suspension moves to the separation zone. Additional ink collection is then achieved under much lower turbulence but over a longer time. The mechanisms of ink collection in terms of probabilities of attachment and detachment of ink particles with air bubbles are very complex. Ink collection is strongly affected by particle size, bubble size and turbulence intensity and scale. The mechanisms of ink separation in terms of stabilisation and removal of the particle bubble aggregates are also strongly affected by hydrodynamic parameters which depend on the flotation technology.

In the most common case of injector cells, a major part of the ink to be removed with the injected air is collected onto the air bubbles in the injector and the feed area where the high turbulence is progressively decreased. As the aerated pulp reaches the cell body, gravity collision between rising bubbles and inks becomes more significant compared to turbulent collision. The additional ink collection obtained within the cell body as turbulence decreases depends on the cell design and operating conditions.

The parameters of decisive importance for gravity collision and bubble separation are the vertical flow component (superficial velocity or surface related pulp flow) and the flow direction (upward or downward) which define the residence time and bubble particle contact time in the cell in connection with the pulp and air introduction levels. Unwanted short circuits and large-scale turbulent mixing may reduce the air removal efficiency if the residence time in the zone below the air introduction level is too short.

Flotation cells with downward pulp flow and thus counter current with respect to the air flow are the most common. If aerated pulp is introduced at one single level [42,44,50,51,55] the cell is essentially used for bubble separation. If aerated pulp is introduced at different levels [46,48,53], the rising distance for air bubbles from the lower injection levels to reach the surface is increased. The contact time for additional particle-bubble collision is increased, but the superficial velocity of the downward flow in the upper cell area has to be decreased to compensate for the increased superficial velocity of the upward air flow. If the air is introduced in the cell at levels lower than the pulp suspension, such as in column flotation, the average contact time is roughly proportional to the cell height for constant superficial velocities and bubble size distributions.

The ink collection mechanisms in column flotation are exclusively governed by gravity mixing caused by the unstable rising motions of the air bubbles through the pulp flow. Large bubbles are most effective to produce some turbulence in the pulp suspension as they have higher buoyancy and rising velocity, but the contact time is lower. On the other hand small bubbles provide much longer contact time and may be entrained downward, since their relative upward velocity is much lower.

Flotation cells with upward pulp flow have also been developed in order to increase the particle bubble contact time [46]. Under these conditions the migration distance of the air bubbles through the pulp is much lower for small bubbles having a low relative rising velocity, than for large bubbles although their residence time in the upward flow area is reduced [48]. As the flow configuration must be downward in the separation zone, upward flow is always connected to downward flow with intermediate horizontal pass. Such flow configuration is observed in different types of cells with multiple pulp aeration [40,46,48,53,55,59] using internal or external re-circulation.

Among global engineering characteristics of flotation cells, specific power, retention time and superficial velocity are most relevant. According to mill experience [36] and equipment suppliers [40,50,55] the specific power consumed by a flotation installation to achieve high ink removal is generally in the range of 20 to 50 kWh/t. Trends to increase the installed power with respect to the cell volume have been pointed out and related to the turbulence observed at the surface of different cells [36]. Values of specific installed power between 2 and 10 kWh/m^3 were reported.

The retention time in a flotation unit is directly related to the superficial pulp flow velocity, cell height and flow configuration. According to the type of cell and operating conditions, the retention time varies between about 20 sec [57] and 10–20 min [40,59]. For complete flotation installations under normal deinking conditions as compared in Table 1, the cumulated retention time is in the range of 2 to 10 min. Low cumulated retention time is observed when ink collection is mainly achieved in the injector and the flotation cell essentially used to remove the air bubbles, while high retention time corresponds to additional ink collection within most of the cell volume.

The superficial downward or upward flow velocities are in the range of 0.5 to 5 cm/s. Velocities between 1 and 2 cm/s are most common according to the values or connected data published by the equipment suppliers. In relation to these upward and downward surface velocities one can assess a cumulated distance of upward and downward flow which is the range of 3 to 10 m for a complete flotation installation. Small superficial velocities are necessary to remove small bubbles and to increase contact time in the case of column flotation and upward flow configurations. Conventional parallel flow between inclined plates [55] and low surface velocity [48] help to remove smaller bubbles. Depending on the large scale turbulent flow velocities in the cell, a minimum distance of about 1 m has to be kept under the aerated pulp introduction level in order to avoid turbulent diffusion of air bubbles which should not be removed in the accept outlet.

Cyclone flotation is a special case in terms of residence time and bubble travel distance, where flotation is achieved in the cyclone [43]. A high centripetal acceleration compared to gravity and a small travel distance depending on the cyclone diameter compensate for a very short residence time to enable the removal of small bubbles. With the rotating flotation cell [56], the residence time is increased while maintaining a high centripetal acceleration, which allows more small air bubbles to be used for particle collection.

The foam removal conditions have an influence on the flotation rejects and efficiency. Depending on the foam removal technique (pressure with control valve, overflow or scraber) and turbulence level in the cell, a minimum distance also has to be kept above the pulp introduction level, in order to selectively remove the inked bubbles. Some additional ink collection, as well as unwanted ink detachment and fibre collection occurs in this foam removal zone. Numerous parameters such as foam height and stability, turbulence level, bubble size and air surface velocity are involved in the separation of the pulp components in this zone.

In the mineral flotation, foam washing is a frequently used and proven process, which has recently gained interest in flotation deinking [39,61,62]. As generally known, by adding liquid onto or within the foam layer, a great part of the hydrophilic particles carried along with the bubbles are washed back into the suspension. The concentration of hydrophobic particles therefore increases in the foam layer and thus in the rejects. Foam washing is performed by spraying water [61] or surfactant [62] on the top of the foam. Significant reductions of the solid flotation losses achieved without sacrificing deinking efficiency were reported. In the flotation reject washing process recently reported in [58] process water is introduced under the foam layer in such a way that free bubbles, instead of foam, are washed by a counter current flow. The reduction of flotation losses showed to be particularly important with respect to the fibre fraction.

Besides foam washing or bubble counter washing, the foam height strongly influences the water and solid losses as the interfacial suspension from collapsed bubbles is drained back to the suspension through the foam. The deinking surfactants have a large influence on the foam stability, which controls the foam height and thus the flotation rejects.

FLOTATION MECHANISMS AND THEORY

As shown by the analysis of the various equipment used in deinking, the flotation process always includes the subsequent aeration, mixing and separation steps. Generally, some overlapping of these subsequent steps and a decreasing turbulence are observed.

Aeration

In the aeration step, the dispersion of the air in the pulp and the bubble size distribution depend on the aeration techniques, on the hydrodynamic conditions and on the pulp properties related to the deinking chemistry, essentially the surface tension of the pulp.

Jameson [63] investigated the bubble formation mechanisms observed in the wake of the paddles of mechanical devices. Barnscheidt [47] analysed the air injector. If porous plates or spargers are used for the introduction of air, basic information can be found in papers reporting experimental and theoretical studies about the formation of bubbles at small orifice [1]. At vanishingly small air flow rates the diameter (d_b) of the bubble formed as it leaves the orifice (diameter d_o) in a steady liquid is determined by a balance between the surface tension (σ) and the pressure gradient due to gravity (g):

$$\pi d_o \sigma = \pi d_b^3 \Delta\rho g/6 \quad \text{or} \quad d_b = (6 d_o \sigma/\Delta\rho\, g)^{1/3} \tag{1}$$

If surface tension can be neglected, the formation of the bubble is governed by the hydrodynamic forces. Theoretical analysis [51] considering the added and virtual mass of the bubble to be accelerated gave, after integration up to detachment, a simple result related to the air flow rate (Q_a) through the orifice:

$$d_b = 1.38\,(Q_a^2/g)^{0.2} \tag{2}$$

The results reported by Julien Saint Amand [38,64,65] about the use of air capillary tubes supplied with pressurised air and connected perpendicularly to the wall of the feed channel of a laboratory flotation cell to produce calibrated bubbles, showed that the measured bubble sizes agreed quite well with Equation 2, as the bubbles were formed under “dynamic” conditions (air and liquid velocities in the order of 1 m/s).

Collection

During the mixing process the ink particles have to be collected and to keep attached onto the air bubbles until the bubble particle aggregate is removed from the pulp. The hydrodynamic aspect of ink collection on air bubbles is complex because it is necessary to consider the whole turbulent flow field and the movement of ink particles and bubbles in each coherent swirl (Figure 26) where they are entrained for a very short time as well as between the swirls. In each coherent swirl ink particles and bubbles migrate according to centripetal and gravity acceleration and to inertial forces.

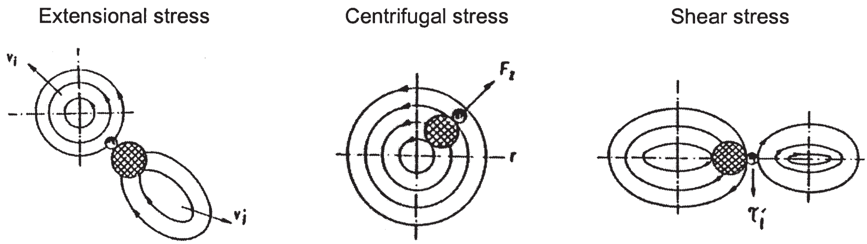

Figure 26 Stresses on the particle-bubble aggregates in the turbulent flow field [16].

Excellent reviews of flotation theory applied to deinking were given by Schulze [14,16] and then by Heindel [29]. The most important flotation micro-processes were analysed:

- the approach of a particle to a bubble in the flow field;
- the formation of a thin liquid film, its rupture at the critical thickness, connected with formation of the three-phase-contact; and
- the stabilisation of the aggregate against external stress forces.

These subsequent micro-processes are described in terms of particle-bubble collision, attachment and stabilisation probabilities in the kinetic Equations of the flotation process.

A global flotation model, which is based on two models, describing the details of the hydrodynamics of bubble-particle interactions and attachment as well as the influence of short range non-hydrodynamic forces on the behaviour of the disjoining film, has been developed to predict deinking flotation efficiencies [17–20,28].

The hydrodynamic model of bubble-particle approach and attachment considered the following three categories of forces [17]:

- Long-range hydrodynamic interactions based on the Stokes' law and including buoyancy forces. The presence of a second particle was shown to have a significant influence on the limiting attachment radius of the bubble first particle interaction.
- Short-range hydrodynamic interactions describing the squeezing-type flow due to the necessity to expel fluid from between the gap which separates the objects, and the tangential shear force due to the relative motion of the two objects.
- Non hydrodynamic interactions lumped into a single term denoted as the critical gap necessary for particle-bubble attachment.

The disjoining film rupture model describing the critical gap necessary for particle-bubble attachment considers surface tension forces, London-Van der Waals dispersion and electrostatic interactions [19]. The disjoining film rupture times were based on a characteristic perturbation wavelength associated with the dimension of the particle. The predictions of the disjoining film rupture were recently correlated with experimental results using a high precision device (resolution in the order of 10 nm) to measure the attractive or separation forces of a bubble-particle pair as they approach each other or are withdrawn from each other [28]. It was shown that hydrophobic attraction can act over very long length scales under certain conditions. Concerns about jump to contact, bubble particle binding energy, the influence of surfactants, particle and bubble size, and the role of angle of attack were discussed and showed to need further investigation.

The global model for predicting flotation efficiency was found to give excellent general agreement with experimental results, in particular regarding the dependence of flotation efficiency on flotation time and particle size, and the influence of numbers of particles present [18–20]. In the case of laser ink flotation the agreement with experimental data was obtained by using different capture radiuses for detached and attached particles [20].

Separation

After the mixing zone where ink particles are collected, pulp enters the flotation cell where turbulence is lower. Additional ink particles may be caught by the rising bubbles, especially in the case of large volume flotation cells. A main role of the flotation cell is to remove the ink-bubble complex, which calls for large bubbles having high rising velocity. If the rising velocity of the bubble in the pulp suspension is lower than the downstream velocity of the accept flow, or if the residence time is too low to allow bubble to reach the surface, the bubbles and the associated ink will not be removed.

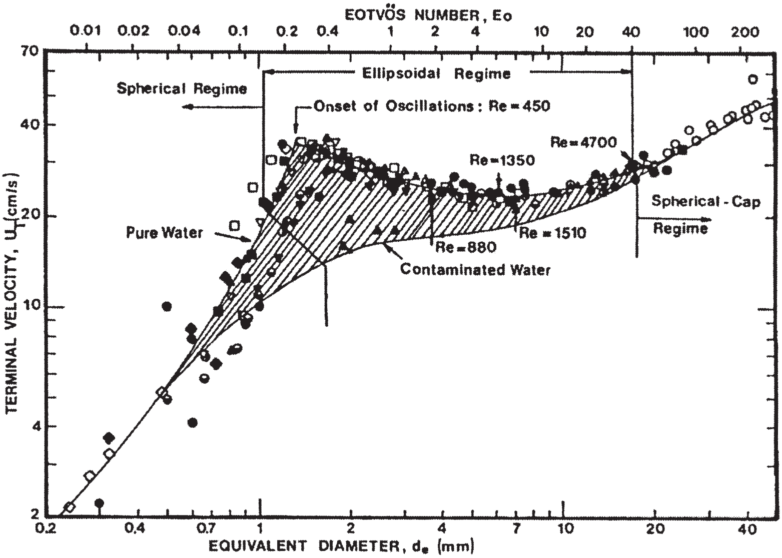

Figure 27 Terminal velocity of air bubbles in water at 20°C [1,16].

The terminal rising velocity or air bubbles in water is shown in Figure 27. The velocity in a fibre suspension is lower. Small bubbles less than 1 mm in diameter are spherical in appearance and rise with a steady rectilinear motion. The rising motion of larger bubbles becomes unstable and their shape is modified to become ellipsoidal or spherical capped bubbles. If the water is “contaminated” with surfactants (as in deinking flotation) the bubble surface becomes rigid and the rising velocity is decreased.

Small bubbles are very effective for deinking but difficult to remove, particularly at increased consistency (sinking velocity is typically a few cm/s in most flotation cells). Consequently, too small bubbles i.e. less than about 0.3 to 0.5 mm and too large bubbles should not be effective for the flotation deinking process. Concerning the air ratio, the relevant parameter is the effective air ratio related to the air removed in the foam.

Comments

In general ink collection is mainly produced by turbulent mixing, i.e. in the mixing zone which is a continuation of the aeration zone. Ink collection occurs as soon as air is in contact with the fibre suspension, i.e. in the aeration zone, and is continued in the separation zone. Ink collection and detachment are simultaneous processes, the latter being increased when bubbles have caught a lot of ink particles, i.e. in the separation zone and for large particles. Consequently, turbulence has to be lower in the separation zone in order to avoid detachment of large particles. A high turbulence produces small bubbles and is necessary for ink collection on these bubbles, while a lower turbulence corresponds to large bubbles. The separation zone is supposed to produce more additional ink attachment for large ink particles and specks than for small particles, especially with large bubbles. In the particular case of cyclone flotation, aeration, mixing and separation are performed in a single process as soon as the bubbles escape from the porous wall. The high acceleration increases drastically the collision rate and the bubble migration velocity, which allows to separate smaller bubbles from the pulp suspension than with conventional flotation. However, the contact time between bubble and particle is reduced as the bubble velocity is increased, which reduces the probability of particle adhesion as reported by Schulze [14].

Flotation kinetics

It is generally agreed that flotation is a first order kinetics process with respect to the number of particles and bubbles of fixed characteristics, which interact per unit volume and time. This has been extensively discussed and shown in mineral flotation [1,2] as well as more recently in the case of ink particles in fibre suspensions [15,20,23].

The simplest form of kinetic Equation describing the flotation micro-processes involved in particle-bubble collection is given by the variation with flotation time of the number of particles in a given cell volume [16,67], where particles collected are effectively removed from this volume:

$$dN_p/dt = -\, z\, N_p N_b P_c P_a P_s \tag{3}$$

where N_p and N_b are the numbers of particles and bubbles per unit volume, $Z = z\ N_p\ N_b$ is the number of particle bubble collisions per unit time and volume, and P_c, P_a and P_s are the probabilities of particle-bubble collision, attachment and stabilisation against external stress forces.

Flotation rate constants usually refer to the flotation time ($k = z\ N_b\ P_c\ P_a\ P_s$ from Equation 3) which is convenient for comparing the relative floatability of different materials under a given set of conditions in laboratory cells with internal re-circulation and aeration, but does not allow different types of laboratory or industrial cells to be compared. Such comparisons are much easier if the volume air to pulp ratio is considered instead of the flotation time to define the flotation rate constants.

If one considers a small relative variation $\Delta N_p/N_p$ of the particle number in a unit volume of aerated pulp during the contact time $\Delta t = t_c$ under given aeration conditions (air ratio and bubble size distribution) and turbulence, assuming that the number ΔN_p of particles collected during the contact time t_c is proportional to the total number N_p of particles in the unit volume (first order kinetics) Equation 1 can be written in the form:

$$\Delta N_p/\Delta t = \Delta N_p/t_c = -\, z\, N_p\, N_b\, P_c\, P_a\, P_s = -\, k\, N_p \qquad (4)$$

A similar Equation can be written with respect to the air ratio T and the associated flotation rate constant K, if one considers a small fraction ΔT of the air ratio:

$$\Delta N_p/\Delta T = -\, K\, N_p \quad \text{or} \quad \Delta N_p/N_p = -\, K\, \Delta T \qquad (5)$$

where ΔT is a function of bubble diameter d_b and number N_b per unit volume:

$$\Delta T = N_b\, (\pi d_b^3/6) \qquad (6)$$

which, from Equation (4) gives:

$$\begin{aligned} \Delta N_p/\Delta T &= -\, z\, N_p\, (6\, t_c\, /\pi d_b^3)\, P_c\, P_a\, P_s \\ \text{or} \quad \Delta N_p/N_p &= -\, z\, P_c\, P_a\, P_s\, (6\, /\pi d_b^3)\, t_c\, \Delta T \end{aligned} \qquad (7)$$

The flotation rate constant K with respect to the air ratio is then given by:

$$K = z\, (6\, t_c\, /\pi d_b^3)\, P_c\, P_a P_s \qquad (8)$$

For small variations of $\Delta N_p/N_p$ and ΔT and after integration, Equation 5 takes the following form where N_{po} is the particle concentration at $T = 0$:

$$\ln N_p/N_{po} = -\, K\, T \qquad (9)$$

The flotation efficiency E for a given air ratio is then defined by:

$$E = 1 - N_p/N_{po} = 1 - \exp(-\, K.T) \qquad (10)$$

In reality, Equations 4–10 are not rigorous to describe real flotation conditions since it is assumed that the successive collection processes at each aeration step (ΔT increase of the air ratio) are achieved under constant conditions (amount of air, bubble size distribution and turbulence) and over a very short time with respect to the proportion of collected particles, which is generally not the case (typically about 50% air and decreasing turbulence at each aeration step of industrial units).

However the approximation is convenient as most of the flotation installations are based either on several aeration steps in the case of continuous industrial flotation installations, or on re-circulation in the case of laboratory batch flotation devices. In the case of column flotation, the successive collection steps are achieved in one aeration step under roughly constant conditions and over the cell height which defines the contact time.

The influence of contact time (t_c) and air ratio (ΔT) is given in Equation 7, which shows that, the particle flotation rate is proportional to the residence time and amount of air introduced in the cell. Equations 9 and 10 can be used to calculate flotation rate constants with respect to the air ratio (Figures 28 and 29) and assess flotation efficiency.

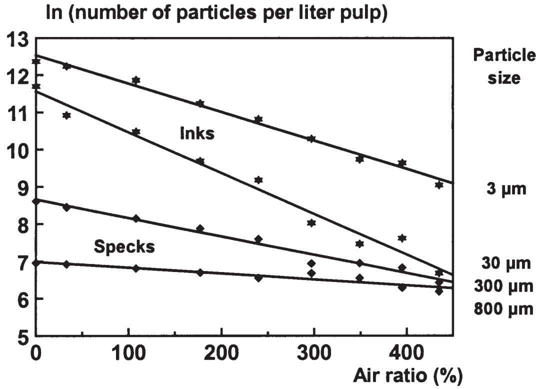

Figure 28 Flotation kinetics of ink particles from repulped magazines with specks [15].

The results shown in Figure 28 to illustrate first order flotation kinetics were obtained with a laboratory flotation cell operated in re-circulation on a feed chest under aeration conditions producing bubbles in the size range of 2–3 mm [15]. Pulp with ink particles from re-pulped magazines and added flat shaped specks (about 5 μm thickness) from re-pulped UV varnished prints

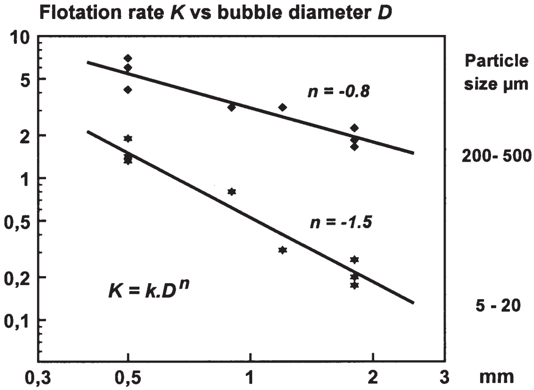

Figure 29 Flotation rate constants of various ink particles versus bubble size [38,65].

were used. The large ink particles gave the highest flotation rate constant (1.2 for the 30 μm particles), and a large decrease of the rate constant with particle size was observed for the specks (from about 0.7 down to 0.2 for 300–800 μm particles). In terms of efficiency, a rate constant of about 1 is necessary to achieve high removal efficiency up to 95% for about 300% air ratio which is a common figure in industrial systems (Table 1). A rate constant lower than 0.2 corresponds to very low floatability while a rate constant higher than 5 ensures almost complete particle removal.

Good correlation should be obtained between laboratory and industrial flotation conditions for similar distributions of bubble size, turbulence level and contact time, as far as the inked particles are correctly removed with the foam. In addition it has to be pointed out that only the ratio of removed air should be considered since small bubbles which may be dragged in the accepts do not contribute to the particle removal efficiency. The smallest bubbles do not contribute significantly to the air ratio whereas relatively few large bubbles may increase significantly the air ratio, though their contribution to the flotation efficiency is low (Figure 29).

The results in Figure 29 were obtained with another laboratory flotation cell, specially designed to produce calibrated bubbles and equipped with a stirrer located in such a way to investigate separately the effects of bubble size and turbulence, since these parameters were linked in the previous design using a stirrer above a porous air injection plate [65].

Indeed, the effects on particle flotation rates of the hydrodynamic parameters such as turbulence and number and size of bubbles and particles are given by Equation 4. This simplified kinetic Equation does not take the balance between free and attached particles into account, since the probability (1-P_s) that a particle-bubble aggregate becomes unstable applies on the number of these aggregates while the cumulated probability (P_c P_a P_s) applies on the numbers of free particles and bubbles [29,68]. It is suggested that particle-bubble detachment should depend on the frequency of external stress in the turbulent flow field which should be related to the collision frequency.

Referring to Equations 4–10 experimental results can be compared to the prediction of the theory [38], on the basis of the Equations and comments given by Schulze [16] about the individual probabilities (P_c, P_a and P_s) of the subsequent collision, attachment and stabilisation micro-processes.

Under turbulent flow conditions (energy dissipation ε) where inertial effects determine the relative velocity of particles about to collide, the number of particle-bubble collisions per unit time and volume is given by the following expression [16,67] adapted from Abrahamson's analysis [69]:

$$Z = (8\pi)^{1/2}\, N_p\, N_b\, d_{pb}^{\,2}(v_{tp}^{\,2} + v_{tb}^{\,2})^{1/2} \tag{11}$$

where $d_{pb} = (d_p + d_b)/2$ is the contact distance and $(v_{ti}^{\,2})^{1/2} = 0.33\ \varepsilon^{4/9}\ d_i^{\,7/9}\ \nu^{-1/3}\ (\Delta\rho/\rho)^{2/3}$ is the effective RMS value of relative velocity between particle or bubble, and the fluid.

As the bubbles are generally much larger than the particles to be collected ($d_b \gg d_p$) and have a higher density difference ($\Delta\rho/\rho$) with respect to the fluid compared to ink particles, d_p and $v_{tp}^{\,2}$ can be neglected in Equation 16 which becomes:

$$Z \approx (\pi/2)^{1/2}\, N_p\, N_b\, d_b^{\,2}(0.33\ \varepsilon^{4/9}\ d_b^{\,7/9}\ \nu^{-1/3}\ \rho^{-2/3}) \approx 0.41\ N_p\, N_b\, d_b^{\,25/9}\ \varepsilon^{4/9}\ \nu^{-1/3} \tag{12}$$

For smaller particles and bubbles, i.e. if d_{pb} is small compared with the smallest eddies in the suspension and particles follow the fluid motion completely, collision is controlled by the velocity gradient within the eddies and particle inertial forces can be neglected. Calculations based on the Smoluchowski mechanism for gradient collision in laminar flow and on the use of the relation between the shear rate $G = (\varepsilon/\nu)^{1/2}$ and the energy dissipation [70], gave [69]:

$$Z = (8\pi/15)^{1/2}\, N_p\, N_b\, d_{pb}^{\,3}(\varepsilon/\nu)^{1/2} \tag{13}$$

As the collision rates have been evaluated in the turbulent flow, one has to consider the collision probability which is governed by the flow lines around the bubble assuming that the particle is much smaller than the bubble. The fact that collision occurs does not imply that a particle-bubble aggregate has formed, but it only means that the particle and the bubble are close enough for physical-chemical forces and thin film dynamics to become significant.

Referring to Figure 30 where R_c is the capture radius which defines the

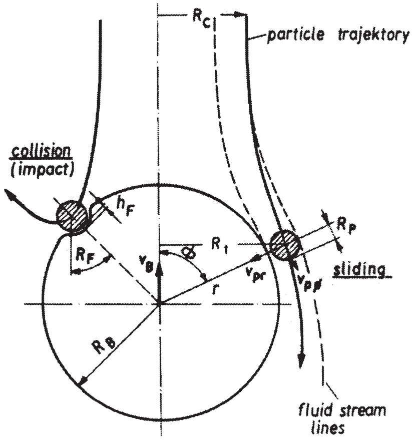

Figure 30 Schematic drawing of particle-bubble collision and sliding processes [16].

streamline tube where the particle must move to be intercepted by the bubble, R_p and R_b the particle and bubble radii, the collision probability is defined as:

$$P_c = (R_c/R_b)^2 \tag{14}$$

The Stokes number St and the bubble Reynolds number $Re_b = v_b\, d_b\, \rho_l/\mu_l$ are critical in defining the flow parameters that define the collision probability P_c. The Stokes number represents a ratio of inertia to drag forces and is defined as:

$$St = Re_b\, \rho_p\, d_p^2 / 9\, \rho_l\, d_b^2 = \rho_p\, d_p^2\, v_b / 9\, \mu_l\, d_b \tag{15}$$

In typical flotation cells Re_b is thought to be in the range of $1 < Re_b < 100$. In this intermediate bubble flow regime, between Stokes flow and potential flow, with a Stokes number $St \ll 0.1$ and with rigid bubble surface, the Equation of the collision probability is given by [14,16,29,71]:

$$P_c = (3/2 + 4\ Re_b^{0.72}/15)\ (R_p/\ R_b)^2 \tag{16}$$

This Equation of the collision probability is valid for particles smaller than 100 μm and bubbles smaller than 1 mm having rigid interface due to adsorbed surfactants [16,71].

The probability of attachment in flotation deinking is mainly described by the sliding process of the particle along the bubble surface since the ink particle density is relatively low with respect to the density of mineral particles where the collision process is more relevant [16,72]. The sliding and collision processes are illustrated in Figure 30. The attachment probability has been evaluated from calculations based on the film drainage time necessary to reach the critical thickness, with respect to the sliding time.

Expressions have been proposed for the critical thickness that the film must thin down in order for rupture to occur, but they cannot be used directly [71]. The Equations of the attachment probability P_a have to be solved numerically [73]. Nevertheless it has been reported that for given physical-chemical conditions (particle surface properties, flotation chemistry and temperature) the attachment probability is reduced as the sliding time decreases, i.e. for large bubbles and higher acceleration, and also as particle size is increased because of the larger film area to be drained off [16].

Concerning the stabilisation probability the results reported in [16] showed that the probability of detachment can be neglected for low density particles (1.1 g/cm3) and size (< 200 μm), even at quite high energy dissipation (130 W/Kg) and for very small bubbles (0.3 mm) with respect to the relevant flotation deinking conditions.

The drawings in Figure 31 illustrate particle-bubble detachment mechanisms, which were postulated to explain experimental results obtained with 0.5 and 1.8 mm bubbles and showing that a turbulence increase improved strongly the flotation rates with small particle (< 20 μm), which is in agreement with the influence of the energy dissipation on the collision rate ($Z \propto \varepsilon 1/2 \propto U$) in Equation 13. The flotation rates only increased slightly with larger particles (> 75 μm) and decreased slightly with the largest particles (> 300 μm) and with the large bubbles only [38,65].

In the case of small 100 μm particles caught at the front side of a large 1.8 mm bubble and entrained along its surface, attachment is achieved if the sliding time is larger than the film drainage time. Once collected onto the bubble, small particles with respect to bubble size are swept to the back of the bubble, where they should be protected from further detachment because of the back flow vortices in the wake.

By contrast, in the case of large particles with respect to the bubble size, the relative contact time under turbulent accelerations may be too low to achieve

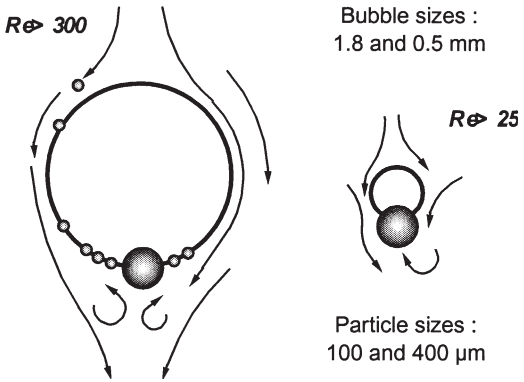

Figure 31 Schematic drawing of particle-bubble aggregates in turbulent flow [65].

particle-bubble attachment and stabilisation. Moreover the particles collected onto the bubble are more subject to detachment under external stress produced by the turbulent flow field since large particles are not caught in the fluid lines around the bubble.

Julien Saint Amand [38,65] discussed the experimental results obtained regarding the influence of bubble size on the basis of the characteristics of the turbulence in the cell and with respect to the theory. From the relations, giving the collision rate for inertial approach mechanisms (Equation 12) and for gradient collision (Equation 13) and combined with Equations 3 and 8, it follows respectively:

$$K = 12\, t_c\, (2/\pi)^{1/2}\, d_{pb}^{\;2}\, d_b^{\;-3}\, (v_{tp}^{\;2} + v_{tb}^{\;2})^{1/2}\, P_c\, P_a\, P_s$$
$$\approx 0.8\, t_c\, d_b^{\;-2/9}\, \varepsilon^{4/9}\, \nu^{-1/3}\, P_c\, P_a\, P_s \qquad (17)$$
$$K = 12\, t_c\, (2/15\pi)^{1/2}\, (d_{pb}/d_b)^3\, (\varepsilon/\nu)^{1/2}\, P_c\, P_a\, P_s \approx 0.3\, t_c\, (\varepsilon/\nu)^{1/2}\, P_c\, P_a\, P_s \qquad (18)$$

which gives the following relation (for $d_b \gg d_p$):

$$K \propto d_b^{\;n}\, \varepsilon^r\, P_c\, P_a\, P_s \quad \text{with} \quad -0.22 < n < 0 \quad \text{and} \quad 0.44 < r < 0.5 \qquad (19)$$

Assuming that particles and bubbles are small compared to the smallest eddies in the flotation cell, the bubble velocity to be used for the calculation of the Reynolds number in Equation 16 is roughly given by the terminal velocity determined in water with surfactants [1]. It follows from the theoretical rising velocities of the bubbles produced in the cell (5 to 15 cm/s for 0.5 to 1.8 mm bubbles), that the collision probability P_c is roughly proportional to $d_b^{-0.9}$ and to d_p^2. In addition it has been shown [71] that P_c varies as $d_b^{-0.46}$ for very large bubbles and as d_b^{-2} for very small bubbles.

Under the experimental flotation conditions and according to a detailed analysis of available theory, the influence of bubble diameter d_b on the probability of collision P_c and on the probability of adhesion by sliding P_a depends on the particle diameter d_p [74]:

$P_c \propto d_b^{-1}$	for	$25 < d_p < 50\ \mu m$
$P_c \propto d_b^{-0.75}$	for	$50 < d_p < 200\ \mu m$
$P_c \propto d_b^{-0.35}$	for	$d_p > 200\ \mu m$
$P_a \propto d_b^{-0.75}$	for	$d_p < 50\ \mu m$
$P_a \propto d_b^{-0.63}$	for	$d_p > 50\ \mu m$

the relations about adhesion probability being only valid for bubbles with a rigid surface i.e. with surfactants (higher dependence of P_a on bubble size with mobile bubble surface).

Assuming that the detachment probability is low ($P_s \approx 1$), which should be valid for the small particles [16] the relation between flotation rate constant and bubble size is then:

$K \propto d_b^n$	with:	$-1.97 < n < -1.75$	for small particles
		$-1.20 < n < -0.98$	for large particles

The higher limits of these n values are in quite good agreement with the experimental results shown in Figure 29, which suggested that the mean collision rate under the flotation conditions in the cell was better described by gradient collision (Equation 13). Experimental results [55] reporting flotation rates of latex particles with different bubble sizes at moderate turbulence, gave n values between −1.1 and −1.5 for particles between 4 and 30 μm and bubbles between 75 and 650 μm. At high turbulence, lower n values between −0.8 and −1 were reported. These results are in agreement with the results shown in Figure 29 for the small particles ($n = -1.5$ at low turbulence), and with the results about the effect of turbulence, i.e. lower influence of bubble size at low turbulence [38,65].

A major conclusion about the effect aeration conditions is that, on average in a large particle size range, the flotation rate constants are roughly proportional to the inverse of the bubble diameter ($n = -1$). This means that, as suggested in [22] and reported in [33], the specific phase interface (total bubble surface area per unit pulp volume) is a most relevant parameter to characterise the effect of bubble size and air ratio.

Concerning the effect of particle size on the flotation rate ($K \propto d_p^m$), Equation 16 and the calculations given in [16] for a low particle density ($\rho_p = 1.1$ g/cm^3) as in the case of laser inks, suggest that the flotation rate constant is proportional to d_p (m = 1), while n values of about 0.7 have been reported for flotation trials on latex particles with small bubbles of about 0.5 mm under agitation [67]. Values of less than unity (0.45–0.65) were reported for toner particles in the microscopic size range, indicating a low dependence of the rate constant on particle size [23].

The experimental results reported in [38,65] indicated a similar influence of particle size in the range of 10–100 μm. The values of m were respectively between about 0.5 and 0.7 for the small bubbles and between about 0.8 and 1.1 for the large bubbles, the lower values of m being obtained at low turbulence. It was pointed out that the large particles used in the experiments were broken particles with a rather spherical shape and a significant surface roughness. This made it difficult to compare experimental and theoretical results with respect to the influence of particle size, since it has been shown that particles with sharp edges are more easily captured by bubbles than spherical particles by accelerating the rupture of the disjoining liquid film [72].

For particles larger than about 100 μm no further increase of the flotation rate was observed with particle size. This observation, commonly reported in the field of flotation deinking where large and usually flat shaped specks show a large efficiency drop with particle size, was believed to be mainly due to the detrimental effect of turbulence on the stabilisation of the particle bubble aggregate, as already discussed (Figure 31).

For very small ink particles in the range of 1 μm, experimental results have shown that the efficiency decrease is much lower than predicted by the theory or by extrapolation of the experimental results obtained on laser ink particles between 10 and 100 μm, which is believed to be due to the fact that very small ink particles may be flocculated and thus removed as larger particles [15].

The ink agglomeration mechanisms depend mainly on deinking chemistry but also on turbulence level and particle size, since large flocs including large particles should not be produced at high turbulence. Physical-chemical interactions are thus believed to be of critical importance for the optimisation of turbulence with respect to particle size.

ANALYSIS OF THE EFFECT OF BASIC FLOTATION PARAMETERS

The global performance of flotation deinking systems is practically evaluated in terms brightness gain as a function of the flotation yield and deinking furnish. This mean that results from field experience are difficult to analyse with respect to the flotation theory. The type of inks and printing techniques applied on the recovered papers has a strong influence on the flotation efficiency in terms of brightness gain, as well as the amount of wood-free and wood-containing furnish and the ash content of the deinking pulp.

Since flotation removes inks and fillers, the brightness gain induced by the removal of the inks might be overshadowed by the removal of fillers if the brightness of the fillers is higher than the brightness of the fibres, such as with ONP/OMG mixtures. A better evaluation of flotation efficiencies is obtained with global ink content measurements based on reflected light analysis in the visible and infrared spectrum (ERIC), but the rigorous evaluation of flotation efficiencies requires free ink particle size distribution measurements since inks attached on fibres should not be removed by the flotation cell.

Such measurements are generally not available, since microscopic image analysis is very time consuming. A new system has been recently developed for the on-line analysis of free and attached ink particle size distributions with a resolution down to 3 μm [75]. These measurements give a better insight in the performance of flotation cells.

Machine and Operating Parameters

The parameters which can be changed with flotation cells are essentially the consistency and the reject rate, while the air ratio is normally kept constant with injector cells at the optimum value which depends on the characteristics of the air injector and of the cell since bubble size decreases as the air ratio is reduced. The influence of the cell design parameters can be assessed by the Equation below obtained from Equations 7–8–13:

$$\Delta N_p/N_p = -(3/10\pi)^{1/2}\,(\varepsilon/\nu)^{1/2}\,T_c\,\Delta T\,P_c\,P_a\,P_s \tag{20}$$

This Equation is interesting as it clearly shows that the flotation kinetics increase with the added air ratio ΔT, the turbulent energy dissipation ε, the contact time T_c and the temperature represented by the viscosity decrease $1/\nu$.

Practically, since the turbulence in the aeration and collection zone is generally high with short contact time and decreases in the collection and separation zone where residence time is longer, one should consider the term $\Sigma(\varepsilon/\nu)^{1/2}\,t_c = \Sigma(\varepsilon\nu)^{-1/2}\,\varepsilon\,t_c$ in Equation 20 which is related to the total energy $\Sigma\varepsilon\,t_c$ dissipated in the flotation cell.

The other practical consequence of the basic research about the influence of bubble size is that the important parameter in the aeration process is the specific phase interface, i.e. the total bubble surface area introduced in the cell with respect to the pulp flow rate. Typical air ratios used in practice are given in Table 1, showing that a minimum amount of air, which depends on the aeration technique, has to be supplied to the cell. The data suggests that smaller bubbles are produced with injectors than with mechanical devices.

A consistency increase is known to reduce the flotation efficiency, though relatively few data has been published in this respect, even in terms of brightness drop. The negative effect of a consistency increase was shown to be higher with large specks compared to microscopic inks [15], since increasing the fibre consistency should reduce the collision rate as turbulence is reduced and increase the detachment probability of large particles.

A reduction of the flotation losses is known to reduce the ink removal efficiency. The results obtained on laboratory scale showed no impact of bubble size as the flotation efficiency was plotted against the fillers and fines losses, which is not surprising as ink particles are in the same size range as fillers and fines [65]. As reported in the first section, there are different means to optimise the foam reject rate with respect to the flotation yield and brightness requirements. The on-line control of the residual ink is therefore a promising tool to control the flotation losses and optimise the final pulp brightness if the characteristics of the deinking furnish are not constant [75].

Material Parameters

The surface properties of the ink particles and the deinking chemicals have clearly the highest impact on the flotation efficiency, since even very small ink particles, which normally should not be removed as their inertia is too small to reach the bubble surface, are effectively removed if proper chemistry is used to collect them in hydrophobic flocs.

The particle surface properties govern the particle-bubble adhesion probability P_a and stabilisation probability P_s. The non-hydrodynamic forces involved in the flotation process have been investigated in several papers [11–14,16–20,28,29,73] on the basis of experimental results and theoretical analysis. The influence of flotation chemicals on the particle surface energy and on the flocculation of ink particles is out of the scope of this paper. A direct relation between the surface energy of hot melt glues and their flotation efficiency was reported in [11], while other investigations showed no direct correlation between laser ink flotation efficiency and surface energy measurements [76]. The flotation ability of PSA particles showed to depend not only on the type of adhesive, i.e. on the particle surface energy, but also on the pulping pH, which suggested that adhesive components might have been dissolved in the pulper [77].

The influence of particle size on flotation efficiency is illustrated in Figure 1 and has been discussed in the previous section. In the specific case of laser inks, which are molten on the paper in printing machines, the flotation kinetics are strongly reduced if the ink is not completely detached from the fibres, as the collection of "hairy" particles on the bubbles is hindered by the fibres attached to the laser particle [23,25].

The influence of particle shape has been investigated in a single-bubble flotation tube with model toner spheres and disks of the same toner and particle volume [24]. The visualisation of the particle-bubble collision and attachment mechanisms showed that flat shaped particles did not float as well as spherical particles. Almost all spheres collisions resulted in attachment ($P_a \approx 1$), whereas only 5% of the discs, which showed a higher collision probability (P_c) than the spheres, attached after collision. The low attachment probability of the discs was due to the fact that the particles either bounced off before attachment could occur, or flipped to the side before contact, giving a long contact time but a large liquid film drainage area which took too long to drain off and rupture for attachment to take place, as shown in Figure 32.

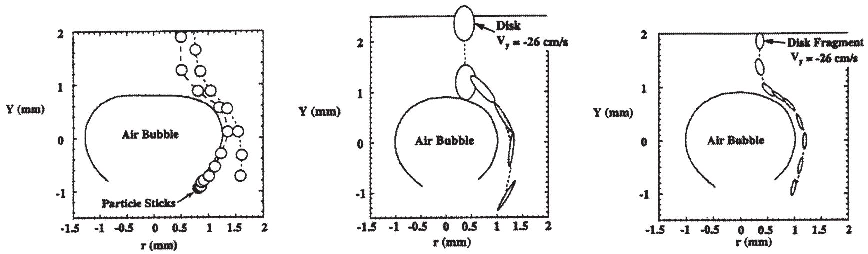

Figure 32 Trajectory of 2 spheres, a disk and a disk fragment colliding with a bubble [24].

The large influence of particle shape on the flotation efficiency was also observed with stickies. Flotation tests performed on deinking pulp containing PSA particles of various shapes and on the same pulp after kneading with PSA particles, which had become more spherical because off the thermal and mechanical action, showed a strong increase of the flotation efficiency after kneading [77]. The implementation of a flotation cell on tailing screen accepts in a post flotation step of a newsprint mill confirmed the possibility to achieve good stickies removal efficiency after hot dispersing [78].

The temperature affects the physical-chemical interactions and reduces the viscosity. A high flotation temperature increases the bubble rising velocities and reduces the liquid film drainage and rupture time in the particle bubble adhesion process, which has a positive influence on the flotation efficiency.

As a practical conclusion about flotation hydrodynamics, it appears that ample air should be supplied to increase ink and speck removal rates, that aeration should be achieved under high turbulent mixing conditions to produce small bubbles and promote collision with the microscopic ink particles, and that subsequent separation should be achieved under lower and optimised turbulence in order to promote stable attachment of large particles on the bubbles and limit fibre losses. Strong agglomeration of the smallest ink particles may be another approach to optimise flotation under lower turbulence.

Current technology generally involves such flotation conditions, with some differences concerning relative optimisation of aeration, turbulence and flotation time. In all cases increasing the amount of small bubbles, turbulence and contact time leads to increased energy and investment costs to achieve the highest flotation efficiencies.

Further improvement of flotation technology with respect to cost effectiveness might be expected on the basis of optimised hydrodynamic parameters such as turbulence, bubble size and contact-time distributions. These must be adapted to particle size, shape and density, as well as to surface chemistry in relation to the decisive micro-processes of ink agglomeration and liquid film drainage and rupture time.

WASHING

Washing commonly refers to two different applications, the washing of virgin pulps and the washing of recycled pulps. As a particle separation process, the second application will be briefly analysed while the first application is out of the scope of this paper.

Washing of secondary fibres is essentially used in the wash deinking process [1]. Physical-chemical aspects of wash deinking will not be treated in this section, which is focused on the mechanical separation phenomena. Washing is basically a dimensional separation process which differs from screening in the fact that accept fibres are retained while contaminants, i.e. the ink particles, pass the barrier. As illustrated in Figure 33, washing is also a fractionation process since fillers and fines are removed with the ink particles, and it is always associated with pulp thickening [2].

The washing process was already used in the early deinking systems. In the late 1970's washing had a world-wide share of about 35% of the total installed deinking capacity, and there was a strong preference for the washing

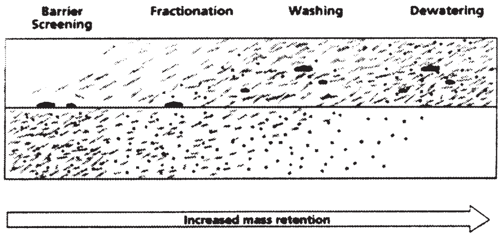

Figure 33 Secondary fibre washing and barrier separation technology [2].

process in North America, while some 90% of the deinking capacity was operated according to the flotation process in Europe and Japan [3]. Washing and flotation are complementary techniques to remove inks in a large particle size range as well as inks with different surface properties [4]. Currently the wash deinking process is mainly used for the production of tissue because of its "deashing" effect while flotation deinking and recently combined processes are used for the production of graphic grades to optimise the deinking yield and the pulp quality. Wash deinking also contributes to the removal of dissolved and colloidal material (more or less removed from the filtrate by dissolved air flotation) from the mill circuits.

In the field of virgin pulp, the washing process aims basically at removing dissolved material and recovering chemicals after the cooking and bleaching stages. Consequently, washing is typically performed at high consistency [6] and the displacement principle can be used to optimise the counter current recovery of the dissolved material (an equal volume of wash water is added to displace in the fibre mat the liquid lost through the separation medium, usually a woven wire mesh as shown in Figure 34). Displacement washing performed on fibre mats in pulp mills is completely different from the washing process used in recycling, which is basically a selective thickening process.

WASHING TECHNOLOGY

The technology used in secondary fibre washing has logically been developed on the basis of thickening (or forming) technology or on the basis of screening technology, as washing is both a thickening and a barrier separation technology (Figure 33). In low consistency washing the task was either to minimise mat formation, as the technology was adapted from thickening (or

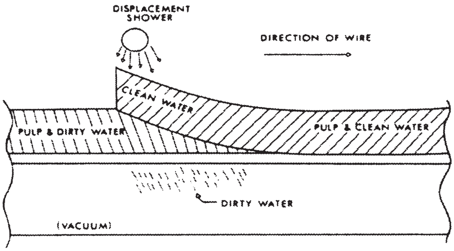

Figure 34 Principle of displacement washing on a rotary vacuum washer [5].

forming) equipment or to minimise the passage of fibres through the screen, as the technology was adapted from screening equipment. On the other hand, the high consistency washing technology is based on the formation of a fibre mat to retain the fibres.

On the whole the washing equipment designed to be operated in a high consistency range, i.e. thickening the pulp from about 3% to 15–30% consistency, is less efficient and more cost effective than low consistency washers where pulp is thickened from about 1% to 5–10% consistency. In addition, the washing water clarification costs depend on the consistency range and on the process water system design.

Low Consistency Washing

The filtering element of low consistency washers is generally a wire screen on which pulp is retained while fine particles are washed through the screen. Some clear water is normally used to clean continuously the wire screen with showers.

The sidehill washer has been one of the first washing equipment used in North America [7]. Low consistency pulp was poured on top of an inclined wire screen. The washed pulp was recovered at the bottom of the sidehill at about 3% consistency. This technology has been dropped because of too large a space requirement. The efficiency and capacity of side hill-type washers can be improved by the addition of mat disrupting means under the wire [8].

Drum washers, known as gravity deckers, have been the most frequently used in the first wash deinking mills. The fibre mat, which is formed in drum thickeners operated at low rotation velocity, is disrupted as the drum velocity is increased (to about 100 m/min) in gravity deckers. The efficiency of gravity deckers can be improved by the addition of a simple mat disrupting device [9].

Disc filters can be used as well for wash deinking by increasing the rotation speed to avoid mat formation [10].

Recently, a new drum-type washer has been developed to improve the efficiency in the high consistency range [11]. The pulp is fed via a headbox between the rotating drum with fabric and a stationary plastic flap. When the consistency has reached 10 to 15% after dewatering of the pulp under low vacuum, the pulp starts to roll and dewatering continues until a consistency of about 25% is reached. A press roll can be added to bring the consistency to 30–40%. The removal of small particles is enhanced at high consistency since the fibre mat is continuously broken up and rolled between the moving fabric and stationary flap.

The old spray filtering technology, which was first used in laboratory washing devices and in mills for the recovery of fibres in process water, has been combined with the drum or disc washing technology. As pulp is sprayed on a wire screen the filtration pressure and the turbulence are increased in such a way to promote the passage of the fine particles through the wire. In the case of rotating discs, the centrifugal force created by the rotation of the discs causes the washed fibres to move radially and discharge from the disc, thus avoiding mat formation [12]. In the case of the rotating drum, the pulp is sprayed onto the drum surface in successive zones in order to maintain the fluidisation of the pulp and avoid mat formation. A compacting zone is used at the end to increase the outlet consistency and consequently the washing efficiency [13].

High-speed belt washers have gained large acceptance over the two last decades because of their advantages in terms of high washing efficiency due to minimal mat formation, high thickening factor, some flexibility and compact design, while disadvantages include increased losses as a consequence of higher efficiency, power consumption, capital costs and maintenance due to high speed and periodic replacement or cleaning of the wires [1].

The first high-speed belt washer proposed on the market was a single belt and single nip washer (Figure 35). Pulp is injected between the wire and the roll. Filtrate is removed through the wire by centrifugal force, wire tension and dynamic head of the inlet jet. Washed pulp is collected by a doctor blade from the centre roll. Production and washing efficiency depend on inlet consistency (about 1%), outlet consistency (6–10%), wire speed (350–1000 m/min) and basis weight, typically 20 to 100 g/m^2 [14]. A version with a second single nip and roll implemented on the same wire is now available.

A double nip single wire high-speed belt washer has been developed more recently [15]. As shown in Figure 36, pulp is injected in the first nip formed by a grooved breast roll and the wire, resulting in high feed pulp capacity. The pulp is deposited on the wire and dewatered around the breast roll, travelling

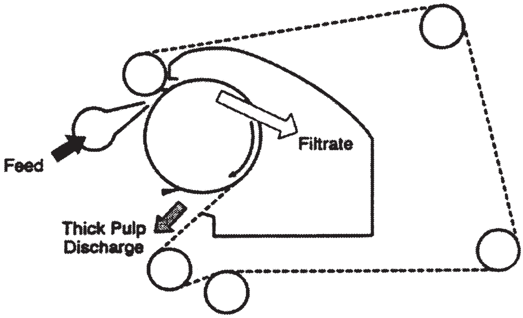

Figure 35 High-speed belt washer with single belt and single nip [14].

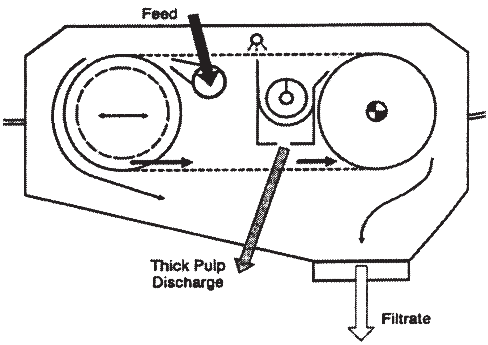

Figure 36 High-speed belt washer with single belt and double nip [16].

to the couch roll where it is dewatered a second time to produce highly washed and thickened stock up to 15% consistency.

The latest high-speed belt washer is a single nip double wire washer, characterised by a two-sided washing [17]. The pulp is injected between two wires and the filtrate is removed from both sides, using blades to improve the drainage. The combination of two-sided dewatering/washing and turbulence generating technology allows to reach a good washing efficiency at higher basis weights compared to single side dewatering. Typically the consistencies are about 1% at the inlet and 11 to 14% at the outlet, with a wire speed of 250 to 500 m/min and basis weight range of 100 to 300 g/m^2.

Pressure screening technology has been adapted to low consistency washing by using finely perforated screen cylinders and a bump rotor [18].

Typically the inlet consistency is about 1% and the "reject" consistency of the washed pulp 5%. The technology can also be used for fibre recovery from process water [19]. Typically, the size range of the micro-holes in the filtering basket is 0.1 to 0.4 mm, using drilling techniques such as the electron beam [20]. The washing technology with pressure screens has also been termed "reverse screening" since contaminants pass the apertures and fibres are retained on the screen cylinder, which is the inverse situation with respect to normal screening.

High Consistency Washing

Basically high consistency thickening equipment, i.e. screw thickeners or screw presses, belt presses, disc or cylinder presses, can be used to produce more or less wash deinking depending on the ink particle size distribution and on the internal thickening process (mat formation, filtering, mixing). Filtration is performed through the fibre mat of fibre flocs formed on perforated cylinder plates with relatively large holes (1 to 2 mm).

Inclined screw thickeners or screw extractors (Figure 37) are operated at a minimum inlet consistency of about 2 to 3% for wash deinking applications in order to avoid excessive fibre losses through the perforated screen cylinder [1,21]. Discharge consistencies are generally in the range of 10 to 15%, depending on the type of pulp and on the outlet design (the counter pressure is mainly produced by the friction of the thick pulp on the cylinder plate).

Screw Presses are basically screw thickeners equipped with additional pressing means designed to increase and control the outlet consistency. They are operated in a higher consistency range, typically from 4 to 5% and more at

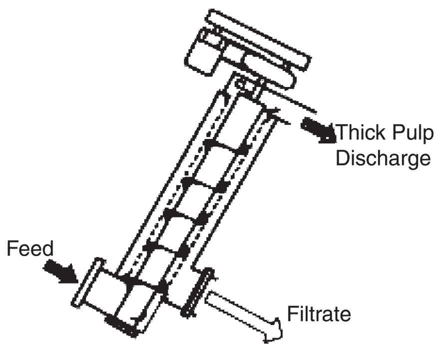

Figure 37 Inclined screw thickener.

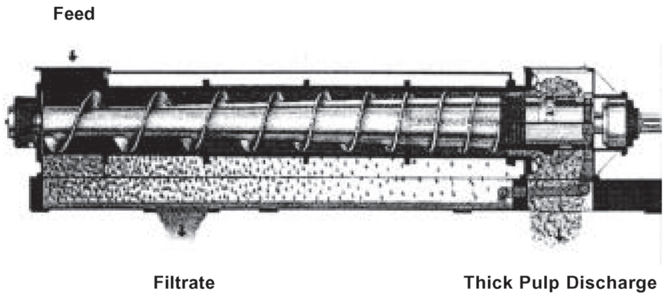

Figure 38 Screw press with conical shaft [28].

the inlet, to about 25 to 35% at the outlet. The tumbling washing process observed inside a screw press (as the fibre mat on the screen surface surrounding the screw is tumbled around, new material is exposed to the screen surface) improves the washing efficiency despite mat formation [22,23].

Belt presses are operated in a similar consistency range than screw presses. The pulp is fed between two low speed wires, squeezed in a dewatering zone and then into a high pressure zone. A continuous fibre mat is formed along the dewatering/washing process. Belt presses as well as screw presses are also used to thicken sludge.

The characteristics of washer and thickeners commonly used in wash deinking are summarised in Figure 39 showing the feed and outlet consistency ranges as well as the hydraulic split range, which is also the theoretical washing efficiency [9].

WASHING MECHANISMS AND THEORY

In the ideal case of wash deinking, the amount of ink removed is proportional to the amount of water removed if, firstly, the ink particles are so small that they are not retained by the fibre mat or filtering element and, secondly, if they are well dispersed, in other words, a redepositing on the fibres is prevented. In practice this is not entirely true because the fibre network always acts like a filter. Once the ideal case has been treated, the theory of secondary fibre washing seems to have been less investigated than in pulp washing, where permeability Equations of fibre mats as well as diffusion Equations and related similitude have been used to predict displacement washing efficiencies [24–26].

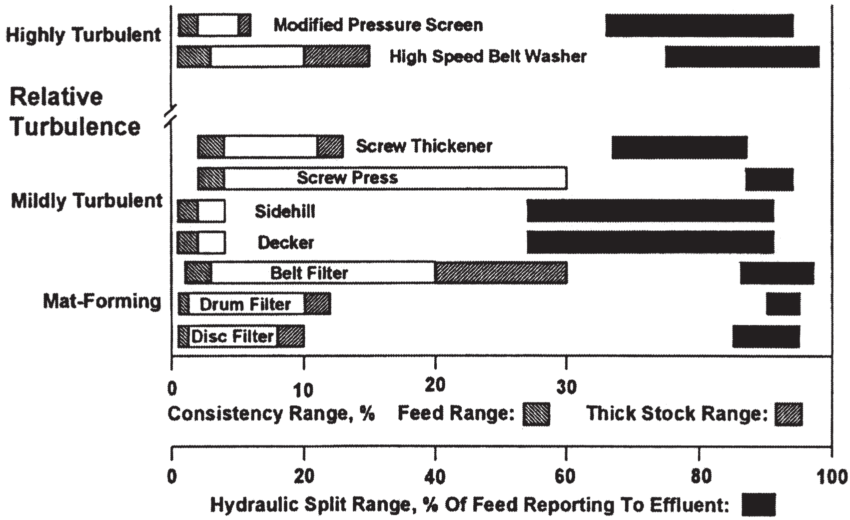

Figure 39 Characteristics of commonly used deink washers and thickeners [9].

Since no dilution water is added in the secondary fibre washing process (neglecting the transport of wire washing water), the theoretical washing efficiency can be easily calculated with a material balance in the ideal case where the amount of fine particles removed is proportional to the amount of water removed, i.e. the concentration of fine particles with respect to the fluid is constant in the washer. With similar definitions and inverse symbols with respect to screening (screen rejects become filtration accepts):

C, c	total concentration, fine particle (ash, ink) concentration, (g/l)
i, a, r	inlet, accepts (washed pulp outlet), rejects (filtrate)
$T = Ca/Ci$	accept (washed pulp) thickening factor
$\mathrm{A} = c/C$	ash, ink or fine particle content
Q	water flow rates
$R\mathrm{w} = Cr\,Qr/Ci\,Qi$	reject rate or total solid loss
$E_R = R\mathrm{w}\,Ar/Ai$	removal efficiency of ash, inks or fine particles
$E_C = 1 - Aa/Ai$	cleanliness efficiency, i.e. deashing or deinking efficiency

and with a constant fine particle concentration (ci = ce = ca) the material balance gives:

$$Th.E_c = 1 - \frac{Ci}{Ca} = 1 - \frac{1}{T}$$

The theoretical washing efficiency (E_C) in this relation refers to the ash or ink content reduction in the washed pulp and is established by using the concentrations (in g/l) of the particles with respect to the water [8]. The theoretical washing efficiency (E_R) with respect to the amount of ash or ink rejected is simply given by the hydraulic split [9]:

$$Th.E_R = \frac{Qr}{Qi}$$

The theoretical washing efficiency (E_R) can be given as a function of the consistencies. If using the consistencies C_m given by the ratio of solid matter with respect to the total pulp (water and solid matter), which is the case of thick pulp consistencies given in %, the material balance gives [7]:

$$Th.E_R = \frac{(C_m a - C_m i)(1 - C_m r)}{(C_m a - C_m r)(1 - C_m i)} \approx \frac{(C_m a - C_m i)}{C_m a(1 - C_m i)} \approx 1 - \frac{C_m i}{C_m a}$$

the first approximation corresponding to $C_m r \ll C_m a$, i.e. to high yield washing and the second also to $C_m i \ll 1$, i.e. to high yield low consistency washing.

The direct relation between the theoretical washing efficiencies and the thickening factor shows the importance to increase the drainage of the pulp. The techniques used to improve the pulp drainage aim at increasing the filtration pressure by gravity, vacuum, jet impact, centrifugal action, squeezing and pressing.

The washing mechanisms in low consistency washers include sheet forming mechanisms as fibres are deposited on the wire. The technology of high-speed belt washers has in fact been adapted from the gap forming technology. The drainage conditions in single belt washers are similar to the drainage conditions in roll formers, while drainage in the double belt washer is similar to drainage in blade formers. The drainage pressure in the nip is given by the dynamic head of the jet with respect to the velocity in the nip in the direction of the wire and by the normal component of the dynamic head if there is an impact angle with respect to the wire direction. The drainage pressure is then, in single belt washers, produced by the wire tension ($P_T = T/R$) and the centrifugal pressure ($P_C = t\,\rho\,V^2/R$ with t: thickness of the pulp layer, V wire speed and R: roll radius). The drainage pressure pulses in the double belt washer also increase with wire tension and speed and depend on blade design.

Information about drainage pressure analysis in roll formers [16,27] and blade formers can be found in several papers about gap forming.

The removal of water along screw presses as the pulp moves forward in the helical channel between the shaft and the screen cylinder, has been described as a filtration process with gradual fibre web built up followed by a pure web consolidation process as the channel is filled with filter cake [28–30]. In the analysis of the water removal process (based on Darcy's law and on pulp specific drainage resistance) the filtered web was assumed to stay fixed on the screen cylinder and then to be doctored by the flight of the screw [30] or to move at the surface of the screen cylinder [28]. In this later analysis, the speed of the filtered web was evaluated with respect to the helical channel assumed to be stationary with a screen plate passing over it. Water removal along the press was measured and the average pulp velocity was found to exceed significantly the apparent forward movement of the flight in the first part of the press. This was explained by assuming a two-phase flow comprising a slowly moving web and fast flowing suspension. As the suspension drains, the moving speed of the web was shown to become the decisive one [28].

Particle Separation

The separation of particles sufficiently small and dispersed to follow the water split is described by the theoretical washing efficiency Equations. Too small particles, which are less sensitive to hydrodynamic forces, might however not be removed according to the water split if the fibres and particles are not chemically dispersed. The separation of the larger particles which can pass the openings of the filter (typically about 0.1 mm) is clearly affected by the fibre consistency and particularly by the formation of a fibre mat. Mat formation and particle retention phenomena in low consistency washers are similar to those observed in paper forming, however with drainage conditions chosen to avoid mat formation, either by reducing the basis weight or by increasing the turbulence.

The ideal particle separation according to the water split becomes much more difficult to achieve in high consistency washers as particle size is increased, because of the higher fibre-particle interactions, the higher turbulence required to avoid pulp flocculation and the faster mat formation for a given drainage rate. The "relative turbulence" (Figure 39) required to avoid mat formation and minimise the fibre-particle interactions increases as the consistency in the washer is increased.

ANALYSIS OF THE EFFECT OF BASIC WASHING PARAMETERS

Performance of washing equipment is generally reported in terms of yield and deinking or deashing efficiency for various deinking furnish. Most of the papers reporting such results are focused on one type of washer and describe the effect of specific parameters. Only general trends are briefly reviewed below because of the large differences between different types of the washing equipment.

Machine and Operating Parameters

As expected from the analysis of the washing mechanisms and theory, the performance of a washing system depends essentially on the thickening factor and on the dispersion level (turbulence, mixing, avoidance of mat formation) achieved in the washer with respect to the inlet to outlet consistency range. The selectivity of the washing process can be evaluated by comparing the real to the theoretical washing efficiency. Table 2 shows the typical theoretical and real ash removal (or deashing) efficiencies reported in [14] and [18] for different wash deinking and thickening equipment.

Table 2 Comparison of washing and thickening equipment according to [14] and [18].

Type of washer	Inlet – Outlet consistency (%)	Theoretical – Real efficiency (%)
Screw press	4.0–28	89.3–35
Inclined screw	3.0–10	72.1–45
Side hill	0.8–3	74.0–60
Decker	0.8–5	84.7–55
Disk filter	0.6–6.8	91.7–50
Pressure screen	0.8–4	80.0–70
High-speed belt washer	0.8–5	84.7–80

As shown in Table 2, low consistency high turbulence washers such as high-speed belt washers, pressure screens or a sidehill-type washer with mechanical mat disruption [8] achieve a more selective washing than high consistency washer. Typical ash removal efficiency ranges of different washing equipment have also been reported in [1,7,11].

Increasing the wash deinking efficiency always reduces the yield since all the parameters which improve the removal of ink particles also increase the

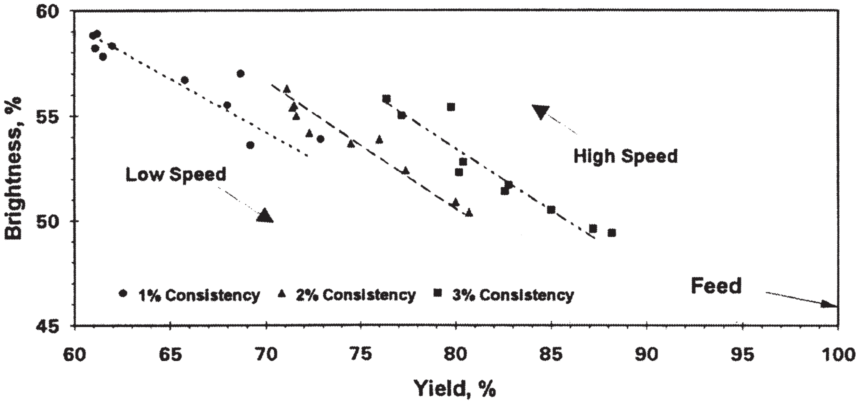

Figure 40 Brightness versus yield for 2-stages high-speed belt washer [9].

removal of fillers and fines, as illustrated in Figure 40, showing the pulp brightness of a 70% ONP 30% OMG furnish reached with a two-stage high-speed belt washer, as a function of the washing yield [9].

The results in Figure 40 confirm the trends observed with all types of washers [11] as the feed consistency is increased, i.e. a decrease of the washing efficiency, and show the effect of the belt speed as the speed range was expanded to 600–1200 m/min. The higher turbulence produced at increasing belt speed improved the deinking efficiency, which, in terms of ash removal, showed to be closed to the theoretical efficiency at the high end of the belt speed range [9].

Material Parameters

The composition of the pulp and the characteristics of the fine particles to remove have a strong influence on the washing efficiency and yield. As previously discussed and illustrated in Figure 1, the wash deinking efficiency decreases strongly as the size of the ink particles is increased from 10 to 100 μm, and to a lesser extent, as the consistency is increased [1,7,18]. Investigations about the relations between efficiency, ink particle size and yield in the case of spray washing, showed that the removal efficiency of large ink particles and the solid losses were increased as the wire opening was increased [12]. Fillers are in general easier to wash out of the pulp than inks because of their smaller size range and the impact of the consistency is lower.

The optimisation of the washing technology depends on the objectives in terms of yield and size range of the particles or matter to be removed. High consistency washers are relatively more competitive for the removal of dissolved matter. Wash water treatment capacity and outlet consistency needs (implementation before dispersing, bleaching storage, screening, etc.) are decisive in the choice of a wash deinking technology.

CONCLUSION

The analysis of the hydrodynamic mechanisms involved in screening, cleaning, flotation and washing, the major particle separation processes used in stock preparation, shows that two different aspects have to be considered: the transport and large scale mixing of the fibre suspension and then the micro-processes which govern the separation of the suspended particles at a smaller scale.

The pulp transport and mixing in the macro-flow of pressure screens, the vortex flow of centrifugal cleaners, the aeration, mixing and separation zones of flotation cells and the various feed flow patterns in the different low consistency washers, can be investigated on the basis of well established knowledge in fluid dynamics, including numerical flow simulation. Commercial CFD codes have however to be adapted to the behaviour of non-diluted fibre suspensions and experimental validation seems to be still necessary.

The separation of the particles in the unsteady micro-flow at the screen plate in pressure screens, in the turbulent and high shear vortex flow in cleaners, in the turbulent three-phase flow in flotation cells and in the turbulent flow at the screen surface in low consistency washers, always involves more or less particle slip with respect to the fluid, contacts with solid walls or with bubbles and contacts between fibres and between fibres and particles to separate from the fibres. Fluid dynamics are more difficult to use at this level because of the unsteady flow at the particle scale, and the numerical simulation of particle motion is particularly difficult with fibres compared to spherical particles.

The behaviour of pulps at higher consistencies and the particle separation mechanisms are believed to be too complex to be treated by numerical simulation in a near future. Progress recently established in the field of fibre flocculation and turbulence interactions on the basis of experimental and theoretical research should contribute to develop a better understanding of the separation processes in concentrated pulps.

Though more fundamental research might become necessary to further develop the understanding of the particle separation processes and numerical simulation will be increasingly used as an engineering tool, applied research based on laboratory and pilot tests will probably still be very important to develop new particle separation equipment and optimise their use in stock preparation.

REFERENCES

1. de Choudens, C., Angelier, R., Combette, Ph., "Pâtes mécaniques de résineux, pâtes chimicomécaniques de feuillus. Nouveau procédé de fabrication", *Revue ATIP*, **38**(8): 405–416, Septembre/Octobre 1984.
2. Kurdin, J.A., Bohn, W.L., "Mechanical pulping by extrusion", TAPPI Pulping Conference, proceedings, 265–274, San Francisco, 12–14 November (1984).
3. de Choudens, C., Angelier, R., "Bleached high yield pulps with the bivis process constituted of two bivis machines in line", *Das Papier*, **43**(10A): 8–12 (1989).
4. de Choudens, C., Angelier, R., Devic, M., Kervennal, J., "Chemithermomechanical pulps at high level of brightness obtained by the bivis process associated with a sulfonation in reducing medium", *Paperi ja Puu*, **72**(3): 248–252 (1990).
5. de Choudens, C., Angelier, R., Brochier, R., Labalette, F., "Manufacture of unbleached high yield pulps for packaging papers by the bivis process from fibre sorghum", 1st European Seminar on Sorghum for Energy and Industry, Toulouse, 1–3 April 1996.
6. de Choudens, C., Angelier, R., "The manufacture of bleached chemical pulps for printing grades from annual plants by the bivis process", International Conference on Sustainable Agriculture for Food, Energy, and Industry, Braunschweig, 27–28 June (1997).
7. Galland, G., Carré, B., Vernac, Y.,, "Deinking difficulties related to waterbased ink printed papers", COST workshop "Waterbased ink and deinking", Grenoble (CTP) 25–26 March, (1998, *Journal of Korea Tappi*, **30**(4): 78 (1998).
8. Julien Saint Amand, F., Perrin, B., De luca P., "Stickies Removal Strategy", *Progress in Paper Recycling*, **7**(4):39–53, August 1998.
9. McCool, M.A., Silveri, L., "Removal of specks and nondispersed ink from deinking furnish", *Tappi J.*, 75–79, November 1987.

Screening

1. McCool M.A., Rosier M.A., "Screening Technology in Recycled Fiber Systems", *Paper Recycling Challenge*, Vol. III: Process Technology, Chapter 3: 29–41, Editors: M.R. Doshi & J.M. Dyer (1998).
2. Julien Saint Amand, F., "Principles and technology of screening", 5th Advanced Training Course on Deinking Technology, CTP, Grenoble, 27–29 March 2001.
3. Selder, H., Siewert, W.H., "The Escher Wyss Fibersorter for the High Density Screening of Recycled Fibres", TAPPI Papermakers Conference, proceedings 1980.
4. Serres, A., Fejoz, R., "Stickies Abscheidung in einem Deinking System. Kritische Punkte. Problemlösungen", *Wochenblatt für Papierfabrikation* **7**, (1989).

5. Lamort, P., "Epuration. Désaération. Evolution des épurateurs sous pression en tête de machine", *Revue ATIP*, **24**(3) (1970).
6. Levis, S.H., "Screening of secondary fibers", *Progress in Paper Recycling*, November 1991.
7. McBride, D., "Deinking systems for office waste paper 'pay now/pay later' choices", *Pulp and Paper*, April 1994.
8. Ingemarsson, B., "Uni-screen meets the test", *Pulp & Paper International*, **13**(5): 52–54, May 1971.
9. Lindström, J., "Removal of abrasive materials with coarse screening on a recycled fiber line", PPI Paper Recycling '96 Conference, London 13–14 November 1996.
10. Fredriksson, B., Olavsen, G., Olsson, G., "High consistency screening of mechanical pulps", EUCEPA International Mechanical. Pulp Conference, proceedings, 39–24, Oslo, 15–17 June 1993.
11. Carvill, R., "High consistency pressurized pulp screening", *Tappi J.*, **51**(9): 104–107, September 1968.
12. Cormack, A.D., "Operating your screening system at maximum efficiency", TAPPI Papermakers Conference proceedings, 141–147, Boston, 9–11 April 1979.
13. Goldenberg, P.H., "Pressure screen improvements with new rotor design", 73rd CPPA Annual Meeting, proceedings, 275–277, January 1987.
14. Yu C.J., "Pulsation measurement in a screen, Part 1: pulse signature and magnitude of s-shape rotor", TAPPI Engineering Conference, proceedings, 767–782, (1994).
15. Frejborg F., "Improvement of new and old screens in cleaning efficiency at maintained or increased capacity" TAPPI Pulping Conference, proceedings, 529–532 (1984).
16. Jepsen, A., "New wave screen baskets upgrade existing systems", TAPPI Pulping Conference, proceedings, 515–520 (1984).
17. Henrich, H.O., Schmidt, K., "Sortierung von mechanischen Holzstoffen mit Schlitzsiebkörben spezieller Bauart", *Das Papier*, **44**(7) (1990).
18. Ora, M., Nerg, H., Saarinen, A., "Advantages of continuous slot screening in broke handling", 81st CPPA Annual Meeting, proceedings, 169–174, Oct./Nov. 1995.
19. Zeeb F. , "Procédé de désencrage. Améliorations et nouvelles technologies", *Revue ATIP*, **48**(5), Septembre/Octobre 1994.
20. Steenberg, B., "Principles of screening system design. Studies in screening theory I", *Svensk Papperstidning*, **56**(20): 771–778, October 1953.
21. Kubat, J., Steenberg, B., "Screening at low particle concentrations. Theory of screening III", *Svensk Papperstidning*, **58**(9): 319–324, May 1955.
22. Wahren, D., "Fundamentals of suspension screening", *Svensk Papperstidning*, **18**: 539–546 (1979).
23. Nelson, G.L., "The screening quotient: a better index for screening performance", *Tappi J.*, **64**(5): 133–134, May 1981.
24. Gooding, R.W., Kerekes, R.J., "Derivation of performance Equations for solid-solid screens", *The Canadian Journal of Chemical Engineering*, **67**: 801–805, October 1989.

25. Gooding, R.W., "The passage of fibres through slots in the pulp screening", Master's Thesis, Dept. of Chemical Engineering, The University of British Columbia, 1986.
26. Kumar, A., "Passage of fibres through screen apertures", PhD Thesis, Dept. of Chemical Engineering, The University of British Columbia, 1991.
27. Tangsaghasaksri, W., "Über die Sortierung von Fasersuspensionen mittels geschlitzter Siebe", PhD Thesis, Technische Hochschule Darmstadt, 1994.
28. Olson, J.A., "The effect of fibre length on passage through narrow apertures", PhD Thesis, Dept. of Chemical Engineering, The University of British Columbia, 1996.
29. Niinimäki, J., "On the fundamentals of pressure screening", PhD Thesis, Faculty of Technology, University of Oulu, 1998.
30. Grégoire, G., "Study and numerical simulation of the flow in an experimental pressure screen", PhD Thesis, Institut National Polytechnique de Grenoble, January 2000.
31. Julien Saint Amand, F., Perrin, B., "Screening: Experimental approach and modelling", TAPPI Pulping Conference, proceedings, 1019–1031, Montreal, 25–29 October 1998.
32. Julien Saint Amand, F., Perrin, B., "Fundamentals of screening: Effect of rotor design and fibre properties", TAPPI Pulping Conference proceedings, 941–955, Orlando, 31 October–4 November 1999.
33. Julien Saint Amand, F., Perrin, B., "Fundamentals of screening: Effect of screen plate design", TAPPI Pulping/Process & Product Quality Conference, proceedings, Boston, 5–8 November 2000.
34. Karvinen, R., Halonen, L., "The effects of various factors on pressure pulsation of a screen", *Paperi ja Puu*, **2**: 80–83 (1984).
35. Schabel, S., "Lässt sich die Sortierung von Stickies noch weiter verbessern", *Wochenblatt für Papierfabrikation*, **21**: 1098–1102, November 1998.
36. Grégoire, G., Favre-Marinet, M., Julien Saint Amand, F., Serres, A., Fernandez de Grado, A., "Modelling of the productive and reverse flow at the screen surface", COST Workshop "Recent Research in Multi-Phase Flows in Paper Making", Paris, 12–13 Novembre 1998.
37. Marko, J.J., LaRivière C.J., "The use of computational fluid dynamics (CFD) in pressure screen design" TAPPI 99, proceedings: 1477–1482 (1999).
38. Wikström, T., Fredriksson, B., "Hydrodynamics in a pressure screen – Consequences on the separation process", 5th Research Forum on Recycling, proceedings, 197–202, Ottawa, 28–30 September 1999.
39. Grégoire, G., Favre-Marinet, M., Julien Saint Amand, F., "Numerical simulation of the flow in a pressure screen", COST Action E7 Final Conference "Multiphase Flows in Papermaking", proceedings poster session, Manchester, 13–14 April 2000.
40. Grégoire, G., Favre-Marinet, M., Julien Saint Amand, F., "Modelling of turbulent fluid over a rough wall without or with suction", paper submitted to the *Journal of Fluids Engineering*.

41. Fredriksson, B., "Screening of recycled fibre pulps at high consistency", EUCEPA Symposium Recycling (1995).
42. Forgas, O.L., Robertson, A.A., Mason, S.G., *Pulp and Paper Magazine Canada*, **59**(9): 117–128 (1958).
43. Duffy, G., Ragnar, E.K., Moller, K., Norman, B., "Hydrodynamics of papermaking fibres in water suspension", 6th Fundamental Research Symposium, trans., session 3, No. 1, Oxford, 18–23 September 1977.
44. Gullichsen, J., Härkönen, E., "Medium consistency technology. Part 1, fundamental data", *Tappi J.*, **64**: 69–72 (1981).
45. Kerekes, R.J., Soszynski, R.M., Tam Doo, P.A., "The flocculation of pulp fibres", 8th Fundamental Research Symposium, Vol. transactions, 1, session 2: 265–310, Oxford, September 1985.
46. Bennington, C.P.J., Kerekes, R.J., "Power requirements for pulp suspension fluidisation", *Tappi J.*, **79**(2): 253–258, (1996).
47. Skali-Lami, P., Fünfshilling, P., Julien Saint Amand, F., "Hydrodynamic behaviour of fibre suspensions and basis similitudes", COST Action E7 Final Conference "Multi-phase Flows in Papermaking", poster session, Manchester, April 2000.
48. Heise, O., Schabel, S., Cao, B., Lorentz, K., "Deformation and desintegration physics of stickies in pressure screens", 5th Research Forum on Recycling, preprints: 187–196, Ottawa, 28–30 September 1999.
49. Shah, P.N., Atsavapranee, P., Thimoty, W., McHugh, J., "The role of turbulent elongational stresses on deflocculation in paper sheet formation", *Tappi J.*, **83**(4): April 2000.
50. Julien Saint Amand, F., Perrin, B., "Basic parameters affecting screening efficiency and fibre loss", 9th PTS/CTP Deinking Symposium, proceedings, paper 26, 9–12 May 2000.
51. Gooding, R.W., Kerekes, R.J., "The motion of fibres near a screen slot", *Journal of Pulp and Paper Science*, **15**(2): 59–62, March 1989.
52. Halonen, L., Ljokkoi, R., "Improvement of screening systems by screen plate design", International Mechanical Pulping Conference, preprints, **2**: 237–247, Helsinky, 1989.
53. Oosthuizen, P.H., Kuhn, D.C.S., Whiting, P., "Fluid and fibre flow near a wall slot in a channel", *Pulp and Paper Canada*, **95**(4): 27–30 (1994).
54. Tangsaghasaksri, W., Göttsching, L., "Einfluss von Schlitz-Konturen auf den Faserdurchgang. Untersuchung mit Hilfe eines Modell-Sortierer", Part 1/2, *Das Papier* **4/5**: 172–179, 235, 247 (1994).
55. Yu, C.J., DeFoe, R.J., "Fundamental study of screening hydraulics. Part 1: Flow patterns at the feed-side surface of screen baskets; mechanisms of fiber-mat formation and remixing", *Tappi J.*, **77**(8): 219–226, August 1994.
56. Yu, C.J., DeFoe, R.J., "Fundamental study of screening hydraulics. Part 2: Fiber orientation in the feed side of a screen basket", *Tappi J.*, **77**(9): 199–124, September 1994.
57. Lawryshyn, Y.A., Kuhn, D.C.S., "Simulation of flexible fibre motion through

screen apertures", *Journal of Pulp and Paper Science*, **24**(12): 404–411, December 1998.
58. Ross, R.F., Klingenberg, D.J., "Simulation of flowing wood fibre suspensions", *Journal of Pulp and Paper Science*, **24**(12): 388–392, December 1998.
59. Dong, S., Salcudean, M., Gartshore, I., "Fiber motion in single and multiple screen slots", 2000 TAPPI Papermakers Conference and Trade Fair, proceedings, 597–602, Vancouver, 16–19 April 2000.
60. Lawryshyn, Y.A., Kuhn, D.C.S., "Large deflection analysis of wet fibre flexibility measurement technique", *Journal of Pulp and Paper Science*, **22**(11): 423–431, November 1996.
61. Kumar, A., Gooding, R.W., Kerekes, R.J., "Factors controlling the passage of fibres through slots", *Tappi J.*, **81**(5): 247–254, May 1998.
62. Olson, J., Roberts, N., Allison, B., Gooding, R., "Fibre length fractionation caused by pulp screening", *Journal of Pulp and Paper Science*, **24**(12): 393–397, December 1998.
63. Olson, J., Wherret, G., "A model of fibre fractionation by slotted screen apertures", *Journal of Pulp and Paper Science*, **24**(12): 398–403, December 1998.
64. Julien Saint Amand, F. , "Epuration: limites techniques et économiques des technologies existantes. Perspectives nouvelles", 38ème Congrès ATIP, Grenoble, 5–7 Novembre 1985.
65. Rienecker, R., "Sortierung – ein Werkzeug zur Sticky-Entfernung: Machinen", *Wochenblatt für Papierfabrikation*, **17**: 787–793 (1997).
66. Julien Saint Amand, F., Perrin, B. , "Le classage des pâtes: Un procédé de séparation hydrodynamique", 50ème Congrès ATIP, Bordeaux, 21–24 Octobre 1997.
67. Julien Saint Amand, F., "Hydrodynamic phenomena involved in stickies removal processes", COST Action E7 Final Conference "Multi-phase Flows in Papermaking", proceedings, Manchester, 13–14 April 2000.
68. Julien Saint Amand, F., Perrin, B., "Fundamental aspects of mechanical pulp screening", International Mechanical Pulping Conference, preprints, session 4, Helsinky, 4–8 June 2001.
69. Goldsmith, H.L., Mason, S.G., "The microrheology of dispersions", *Rheology, Theory and Applications*, **4**(2): 85–250, Eirich Edition, Academic Press (1967).
70. Julien Saint Amand, F., Perrin, B., "Fragmentation and removal of PSA particles in screens and cleaners", 3rd PTS Stickies Symposium, Munich, 13–14 November 2000.
71. Paul, S.T., Duffy, G.G., Chen, X.D., "Viscosity control as a new way to improve pressure screen performance", *Tappi J.*, **83**(9), September 2000.
72. Meersman, T., "Improved contaminant removal in deinking systems", TAPPI Pulping Conference, proceedings, 1005–1019, San Francisco, 19–23 October 1997.
73. Gassmann, H., "Avoidance of adhesive impurities by mechanical separation in pressure screen and cleaner", 6th International Conference on New Available Technologies, proceedings, 509–513, Stockholm, 1–4 June 1999.
74. Heise, O., Cao, B., Schabel, S., "A novel application of Tappi 277 to determine macro stickies disintegration and agglomeration in the recycling process", TAPPI Recycling Symposium, proceedings, 631–644, Washington DC, 6–8 March 2000.

75. Baehr, T., Rienecker, R., "A new generation of pressure screens for stock preparation systems", TAPPI Pulping Conference, proceedings, 1991.
76. Kanazawa, T., "Experience and proposal to improve sticky problems in deinking plant and in recycling paper processing for paper board", Pan Pacific Pulp and Paper Technology Conference, proceedings, 1992.
77. Vitori C.M., "Stock velocity and stickies removal efficiency in slotted pressure screens", *Pulp and Paper Canada* **94**(12) (1993).
78. Lascar, A., Fejoz, R., "Concept expertise and field experience in fine slot screening", 8th PTS CTP Deinking Symposium, proceedings, Paper **15**, Munich, May 1998.
79. Delagoutte, Th., Laurent, A., "Characterisation of stickies after enzymatic digestion of fibres: a promising new method for the quantification of primary stickies in recycled pulps", 3rd CTP Research Forum, Recycled Fibres, Paper **16**, Grenoble, 30–31 January 2001.
80. Delagoutte, Th., Julien Saint Amand, F., "Pilot plant procedure for the assessment of the screening ability of pressure sensitive adhesive", TAPPI Recycling Symposium, proceedings, Washington DC, 6–8 March 2000.
81. Wakelin, R.F., Corson, S.R., "TMP long fibre fractionation with pressure screens", International Mechanical Pulping Conference, proceedings, 257–265 (1995).
82. Repo, K., Sundholm, J., "The effect of rotor speed on the separation of coarse fibers in pressure screening with narrow slots", International Mechanical Pulping Conference, proceedings, 271–275 (1995).
83. Niinimäki, J., Dahl, O., Kuopanportti, H., Ämmälä, A., "A comparison of pressure screen baskets with different slot widths and profile heights", *Paperi ja Puu*, **80**(8): 601–605, (1998).
84. Weckroth, R., Grundström, K.J., "Effect on screening performance with different screen cylinder aperture design", *African Pulp & Paper Week*, Durban, 17–19 October 2000.
85. Serres, A., Fernandez de Grado, A., Vitori, C., McCarthy, C., "Contribution to the understanding of the screening process on the example of a newly developed fine screen with slotted basket", 9th PTS CTP Deinking Symposium, proceedings, Paper 27 Munich; 9–12 May 2000.
86. Bohn, B., Hernesaho, M., Nerg, H., "New screening techniques for the new millennium – The MuST screen", TAPPI Papermakers Conference and Recycling Symposium, proceedings, 1469–1476, 1–4 March 1999.
87. Brettschneider, W., "Screening systems – A contribution towards selecting the correct system arrangement", *Wochenblatt für Papierfabrikation*, **13** (1993).
88. Julien Saint Amand, F., Perrin, B., "Removal of Low Density Contaminants: Limits of Current Screening and Cleaning Technology", *Revue ATIP,* **53**(6): 156–168, Novembre-Décembre 1999.
89. Olson, J.A., "Fibre length fractionation caused by pulp screening, slotted screen plates", 86th Annual Meeting PAPTAC, proceedings, 21–28 February 2000.
90. Allison, B.J., Olson, J.A., "Optimization of multiple screening stages for fibre length fractionation: two stage case", *Journal of Pulp and Paper Science*, **26**(3): 113–119, March 2000.

91. Julien Saint Amand, F., Perrin, B., De luca P., "Stickies Removal Strategy", *Progress in Paper Recycling*, **7**(4): 39–53, August 1998.

Cleaning

1. Julien Saint Amand, F., "Principles and technology of cleaning", *Paper Recycling Challenge*, Process Technology, **III**(4): 42–70, Editors: M.R. Doshi and J.M. Dyer (1998).
2. Larsson, T., "A new type of hydrocyclone", BHRA International Conference on Hydrocyclones, 83–98, Cambridge, October 1980.
3. Bouchillon, C.W., Franko, A., "Computer Modeling Improves the Design of Hydrocyclones for Pulp Cleaning", Part 2, *Paper Trade Journal*, November 1985.
4. Larsson, T. , "Les épurateurs cyclones de demain pour l'industrie papetière", *Papier, Carton, Cellulose*, **27**(10): 38–41 Octobre 1978.
5. Chivrall, G.B., "Stock preparation and strategies for brown grades-highlighting new developments", PIRA Conference Brown packaging grades-current and future trends, proceedings, 10–11 September 1991.
6. Lindqvist, S., Moss, C., "Advanced cleaner technology for the year 2000", *Progress in Paper Recycling*, **2**(2): 35–40, February 1993.
7. Moss, C.S., "A new generation of cleaners: The high consistency sand and the neutral buoyancy stickies removal cleaner", PPI Paper Recycling '96 Conference, Session 3, London, 13–14 November 1996.
8. Clay, J., "Bergstrom finds reverse cleaning answer to lightweight contaminants", *Paper Trade Journal*, **164**(15): 28–30, August 1980.
9. Sjogren, K., Larsson, T., "Albia hydrocyclones and their application in the pulp and paper industry", *Appita*, **41**(4): 313–316, July (1986).
10. Bliss, T., "Through-flow cleaners offer good efficiency with low pressure drop", *Pulp and Paper*, **59**(3): 61–65, March 1985.
11. Maze, E.L., "New cleaner development for lightweight contaminant removal", *Progress in Paper Recycling*, **xx**(0): 40–47, May 1997.
12. Chivrall, G.B., "The BELOIT Uniflow Cleaner, a novel concept in hydrocyclone technology", SPCI World Pulp and Paper week, proceedings, 266–271, Stockholm, 10–13 April 1984.
13. Karneth, A.M, Bach, R.H., Sferrazza, M.J., Horn, D.J., "Die Auswirkungen von Druckfarbe und Strich auf den Deinkingprozess", *Wochblatt für Papierfabrikation*, **1**: 8–12 (1995).
14. Pfalzer, T., "Deinking Process Technology", *Progress in Paper Recycling*, **1**(2): 21–29, February 1992.
15. Julien Saint Amand, F., "Etude d'un épurateur à vortex libre en paroi tournante", PhD Thesis, INPG Technical University of Grenoble, 8 July 1980.
16. Julien Saint Amand, F., Charuel, R. , "Etude d'un épurateur à vortex libre en paroi tournante", *Revue ATIP*, **36**(6–7): 323–331, June/September 1982.
17. Julien Saint Amand, F., Bernard, E., Lamort, P., "Entwicklung eines rotierenden Cleaners fur hocheffiziente Leichtschmutzentfernung", *Wochenblatt für Papierfabrikation*, **113**(20): 779–784, October 1985.

18. Serres, A., Julien Saint Amand, F., "Entwicklung des Leichtschmutzcleaners Gyroclean GYT", *Wochenblatt für Papierfabrikation*, **118**(23/24): 1059, December 1990.
19. Serres, A., Levis, S.H., "Recent Developments in the removal of lightweight contaminants", CPPA 77th Annual Meeting Preprints: A151–A155 (1991).
20. Kelsall, D.F., "A study of the motion of solid particles in a hydraulic cyclone", *Chemical and Process Engineering*, **33**: 261 (1952).
21. Bradley, D., *The Hydrocyclone*, Pergamon Press, Oxford, 1965.
22. Rietema, K., "The mechanisms of separation of finely dispersed solids in cyclones", *Cyclones in Industry*, Chapter 4, Elsevier, London 1961.
23. Sevilla, E.M., Branion, R.M.R., "Computational fluid dynamics calculations for flow in hydrocyclones", 81st Annual Meeting, CPPA, Preprints: B127–B135 (1995).
24. Sevilla, E.M., Branion, R.M.R., "The Fluid Dynamics of Hydrocyclones", *Journal of Pulp and Paper Science*, **23**(2): 85–93, February 1997.
25. Schabel., "Computational fluid dynamics in stock preparation machine development", COST Action E7 Final Conference "Multi-phase Flows in Papermaking", proceedings, Paper 5, Manchester, 13–14 April 2000.
26. Bouchillon, C.W., Franko, A., "Computer Modeling Improves the Design of Hydrocyclones for Pulp Cleaning. Part 1", *Paper Trade Journal*, **168**(17): 54–56, November 1984.
27. Comolet, R.: "Mécanique expérimentale des fluides, Tome II, Dynamique des fluides réels – Turbomachines", *Masson et Cie Editeurs*, Paris, 1963.
28. Lamb, H., *Hydrodynamics*, Cambridge University Press, 6th Edition, 1975.
29. White, F.M., *Viscous Fluid Flow*, McGraw-Hill, New York, 1991.
30. Rhemat, T., Branion, R., "Fibre fractionation in hydrocyclones", 81st CPPA Annual Meeting, proceedings, 105–125, Oct./Nov. 1995.
31. Lawryshyn, Y.A., Kuhn, D.C.S., "Large deflection analysis of wet fibre flexibility measurement techniques", *Journal of Pulp and Paper Science*, **22**(11): 423–431, November 1996.
32. Schubert, H., "Zur prozessbestimmenden Rolle der Turbulenz bei Aufbereitungsprozessen I", *Aufbereitungs Technik*, **9**: 501–512, (1974).
33. Svarovsky, L., *Hydrocyclones*, Holt, Rinehart and Winston, London, 1984.
34. Bermond, C., Bollard, J. Palassoff, S., "Modelisation de l'hydrocyclone", *Revue ATIP*, **41**(10): Décembre 1987.
35. Julien Saint Amand, F., Perrin, B., Bernard, E., "Modellierung und Dimensionierung von Cleanern Eine vergleichende Untersuchung zur Abscheidung von Schmutzpunkten aus deinktem Altpapierstoff", *Wochenblatt fur Papierfabrikation*, **8**: 295–302 (1992).
36. Julien Saint Amand, F., "Epuration: limites techniques et économiques des technologies existantes. Perspectives nouvelles", 38ème Congrès ATIP, Preprints, Grenoble, 5–7 November 1985.
37. Julien Saint Amand, F., Perrin, B., "The effect of particle size on ink and speck removal efficiency of the deinking steps. Part II: Cleaning", *Pulp and Paper Canada*, **94**(10): 284–287, October 1993.

38. Grimes, D.B., "The use of flow pattern modeling in paper pulp hydrocyclone cleaners", TAPPI Recycling Symposium, proceedings, 379–391 (1994).
39. Sutman, F.J., Philippe, I.J., Le Blanc, P., "Medium consistency Forward cleaning development for laser deinking systems", TAPPI Recycling Symposium, proceedings, 399–406 (1994).
40. Julien Saint Amand, F., Bernard, E., "Centrifugal cleaning for the production of brown grades", *Progress in Paper Recycling*, **2**(3), May 1993.
41. Julien Saint Amand, F., Perrin, B., "Removal of Low Density Contaminants: Limits of Current Screening and Cleaning Technology", *Revue ATIP*, **53**(6): 156–168, Novembre-Décembre 1999.
42. Bliss, T., "Reverse cleaning – its use in removing lightweight and sticky contaminants", *Tappi J.*, **63**(6): 87–90, June 1980.
43. Wight, M.O., "Performance of Forward Cleaners", *Progress in Paper Recycling*, **1**(4): 38–45, August 1992.
44. Kerekes, R.J., "Characterizing fibre suspension", TAPPI Engineering Conference, proceedings, 21–28 (1996).
45. Bliss, T., "Secondary fibre fractionation using centrifugal cleaners", TAPPI Pulping Conference, proceedings, 217 (1984).
46. Wood, J.R., Grondin, M., Karnis, A., "Characterization of mechanical pulp fines with a small hydrocylone. Part I: The principle and nature of the separation", *Journal of Pulp and Paper Science*, **17**(1): J1 (1991).
47. Gavelin G., Backman, J., "Fractionation with hydrocyclones", TAPPI Pulping Conference, proceedings, 753–774 (1991).
48. Paavalainen, L., "The possibility to fractionate softwood sulfate pulp according to cell wall thickness", *Appita*, **45**(5): 319–326, September 1992.
49. Ho, S.L., Rehmat, T., Branion, R., "Fractionation in hydrocyclones", 86th Annual Meeting PAPTAC, Preprints, 193–215, February 2000.
50. Omholt, I., "The effect of hydrocyclone separation and reject refining on the TMP fibre properties", 3rd Fundamental Mechanical Pulp Research Seminar, proceedings, Helsinky, 20 June 2001.
51. Dessureault, S., Michaud, G., Tremblay, S. and Massicotte, C., "Cleaning systems for recycled pulps from laser/xerox printed wastepaper". TAPPI Pulping Conference proceedings, 875–884 (1993.
52. Olson, C.R., Richmann, S.K., Sutman, F.J., Letscher, M.B., "Deinking of laser-printed stock using chemical densification and forward cleaning", *Tappi J.*, **76**(1): 136, January 1993.
53. Bormett, D.W., Lebow, P.K., Ross N.J. and Klungness J.H., "Removal of hot-melt adhesives with through flow cleaners", *Tappi J.*, **78**(8): 179–184, August 1995.
54. Banerjee, S., Grimes, D.B., "Improving centrifugal cleaner efficiency through temperature mismatching", *Tappi J.*, **84**(1), January 2001.
55. Gassmann, H., "Avoidance of adhesive impurities by mechanical separation in pressure screen and cleaner", 6th International Conference on New Available Technologies, proceedings: 509–513, Stockholm, 1–4 June 1999.
56. Julien Saint Amand, F., "Hydrodynamic phenomena involved in stickies removal

processes", COST Action E7 Final Conference "Multi-phase Flows in Papermaking", proceedings, Paper 1, Manchester, 13–14 April 2000.

Flotation

1. Ives, K.J., *The scientific basis of flotation*, Martinus Nijhoff Publishers, 1984.
2. Laskowski, J.S., *Frothing in flotation*, Gordon and Breach Science Publishers, 1989.
3. Schweizer, G.: *Wochenblatt für Papierfabrikation*, **93**(19): 823–830 (1965).
4. Bechstein, G., Unger, E., "Ein Beitrag zur Klärung der Wirkungsweise von Sammlern beim Deinking flotationsprozess", *Zellstoff und Papier*, **10**: 297–306 (1972).
5. Ortner, H., Wood, R.F., Gartemann, H., "Deinking – Stand und Entwicklung", *Wochenblatt für Papierfabrikation*, **103**(6): 597–601 (1975).
6. Galland, G., Bernard, E., Sauret, G. , "Aspect physico-chimique du désencrage", *Revue ATIP*, **31**(10): 374–378, Decembre 1977.
7. Fischer, S., "Modellvorstellungen für die physikalish-chemischen Vorgänge in der Flotationsstufe des Deinking-Prozesses", *Wochenblatt für Papierfabrikation*, **110**(14): 511–514 (1982).
8. Hornfeck, K., "Flotationshilfsmittel und deren Einfluss auf den Deinking Prozess", *Wochenblatt für Papierfabrikation*, **110**(15): 542–544 (1982).
9. Larson, A., Stenius, P., Ström, G., "Zur Oberflächenchemie des Deinking Prozesses", *Wochenblatt für Papierfabrikation*, **110**(14): 502–506 (1982).
10. Putz, H.J., Schaffrath, H.J., Göttsching, L., "Deinking of oil and water-born printing inks – a new flotation deinking model", 1st Research Forum on Recycling, proceedings, 183–190, Toronto, 1991.
11. Stratton, R.A., "The surface chemistry of flotation of stickies and laser printed inks", *Journal of Pulp and Paper Science*, **18**(6): 221–224, November 1992.
12. Hou, M.J., Hui, S.H., "Interfacial phenomena in deinking. Part 1: Stability of ink particle-air bubble aggregates in flotation deinking", TAPPI Pulping Conference, proceedings, 1125–1142 (1993).
13. Beneventi, D., Carré, B., "The mechanisms of flotation deinking and the role of fillers", *Progress in Paper Recycling*, (2): 77–85, February 2000.
14. Schulze, H.J., "The fundamentals of flotation deinking in comparison to mineral flotation", 1st Research Forum on Recycling, proceedings, 161–167, Toronto, 29–31 October 1991.
15. Julien Saint Amand, F., Perrin, B., "The effect of particle size on ink and speck removal efficiency of the deinking steps", 1st Research Forum on Recycling, proceedings, 39–47, Toronto, 29–31 October 1991.
16. Schulze, H.J., "Zur Hydrodynamik der Flotations-Elementarvorgänge", *Wochenblatt für Papierfabrikation*, (5): 160–168 (1994).
17. Pan, R., Bousfield, D.W., Thompson, E.V., "Modelling particle-bubble dynamics and adhesion in air bubble/solid particle/liquid systems", TAPPI Pulping Conference, proceedings, 941–956 (1992).
18. Paulsen, F.G., Pan, R., Bousfield, D.W., Thompson, E.V., "The dynamics of

bubble/particle approach and attachment during flotation and the influence of short-range nonhydrodynamic forces on disjoining film rupture", CPPA 2nd Research Forum on Recycling, proceedings, 1–12 (1993).

19. Pan, R., Paulsen, F.G., Johnson, D.A., Bousfield, D.W., Thompson, E.V., "A global model for predicting flotation efficiencies: model results and experimental studies", TAPPI Pulping Conference, proceedings: 1155–1164 (1993).
20. Pan, R., Paulsen, F.G., Kocer, H., Nerez, R., Johnson, D.A., Bonsfield, D.W., Thompson E.V., "A global model for predicting flotation efficiencies. Part II: Particle size and flotation rate predictions, and experimental studies and comparisons", TAPPI Recycling Symposium, proceedings, 291–301 (1994).
21. Klein, R., Schwarze, D., Grossmann, H., "Beitrag zur Berwertung des Einflusses der Luftblasengrösse auf das Deinkingergebnis", 6th PTS Deinking Symposium, 15–18 March 1994.
22. Göttsching, L., Hunold, M., Krauthauf, T., Müller, J., Putz, H.J., "Effect of Air Volume and Air Bubble Size Distribution on Flotation in Injector Aerated Deinking Cells", CPPA 3rd Research Forum on Recycling, proceedings, 17–25, Vancouver, 20–22 November 1995.
23. Dorris, G.M., Pagé, M., "Deinking of toner printed papers. Part 1: Flotation kinetics, froth stability and fibre entrainment", 3rd Research Forum on Recycling, proceedings, 215–225, Vancouver, 20–22 November 1995.
24. Schmidt, D.C., Berg, J.C., "The effect of particle shape on the flotation of toner particles", Progress in Paper Recycling, 67–77, February 1996.
25. Vidotti, R.M., Johnson D.A., Thompson, E.V., "Hydrodynamic particle volume and its relationship to mixed office waste paper flotation efficiency, Part. 1", TAPPI Pulping Conference, proceedings, 203–213 (1995).
26. Kocer, H., Johnson, D.A., Thompson, E.V., "Influence of air flow rate, time and total air volume on efficiency of toner removal in mixed office waste flotation", TAPPI Recycling Symposium, proceedings, 65–72, 1995.
27. Ajersch, M., Pelton, R., "Mechanisms of pulp loss in flotation deinking", 3rd Research Forum on Recycling, proceedings, 27–40, Vancouver, 20–22 November 1995.
28. Paulsen, F.G., Pan, R., Bousfield, D.W., Thompson, E.V., "Measurement of long-range hydrophobic attraction forces and their relationship to deinking flotation", TAPPI Pulping Conference, proceedings, Nashville, 27–31 October 1996.
29. Heindel, T.J., "The fundamentals of flotation deinking", TAPPI Pulping Conference, proceedings, 521–533, San Francisco, 19–23 October 1997.
30. Ajersch, M., Pelton, R., "Modelling fibre loss by entrainment during flotation of flocculated pulps", *Journal of Pulp and Paper Science*, **25**(1): 30–36, January 1999.
31. Hardie, C.A., Gomez, C.O., Finch, J.A., "A venturi aerated column cell for deinking: Effect of design and operating parameters", *Progress in Paper Recycling*, 33–40, August 1999.
32. Catsburg, R.W., "Flotation deinking research of the future: Parallel process simulation", *Paper Technology*, 35–39, November 1999.
33. Yoon, R.H., "Application of mineral processing techniques for recycling", TAPPI Recycling Symposium, proceedings, 33–45 (2000).

34. Garnier, A.E., Heindel, T.J., "The effect of fibre type on bubble size", *Journal of Pulp and Paper Science*, **26**(7): 30–36, July 2000.
35. Ferguson, L.D., "A review of flotation deinking technology", *Progress in Paper Recycling*, 17–23, November 1991.
36. Floccia, L., "Some comments about industrial cells for DIP", 4th International Wastepaper Technology Conference, proceedings, London Gatwick, 13–15 June 1995.
37. Mac Kinney, R., "Flotation deinking overview", *Paper Recycling Challenge*, Process Technology, **III**(7): 99–114, Editors: M.R. Doshi and J.M. Dyer, 1998.
38. Julien Saint Amand, F., "Hydrodynamics of deinking flotation" *International Journal of Mineral Processing*, **56**(1–4): 277–316, April 1999.
39. Kemper, M., "Flotation deinking. State of the art, new applications and technologies" 6th International Conference on New Available Technologies, proceedings, 485–492, 1–4 June 1999.
40. Gilkey, M.W., Yoshida, H., "A new high efficiency flotation device", 78th CPPA Annual Meeting, proceedings, B153–B158, 31 January 1992.
41. Gilkey, M.W., Conte, T.O., Seifert, P., "Field experiences with a new high air rate flotator", TAPPI Recycling Symposium, proceedings, 163–170 (1994).
42. MacCool, M.A., Carroll, W.P., "Pressurized deinking module", TAPPI Pulping Conference, proceedings, 145–152 (1990).
43. Torregrossa, L.A., Chamblee, J.W., Platner, G., "Flotation deinking with the gas sparged cyclone", Pan–Pacific Pulp and Paper Technology Conference, proceedings, 101–104, Tokyo, 8–10 September 1992.
44. Carlton, K.A., "New deinking system combines GSC contacting with tower flotation technology", TAPPI Recycling Symposium, proceedings, 325–331 (1996).
45. Dessureault, S., Levesque, M., Barbe, M.C., "Column flotation: a new technology for deinking recycled pulp", TAPPI Recycling Symposium, proceedings, 251–255 (1995).
46. Barnscheidt, W., "Die Weiterentwichlung des Verticell Verfahrens", *Wochenblatt für Papierfabrikation*, **113**(13): 484–485 (1985).
47. Barnscheidt, W., "Uberlegungen zur Auslegung eines Deinkinginjektors", PTS Deinking Symposium, 85, Munich, 1987.
48. Serres, A., Colin, E., "The MAC flotation cell on a new deinking concept: Theory and practical results", 7th PTS Deinking Symposium, Munich 7–9, May 1996.
49. Pfalzer, L., Schweiss, P., "Die Voith Multi-Injectorzelle – Fonktionsweise und Anwendung in einer modernen Deinkinganlage", *Wochenblatt für Papierfabrikation*, **8**: 303–307 (1988).
50. Kurz, E., Frymark, J., "The voith multi injector flotation cell", Pan Pacific Pulp and Paper Technology Conference, proceedings, 131–138, Tokyo, 8–10 September 1992.
51. Britz, H., "Flotations deinking – Grundlagen und Systemeinbindung", *Wochenblatt für Papierfabrikation*, **10**: 394–401 (1993).
52. Britz, H., Peschl, A., "Flotationsdeinken bei erhöhten Stoffdichten – oder wirtschaftlich flotiert", *Wochenblatt für Papierfabrikation*, **15**: 603–608 (1994).

53. Carletti, C., Wood, R.J., “Spidercel Reactor technology improves flotation deinking efficiency”, TAPPI Recycling Symposium, proceedings, 321–324 (1996).
54. Hori, H., “The present state of small scale papermaking in Japan. Treatment of waste paper”, *Japan Pulp and Paper*, **28**(4): 19 (1996).
55. Chudacek, M.W., Fichera, M.A., Estrina, H., Marshall, S.H., “Initial experiments on newsprint deinking by the Fastflot process”, *Progress in Paper Recycling*, 26–31, May 1995.
56. Grossmann, H., Hanecker, E., Schulze, G., “Flotation of recycled pulp in a centrifugal force field”, TAPPI Recycling Symposium, proceedings, 65–72, Chicago, 14–16 April 1997.
57. Linck, E., Siewert, W.H., “The new Escher Wyss flotation cell in an improved deinking system”, TAPPI Pulping Conference, proceedings 605–610 (1994).
58. Serres, A., “Reduction of losses during deinking”, 5th Research Forum on Recycling, proceedings, 113–120, 28–30 September 1999.
59. Heimonen, J., Pousi, J., “Optimisation of flotation cell performance”, 5th Research Forum on Recycling, proceedings, 121–127, 28–30 September 1999.
60. Ajersch, M., Pelton, R., “The growth of bubbles on pulp fibers and on carbon black dispersed in supersaturated carbon dioxide solutions”, 2nd CPPA Research Forum on Recycling, proceedings, 129–134 (1993).
61. Robertson, N., Patton, M., Pelton, R., “Washing the fibers from foam for higher yields in flotation deinking”, *TAPPI J.*, **81**(6): 138–142 (1998).
62. Zhu, J.Y., Wu, G.H., Deng, Y., “Flotation deinking of toner-printed papers using frother spray”, *Journal of Pulp and Paper Science*, **24**(9): 295–299 (1998).
63. Jameson, G.J., “Physics and hydrodynamics of bubbles”, in *The scientific basis of flotation*, Martinus Nijhoff Publishers, 1984.
64. Julien Saint Amand, F., De Luca, P., “Hydrodynamics of flotation: Experimental studies and technological aspects”, 7th PTS Deinking Symposium, Munich, 7–9 May 1996.
65. Julien Saint Amand, F., “Hydrodynamics of flotation: Experimental studies and theoretical analysis”, TAPPI Recycling Symposium, proceedings, Chicago, 14–16 April 1997.
66. Clift, R., Grace, J.R., Weber, M.E., *Bubbles, Drops and Particles*, Academic Press, New York, 1978.
67. Ahmed, N., Jameson, G.J., “Flotation kinetics”, *Mineral Processing and Extractive Metallurgy Review*: **5**: 77–99 (1989).
68. Plate, H., Schulze, H.J., “Modeling of the overall flotation process based on physico-chemical micro-processes – Technique and application”, XVII International Mineral Processing Congress, Dresden, 23–28 September 1991.
69. Abrahamson, J., “Collision rates of small particles in a vigorously turbulent fluid”, *Chemical Engineering Science*, **30**: 1371–1379, (1975).
70. Bird, R.B., Stewart, W.E., Lightfoot, E.N., *Transport phenomena*, John Wiley & Sons (1960.
71. Yoon, R.H., Luttrell, G.H., “The effect of bubble size on fine particle flotation”, *Mineral Processing and Extractive Metallurgy Review* (5): 101–122 (1989).
72. Nguyen-Van, A., Kmet, S., Schulze, H.J., “Collection events in flotation: the

quantitative analysis of the particle-bubble collision and the attachment of particle onto bubble surface", XIX International Mineral Processing Congress, San Francisco, 22–27 October 1995.

73. Schulze, H.J., "Probability of particle attachment on gas bubbles by sliding", *Advances in Colloid and Interface Science*, **40**: 283–305 (1992).
74. Schulze, H.J., Personal communication (1996).
75. Julien Saint Amand, F., Eymin Petot Tourtollet, G., Perrin, B., Sabater, J., "Advanced deinking process control using new on-line sensors", *Progress in Paper Recycling*, **8**(3): 37–52, May 1999.
76. Cathie, K., Mallouris, M., "use of surface energy measurements and other parameters to predict the deinkability of laser printed papers", 2nd CPPA Research Forum on Recycling, proceedings, 179–199, October 1993.
77. Julien Saint Amand, F., Perrin, B., De luca P., "Stickies Removal Strategy", *Progress in Paper Recycling*, **7**(4): 39–53, August 1998.
78. Heise, O., Kemper, M., Wiese, H., Krauthauf, E., "Removal of residual stickies applying new flotation technology at Haindl Paper – Schöngau", TAPPI Recycling Symposium, proceedings, 693–710, Atlanta, 1999.

Washing

1. Gilkey, M., "Washing of secondary fibres", *Paper Recycling Challenge*, Process Technology, **III**(8): 115–130, Editors: M.R. Doshi and J.M. Dyer (1998).
2. McCool M.A., Rosier M.A., "Screening Technology in Recycled Fiber Systems", *Paper Recycling Challenge*, Process Technology, **III**(3): 29–41, Editors: M.R. Doshi and J.M. Dyer (1998).
3. Pfalzer, L., "Deinking by Washing or Flotation – A comparison from the view-point of process engineering and process application", TAPPI Pulping Conference, proceedings, Seattle (1979).
4. Galland, G., Carré, B., "Waterbased ink and deinking – Summary and main conclusions of the COST workshop", 8th PTS/CTP Deinking Symposium, proceedings: **8**, Munich, 5–8 May 1998.
5. Smook, G.A., "Handbook for pulp and paper technologists", TAPPI Press, 91–99, 196–221 (1982).
6. Ricketts, J.D., "An overview of modern pulp washing systems", CPPA/TAPPI Pulp Washing '96 Conference, proceedings, 103–108, Vancouver, 7–10 October, 1996.
7. Horacek, R. and Matthew, J.: *Beloit Corporation Deinking Manual*, 2nd Edition, September 1979.
8. Julien Saint Amand, F., "Evaluation des techniques d'épuration en fonction des caractéristiques physiques des contaminants. Recherche de modèles", *Revue ATIP*, **45**(4): 145–164, Juin/Juillet, 1991.
9. Bliss, T., Dietrich, G., Seifert, P., "Controlling yield in washing deink systems", TAPPI Pulping Conference, proceedings, 1011–1024, San Diego, 6–10 November 1994.
10. Holle, D., "Eindicken, Entaschen und Entsorgen der Druckfarbe beim Deinking

mit dem AKSE Scheibeneindicker", *Wochenblatt fûr Papierfabrikation*, **19**: 711–815 (1985).
11. Kleuser, J., Egenes, T.H., "Selection and configuration of washing systems for secondary fibres", *Paper Technology*, 42–48, June 1996.
12. Backman, J., Kempe, A., Lindqvist, J., "Particle removal by centrifugal cleaning and washing", Pira Conference "Developments in wastepaper technology", proceedings, 24–25 March 1993.
13. Moss, CS., Smith R.M., "A new type of washer", TAPPI Recycling Symposium, proceedings, 443–477, March 1996.
14. Linck, E., Mayer, H., Siewert, W.H., "Der Vario Split – Eine neue Maschine zur Verbesserung von AP-Rohstoffen", *Wochenblatt für Papierfabrikation*, **109**(21), 787–796 (1981).
15. Gilkey, M., McCarthy, C., "A new device for high efficiency washing of deink furnishes", TAPPI Pulping Conference, proceedings, New Orleans, 1988.
16. Seifert, P., "Understanding washing of secondary fiber", TAPPI Pulping Conference, proceedings, 917–923 (1992).
17. Nerg, H., Pousi, J., Hourula; V., Heimonen, J., "How to simplify the RCF process?", TAPPI Papermakers Conference and Recycling Symposium, proceedings, 985–999, March 1999.
18. Rangamannar, G., Butler, R., "The Dynamic Washer – A new approach for washing recycled fibers", TAPPI Recycling Symposium, proceedings, 247–264 (1993).
19. Patel, R., "The dynamic washer and filter", Recycling '95 EUCEPA Symposium, proceedings, Manchester, 16–18 October 1995.
20. Locke, R.E., Kerr, J.C., Vitori, C.M., "Successfully recycling waxed corrugated containers", TAPPI Pulping Conference, proceedings, 313–319 (1993).
21. Aikawa, Y., Kanazawa, T., "Recent trend in Aikawa-Lamort deinking system in Europe*", Japan Pulp and Paper*, 61–74, February 1983.
22. Bottegard, O., Norli, L., "Tumbling washing with screw presses", *Korean TAPPI* (1990).
23. Egenes, T. Helle, T., Bendiksen, P.B., Hegstad, G., "Removal of water and contaminants from ONP-stocks in a screw press", CPPA 2nd Research Forum on Recycling, proceedings, 71–78 (1993).
24. Hakan, D., Urban, G., "Displacement washing of pulp fibre beds – Comment on the influence of permeability", CPPA/TAPPI Pulp Washing '96 Conference, proceedings, 9–12, Vancouver, 7–10 October 1996.
25. Antkowiak, J., LaRivière, C., Lennon, V., Miller, W., "Discharge consistency impact on washer efficiency", CPPA/TAPPI Pulp Washing '96 Conference, proceedings, 13–16, Vancouver, 7–10 October 1996.
26. Qvintus, H., Tervola, P., "Methods to intensify displacement washing", CPPA/TAPPI Pulp Washing '96 Conference, proceedings, 17–22, Vancouver, 7–10 October 1996.
27. Holik, H., Kurtz, R., "The Tisco Former, a new double wire former", *Wochenblatt für Papierfabrikation* 11/12 (1978).
28. Egenes, T.H., Helle, T., "Flow characteristics and water removal from pulp

suspensions in a screw press", *Journal of Pulp and Paper Science*, **18**(3): 93–98, May 1992.

29. Shirato, M., Murase, T., Hayashi, N., Miki, K., Fukushima, N., Tazima, T., "Fundamental studies on continuous extrusion using a screen press", *International Chemical Engineering*, **18**(4): 680–688 (1978).
30. Seifert, P., "Analysis of a pulp thickener", *Tappi J.*, **52**(12): 2416–2419, December 1969.

Transcription of Discussion

STOCK PREPARATION PART 2 – PARTICLE SEPARATION PROCESSES

François Julien Saint Amand

Centre Technique du Papier (CTP)

Derek Page Institute of Paper Science & Technology

I would like to ask one question. Could you put up your first slide (Figure 1)? Many years ago I tried to find the origin of this graph which has been reproduced by many people. The first version I saw had no data points and neither has any version since. Does data exist anywhere or is this one of those diagrams that are passed from generation to generation without having an experimental basis?

François Julien Saint Amand

In the beginning there was no scale for particle size. This curve comes from experimental data gained in the field of de-inking only. Secondly it assumes that in flotation we have hydrophilic particles and that for cleaning you have high density particles. This equation only takes high density inks into account, so it is for the field of de-inking but it is also used a lot for teaching purposes and it's very easy to introduce into all of the separation process

Derek Page

So you don't have any data points that we don't know about?

François Julien Saint Amand

I have never seen a curve with data points.